PB84-160514

Evaluation of an Air Curtain Hooding System for a Primary Copper Converter
Volume 1

PEDCo Environmental, Inc.
Cincinnati, OH

Prepared for

Industrial Environmental Research Lab.
Cincinnati, OH

Feb 84

U.S. Department of Commerce
National Technical Information Service
NTIS

PB84-160514

EPA-600/2-84-042a
February 1984

EVALUATION OF AN AIR CURTAIN HOODING SYSTEM FOR A PRIMARY COPPER CONVERTER

Volume I.

by

PEDCo Environmental, Inc.
Cincinnati, Ohio 45246

Contract No. 68-03-2924
Work Directive 9

and

Contract No. 68-02-3546
Task Assignment No. 12

Project Officers
John O. Burckle
Industrial Pollution Control Division
Industrial Environmental Research Laboratory
Cincinnati, Ohio 45220

and

Alfred Vervaert and Frank Clay
Office of Air Quality Planning and Standards
Emission Standards and Engineering Division
Research Triangle Park, North Carolina 27711

INDUSTRIAL ENVIRONMENTAL RESEARCH LABORATORY
OFFICE OF RESEARCH AND DEVELOPMENT
U.S. ENVIRONMENTAL PROTECTION AGENCY
CINCINNATI, OHIO 45268

REPRODUCED BY
NATIONAL TECHNICAL
INFORMATION SERVICE
U.S. DEPARTMENT OF COMMERCE
SPRINGFIELD, VA. 22161

TECHNICAL REPORT DATA

(Please read Instructions on the reverse before completing)

1. REPORT NO.
EPA-600/2-84-042a

2.

3. RECIPIENT'S ACCESSION NO.
PB84 160514

4. TITLE AND SUBTITLE
Evaluation of an Air Curtain Hooding System for a Primary Copper Converter - Volume I

5. REPORT DATE
February 1984

6. PERFORMING ORGANIZATION CODE

7. AUTHOR(S)

8. PERFORMING ORGANIZATION REPORT NO.

9. PERFORMING ORGANIZATION NAME AND ADDRESS
PEDCo Environmental, Inc.
Cincinnati, OH

10. PROGRAM ELEMENT NO.
DU A-119

11. CONTRACT/GRANT NO.
68-03-2924

12. SPONSORING AGENCY NAME AND ADDRESS
US Environmental Protection Agency
Office of Research and Development
Industrial Environmental Research Laboratory
Cincinnati, OH 45268

13. TYPE OF REPORT AND PERIOD COVERED
Final

14. SPONSORING AGENCY CODE
EPA/600/12

15. SUPPLEMENTARY NOTES
Project Officer: John O. Burckle

16. ABSTRACT

This report presents the results of tests conducted to evaluate the effectiveness of a full-scale air curtain capture system installed on a primary copper smelter for capture of low level fugitive particulate, including trace metals, and sulfur dioxide. The test work was performed onsite at ASARCo'S Tacoma Smelter on the first domestic full-scale prototype system, resulting in the first published evaluation of full-scale fugitive capture system based upon the air curtain approach as applied to a primary copper converter.

The installation of the air curtain hooding system has permitted a quantitative approach to the direct measurement of the fugitive emissions for the first time. In this program, the fugitives captured by the air curtain were measured at a downstream sampling point in the exhaust side of the air curtain system during the various portions of the converter cycle. Emission factors were established for sulfur dioxide, filterable particulate (method 5), inhalable particulate, and selected trace elements.

17. KEY WORDS AND DOCUMENT ANALYSIS

a. DESCRIPTORS	b. IDENTIFIERS/OPEN ENDED TERMS	c. COSATI Field/Group
		13B

18. DISTRIBUTION STATEMENT
RELEASE to PUBLIC

19. SECURITY CLASS *(This Report)*
UNCLASSIFIED

20. SECURITY CLASS *(This page)*
UNCLASSIFIED

21. NO. OF PAGES
194

22. PRICE

EPA Form 2220-1 (Rev. 4-77) PREVIOUS EDITION IS OBSOLETE

DISCLAIMER

The information in this document has been funded wholly or in part by the United States Environmental Protection Agency under Contracts 68-03-2924 and 68-02-3546 to PEDCo Environmental, Inc. It has been subject to the Agency's peer and administrative review, and it has been approved for publication as an EPA document. Mention of trade names or commercial products does not constitute endorsement or recommendation for use.

FOREWORD

When energy and material resources are extracted, processed, converted, and used, the related pollutional impacts on our environment and even on our health often require that new and increasingly more efficient pollution control methods be used. The Industrial Environmental Research Laboratory in Cincinnati (IERL-Ci) assists in developing and demonstrating new and improved methodologies that will meet these needs both efficiently and economically.

This report presents the findings of an evaluation of a secondary hooding system for the capture of fugitive air pollutant emissions from primary copper smelter converters. The converter operation is the most significant source of fugitive emissions in the copper smelter. These emissions contain sulfur dioxide and particulates (total suspended particulates, inhalable particulate matter, and trace metals including arsenic, lead, antimony, bismuth, and selenium). They are emitted within the smelter, exposing the worker, and exit the smelter through roof ventilation resulting in fumigation of the areas close to the smelter. A number of approaches to the control of these emissions have beeen attempted by industry with unsatisfactory results. The major barrier to the development of an acceptable secondary hood has been the inability to design a system capable of permitting crane and ladle access while simultaneously providing for reasonably effective capture of fugitive emissions. This application of the air curtain secondary hooding system has successfully overcome this barrier. The findings of this study will also be useful to other Agency components and the industry in dealing with environmental problems involving fugitive emissions capture. The Nonferrous Metals and Minerals Branch of the Industrial Pollution Control Division should be contacted for any additional information desired concerning this program.

David G. Stephan
Director
Industrial Environmental Research Laboratory
Cincinnati

ABSTRACT

This report presents the results of tests conducted to evaluate the effectiveness of a full-scale air curtain capture system installed on a primary copper smelter for capture of low level fugitive particulate, including trace metals, and sulfur dioxide. The test work was performed onsite at ASARCO's Tacoma Smelter on the first domestic full-scale prototype system, resulting in the first published evaluation of a full-scale fugitive capture system based upon the air curtain approach as applied to a primary copper converter.

The installation of the air curtain hooding system has permitted a quantitative approach to the direct measurement of the fugitive emissions for the first time. In this program, the fugitives captured by the air curtain were measured at a downstream sampling point in the exhaust side of the air curtain system during the various portions of the converter cycle. Emission factors were established for sulfur dioxide, filterable particulate (Method 5), inhalable particulate, and selected trace elements.

This report is given in two volumes. The first volume contains an overview of procedures, major findings, and conclusions. The second volume contains raw field data.

CONTENTS

Page

Foreword iii
Abstract iv
Figures vii
Tables ix
Acknowledgment xiv

1. Introduction and Summary 1
    1.1 Introduction 1
    1.2 Capture effectiveness 3
    1.3 Emission characterization 5

2. Process Description 10
    2.1 Converter operation 10
    2.2 Converter emissions 14
    2.3 Air curtain hooding system 15

3. Process Operation and Test Log 19

4. Air Curtain Capture Efficiency 27
    4.1 Tracer gas mass balance 27
    4.2 Opacity 64
    4.3 Visual observations 70

5. Emission Factor Development 85
    5.1 Sulfur dioxide (SO_2) 86
    5.2 Filterable particulate emissions 98
    5.3 Filterable and gaseous arsenic 103
    5.4 Particle size results 108
    5.5 Trace metals--antimony, bismuth, cadmium, lead, and selenium 153
    5.6 Process samples 155

6. Quality Assurance 157

7. Sampling and Analytical Plan 169
    7.1 Sample location 169
    7.2 Velocity and gas temperature 169
    7.3 Molecular weight 172

CONTENTS (continued)

Page

7.4 Particulate/arsenic 172
7.5 Particle size distribution 173
7.6 Sulfur dioxide manual method 174
7.7 Continuous monitoring for sulfur dioxide 175
7.8 Sulfur hexafluoride tracer as an indicator of hood capture efficiency 176
7.9 Opacity 177

Appendices

A Opacity and Transmissometer Data, Velocity and Particulate Loading Calculations, Particle Size Calculations, and SO_2 Concentration Calculations A-1
B Field Data B-1
C Laboratory Results C-1
D Sampling and Analytical Procedures D-1
E Calibration Procedures and Results E-1
F Quality Assurance Project Plan F-1
G Project Participants G-1
H Visual Observation Logs H-1
I Interlaboratory Comparison Study of Proposed Method 108 I-1

FIGURES

Number		Page
1	Typical Peirce-Smith Primary Copper Converter	11
2	Converter with Primary Hood	12
3	Copper Converter Operation	12
4	Converter Air Curtain/Secondary Hooding System (No Scale)	16
5	Air Curtain Control System	17
6	SF_6 Concentration Profile	35
7	Graphical Presentation of Air Curtain Tracer Injection	39
8	Injection Point Matrix Used for Preliminary Tracer Gas Tests	40
9	Velocity Profile for Low Flow Condition	49
10	Velocity Profile for High Flow Condition	49
11	SF_6 Injection Locations	51
12	Tracer Injection Matrix	52
13	Comparison of Hood Collection Efficiency and Matrix Port Injection	54
14	Comparison of Hood Collection Efficiency and Matrix Point Injection	54
15	Average Opacity vs. Converter Operation	68
16	Individual Particle Size Distributions for the Charging Mode Sample Runs	115
17	Individual Particle Size Distributions for the Skimming Mode Sample Runs	116

FIGURES (continued)

Number		Page
18	Individual Particle Size Distributions for the Blowing Mode Sample Runs	117
19	Average Particle Size Distribution for the Charging Mode	119
20	Average Particle Size Distribution for the Skimming Mode	120
21	Average Particle Size Distribution for the Blowing Mode	121
22	Comparison of Elemental Concentrations for the Charging Mode (Run Nos. PSMC-1, -2, -3)	134
23	Comparison of Elemental Concentrations for the Charging Mode (Run Nos. PSMC-4, -5)	135
24	Comparison of Elemental Concentrations for the Skimming Mode	143
25	Comparison of Elemental Concentrations for the Blowing Mode	151
26	Audit Report Dry Gas Meter (Meter Box No. FB-4)	160
27	Audit Report Dry Gas Meter (Meter Box No. FB-5)	161
28	Audit Report Dry Gas Meter (Meter Box No. FB-7)	162
29	Audit Report Dry Gas Meter (Meter Box No. FB-9)	163
30	Audit Report SO_2 Analysis	165
31	No. 4 Converter Air Curtain Exhaust Duct Sample Site	171
32	Transmissometer Installation on Secondary Hood	178

TABLES

Number		Page
1	Converter Cycle and Tests Conducted	20
2	Sample Matrix	21
3	Test Log	22
4	Summary of Preliminary Tracer Recovery Efficiency Data	34
5	Summary of Single Point Tracer Recovery Efficiency Tests	36
6	Summary of Tracer Recovery Efficiency at Air Curtain Suction Inlet	37
7	Summary of Tracer Recovery Test Data on Exhaust Side	41
8	Summary of Tracer Recovery Test Data on Jet Side	43
9	Summary of Matrix Area Tracer Recovery Efficiency Data	44
10	Collection Efficiency of SF_6 Within the Air Curtain Matrix Area (December 1982)	45
11	Summary of Volumetric Flow Data	48
12	Tracer Recovery Efficiency Within the Air Curtain Control (Matrix) Area (January 14, 1983)	54
13	SF_6 Collection Efficiency Within the Control (Matrix) Area (January 17, 18, 19, 1983)	54
14	Summary of Tracer Recovery Efficiency for Upper Control Volume	55
15	Summary of Matrix Injection Test Data, 1/14/83	57
16	Summary of Matrix Injection Test Data, 1/17/83	59
17	Summary of Matrix Injection Test Data, 1/18/83	60

TABLES (continued)

Number		Page
18	Summary of Matrix Injection Test Data, 1/19/83	61
19	Summary of Tracer Recovery Efficiency for Lower Control Volume	62
20	Summary of Sample and Analytical Data for Special Injection Point Tests	65
21	Summary of Opacity of Emissions Escaping Air Curtain	68
22	Summary of Visual Observations of Hood Capture Effectiveness by Converter Event	70
23	Summary of Visual Observations Logs by Event	74
24	SO_2 Emission Summary	88
25	SO_2 Emission During Matte Charges	89
26	SO_2 Emission During Slag Skims	90
27	SO_2 Emission During Copper Pour	92
28	SO_2 Emission During Cold Additions	93
29	SO_2 Emission During Standby, Blow, and Idle Modes	94
30	SO_2 Emission During Converter Rolls	96
31	SO_2 Emission During Upset Conditions	97
32	Comparison of SO_2 Emission During Normal and Upset Primary Hood Operation	99
33	Summary of Filterable Particulate Emissions Data	100
34	Particulate Emission Factor Development	103
35	Summary of Filterable and Gaseous Arsenic Emission Data	104
36	Development of Arsenic Emission Factors	107
37	Particulate Loading and Impactor Flow Rate Data for the Particle Size Runs	109

TABLES (continued)

Number		Page
38	Summary of Filterable Particulate Concentrations for the Particle Size Runs	111
39	Summary of Filterable Particulate Emission Rates for the Particle Size Runs	112
40	Summary of Inhalable Particulate Concentrations During the Particle Size Runs	122
41	Summary of Inhalable Particulate Emission Rates During the Particle Size Runs	123
42	Summary of Arsenic Concentration and Mass Emission Rate for the Particle Size Runs for the Charging Mode	127
43	Summary of Selenium Concentration and Mass Emission Rate for the Particle Size Runs for the Charging Mode	128
44	Summary of Cadmium Concentration and Mass Emission Rate for the Particle Size Runs for the Charging Mode	129
45	Summary of Antimony Concentration and Mass Emission Rate for the Particle Size Runs for the Charging Mode	130
46	Summary of Lead Concentration and Mass Emission Rate for the Particle Size Runs for the Charging Mode	131
47	Summary of Bismuth Concentration and Mass Emission Rate for the Particle Size Runs for the Charging Mode	132
48	Summary of Arsenic Concentration and Mass Emission Rate for the Particle Size Runs for the Skimming Mode	136
49	Summary of Selenium Concentration and Mass Emission Rate for the Particle Size Runs for the Skimming Mode	137
50	Summary of Cadmium Concentration and Mass Emission Rate for the Particle Size Runs for the Skimming Mode	138

TABLES (continued)

Number		Page
51	Summary of Antimony Concentration and Mass Emission Rate for the Particle Size Runs for the Skimming Mode	139
52	Summary of Lead Concentration and Mass Emission Rate for the Particle Size Runs for the Skimming Mode	140
53	Summary of Bismuth Concentration and Mass Emission Rate for the Particle Size Runs for the Skimming Mode	141
54	Summary of Arsenic Concentration and Mass Emission Rate for the Particle Size Runs for the Blowing Mode	145
55	Summary of Selenium Concentration and Mass Emission Rate for the Particle Size Runs for the Blowing Mode	146
56	Summary of Cadmium Concentration and Mass Emission Rate for the Particle Size Runs for the Blowing Mode	147
57	Summary of Antimony Concentration and Mass Emission Rate for the Particle Size Runs for the Blowing Mode	148
58	Summary of Lead Concentration and Mass Emission Rate for the Particle Size Runs for the Blowing Mode	149
59	Summary of Bismuth Concentration and Mass Emission Rate for the Particle Size Runs for the Blowing Mode	150
60	Comparison of the Total Particulate Concentration Measured by the Particle Size Runs to the Elemental Concentrations	152
61	Summary of Trace Metal Emission Results	154
62	Arsenic and Lead in Process Samples	156
63	Field Equipment Calibration	159
64	Example Blank Filter and Reagent Analysis	164

TABLES (continued)

Number		Page
65	Arsenic and Selenium QA Audit	164
66	Comparison of Manual and CEM SO_2 Results	166
67	Summary of SF_6 Background Analysis	167
68	Sample Matrix	170

ACKNOWLEDGMENT

Overall project coordination and test supervision were performed for the U.S. EPA by Messrs. John Burckle and Al Vervaert of the EPA's Industrial Environmental Research Laboratory (Cincinnati) and Office of Air Quality Planning and Standards. Mr. Frank Clay, also of the Office of Air Quality Planning and Standards, coordinated the transmissometer portion of this project. Messrs. Melvin Belich and Robert Budd represented ASARCO during the test program and coordinated the scheduling and process operations. Mr. James Nolan of the Puget Sound Air Pollution Control Authority also observed the test program. Mr. Mark Hooper assisted in developing and coordinating the project for Region X. Messrs. Chuck Bruffey and Thomas Clark were the PEDCo project managers. Principal authors were Messrs. Chuck Bruffey, Paul Clarke, Thomas Clark, and Mark Phillips.

SECTION 1

INTRODUCTION AND SUMMARY

This report presents the results of tests conducted to evaluate the effectiveness of a full-scale air curtain capture system installed on a primary copper smelter converter for capture of low-level fugitive particulate, including trace metals and sulfur dioxide. The test work was performed onsite at ASARCO's Tacoma smelter on the first domestic full-scale prototype system, resulting in the first published evaluation of a full-scale fugitive capture system based upon the air curtain approach as applied to a primary copper converter.

1.1 INTRODUCTION

Copper converting is a batch operation conducted in two stages to convert copper matte produced in a smelting furnace into blister copper. The Peirce-Smith converter, used in all but one U.S. smelter, is acknowledged to be the major source of fugitive emissions in the smelter. These fugitive emissions first enter the workplace and, because they are present in relatively high concentrations, are considered hazardous to worker health. They are emitted from the smelter at relatively low elevations through roof monitors and other openings in the building. These emissions cause deterioration of the air quality and are believed to cause adverse health impacts on the general population suffering prolonged exposure. While some dispersion and dilution of the fugitives occur upon leaving the smelter workplace, the ambient exposure concentrations are high relative to a well-dispersed emission from a tall stack.

A number of approaches to the control of these emissions have been attempted by industry with unsatisfactory results. The major barrier to the development of an acceptable secondary hood has been the inability to design a system capable of permitting crane and ladle access while simultaneously providing for reasonably effective capture of fugitive emissions. The air curtain principle offers an alternative approach for the capture of the fugitives without interference with the normal crane-ladle operation.

The air curtain is formed by blowing air from a supply plenum or a row of nozzles which is especially designed to form an air sheet, or curtain, with as little turbulence as possible. This curtain is directed over the open space, well above the converter, which permits crane access. On the opposite side of the space, the curtain and entrained air are captured by an exhaust system. Fumes which rise from the source are directed into the suction plenum by the curtain. Air is also pulled into the curtain from both above and below. Since all air flow is inward, into the curtain, there is no opportunity for fumes to escape a properly designed and operated curtain, and a high capture efficiency is achievable.

Because the fugitive emissions are captured by the air curtain and are collected by ducting, it becomes possible to completely characterize these emissions in order to provide actual engineering data for design. This is of significant importance because in the past it has been possible to estimate only very approximately, the quantity and composition of the converter fugitives for defining control strategies and needs, making actual design and selection of equipment somewhat risky.

The test program was designed to achieve two major objectives: estimation of the effectiveness for capture of the converter fugitives not controlled by the primary hood and characterization of the captured fugitives by the "quasi-stack" method.

41.2 CAPTURE EFFECTIVENESS

The effectiveness of capture was evaluated using three techniques.

- Mass balance using sulfur hexafluoride as a tracer
- Opacity of emissions escaping through the slot
- Observation of visible emissions

1.2.1 Tracer Experiments

Sulfur hexafluoride was injected into various points within the air curtain control volume, defined by the top, sides, and front of the air curtain structure and the converter and primary hood which formed the back of the structure. The tracer experiments were of two types, those in which the tracer was injected into the air curtain volume above the converter (the upper portion of the air curtain control volume) and those in which the tracer was injected below the plane of the top of the converter and near the front of the air curtain side walls (the lower portion of the air curtain control volume).

1.2.2 Opacity Measurements

An opacity monitor was mounted on the top of the air curtain below the crane rail in order to obtain information on emissions escaping capture by the air curtain and passing through the slot. A total of 86 discrete observations were made with results ranging from 2 to 54 percent opacity for the major converter operations. During slag and finish blowing, no attenuation of the monitor's light beam was observed resulting in zero percent opacity. The instrument output range was 0 to 20 milliamps which corresponds with 0 to 98.4 percent opacity. The relationship of the instrument output to opacity was exponential, with 5 milliamps corresponding with 50 percent opacity. Therefore, emissions during the test program were in the lower end of instrument response. No correlation between opacity and capture effectiveness could be made because of emissions from the front of the air curtain system.

1.2.3 Visual Emissions

Two observers visually monitored the air curtain capture effectiveness by noting the location, approximate opacity, duration, and significance of visible emissions. Their estimates of capture efficiency were within 5 to 10 percent with only a few exceptions. Most variability in the estimates occurred for those operations involving rapid evolution of emissions over a short period, such as roll-in, roll-out, and pouring. The average of the observations for the various converter operating conditions displayed the same trends as the tracer experiments and indicates a reasonably effective capture of fugitives.

1.2.4 Conclusions

In summary, the visual observation and tracer recovery data indicated that the fugitive emissions capture effectiveness of the secondary hood is greater than 90 percent, averaging about 94 percent overall. The capture effectiveness during converter roll-in and roll-out and slag skimming operations is more variable than other converter modes since fugitive emissions generated during these events are more dependent upon converter and crane operations. It is also evident that capture efficiencies of 90 percent or better are achievable for these events under the proper crane and converter operating conditions to minimize fume "spillage" into the converter aisle.

Thermal lift plays a significant role in increased collection efficiencies for fume generated in the lower portion of the control area. Also, the lower tracer recovery efficiencies for the various converter roll-out modes are indicative of fume "spillage" outside of the control area.

It is believed that no practical correlation can be made between opacities recorded by the observers and the transmissometer. The transmissometer was mounted perpendicular to the longitudinal axis of the slot, whereas the position of the visual observers was such that their view was parallel to the longitudinal axis of the slot, which resulted in a considerably longer path length through the escaping emissions. The apparent opacity increases as the path length through the emissions increases. Also, when positioned in front of the converter, the overhead crane interfered with visual observations above the slot area.

1.3 EMISSION CHARACTERIZATION

The capture of the fugitive emissions by the air curtain permitted their characterization by the "quasi-stack" method using standard EPA stack sampling techniques in the exhaust duct. The converter is a batch operation comprised of a number of steps requiring the roll-out, charge or pour, and roll-in of the converter. The generation of fugitive emissions occurs primarily during these operations because the primary hood is raised and the draft to the primary hood is closed off to prevent dilution of the strong sulfur dioxide gases processed in the acid or liquid SO_2 plants. During the blowing phase of the operation, a small amount of fugitives are seen to occasionally escape the primary hood. Because of the large number of different operations (i.e., roll-in and roll-out; charging of matte, anode slag, various reverts, and scrap; slag skims; copper pours; and blowing and holding), we recognized that we could not characterize emissions for each individual condition. Therefore, the test was structured to provide composite data for selected operations.

The Emission Characterization section summarizes emission test results for sulfur dioxide, filterable particulate, particle size distribution (inhalable particulate), and trace metals including filterable and gaseous arsenic in the exhaust stream of the secondary hood, or air curtain system. Results for each pollutant are reported and where applicable, emission factors have been developed for overall converter operation and specific operational modes (charging, skimming, and blowing).

1.3.1 Sulfur Dioxide Emissions

The concentration of sulfur dioxide in the air curtain exhaust was monitored by a continuous emission monitor. More than 470 individual data points were utilized to characterize the converter emissions, resulting in an emission factor of 3.0 kg/Mg of blister copper for the total converter cycle and 0.1 kg/Mg when the converter was in the blowing or standby mode.

1.3.2 Particulate Emissions

Total filterable particulate was sampled using EPA Method 5. For each of the three converter cycles, a sample was taken compositing all emissions over the total converter cycle by traversing the exhaust duct. Single point sampling was used to obtain a composite sample representing the emissions during those converter operations where the primary hood was open, i.e., charging or discharging. The emission factor for the total cycle was calculated as 0.45 kg/Mg of blister copper for the total cycle and 0.43 kg/Mg for those operations where the converter was rolled out.

1.3.3 Particle Size

Particle size samples were taken by impactors to define the particle size distribution within the inhalable particulate range of 10 μm and less by aerodynamic size. The tests were conducted at points of average velocity simultaneously with, but at points different from, those at which the particulate samples were taken. The sampling was conducted in such a manner so as to provide a composite over a converter cycle for each major converter operating condition, i.e.:

- Charging mode which consists of all additions to the converter such as matte, anode slag, and cold additions such as scrap
- Skimming mode, which consists of slag skimming and pouring of blister copper
- Blowing mode, which consists of all operating conditions during which the primary hood is closed, including the slag, cleanup, and finish blows

The average particle size distribution for each mode indicates that: 1) the bulk of the particulate (88 to 98%) is above 10 μm during blowing; 2) the particulate is composed of both fine and coarse particulate (70 to 84% less than 10 μm) during charging; and 3) the particulate during skimming and pouring is predominantly (86 to 92% less than 10 μm) in the inhalable range.

The cumulative particulate emission rates were obtained by calculation from the particulate concentration and volumetric flow rates sampled by the impactors for the total, less than 10-μm, less than 5-μm, and less than 2.5-μm size fractions.

1.3.4 Trace Metal Emissions

Arsenic, emitted in the form of arsenic trioxide, was measured to determine both the filterable particulate and gaseous emission rates. The samples were obtained from the same Method 5 sampling trains used for total particulate with the impinger solutions modified for arsenic removal (Method 108). The filterable arsenic fraction represents material collected in the sample probe and on the filter, both of which were heated to approximately 121°C (250°F). The gaseous arsenic fraction represents material that passed through the heated filter and condensed or was trapped in the impinger section of the sample train, which was maintained at a temperature of 20°C (68°F) or less. In retrospect, the sampling train should have been operated at the temperature of the stack gas, i.e., 15° to 30°C, to prevent revolatilization of arsenic trioxide and passage through the filter. Should revolatilization occur, the amount of arsenic reported as gaseous will be increased, which could lead to a false conclusion regarding the amount which could be removed by dry collectors.

During Test 2, the gaseous arsenic concentration was considerably greater than in the other tests. During this test, the loss of draft in the primary hood caused by operational problems at the chemical plant resulted in frequent releases of smoke and fumes from the primary hood. Significant quantities of heavy smoke escaped the primary hood systems, and much of these emissions were captured by the secondary hood. Sampling continued throughout these intermediate upsets, but was finally stopped when the air curtain control system became overwhelmed by continuous and heavy emission discharge from the primary hood. Therefore, it is reasonable to conclude that fugitive emissions generated by the malfunctioning primary hood draft contributed to the higher arsenic concentrations observed during this second cycle test.

1.3.5 Conclusions

The bulk of the fugitive sulfur dioxide emissions (over one-half) were emitted during those converter operations involving the rolling in or out of the converter and the charging of cold additions, particularly anode slag. The remaining operations in order of significance were matte charging; slag skimming; and copper pouring and blowing, including standby and idle. The results of the total particulate sampling indicated that the bulk of the fugitive particulate emissions occur during those operations occurring when the converter is charging or discharging. This suggests that the primary hood system is quite effective in preventing the escape of emissions during blowing.

The particulate size information leads to the conclusion that the bulk (90%+) of the fugitive particulate emitted during blowing is greater than 10 µm while that emitted during the charging or discharging is predominantly (70 to 90%) in the inhalable range. Emissions which occurred during a process upset in the blowing mode exhibited an increase in the proportion of emissions in the fine (less than 2.5 µm) particle range, in addition to the increase in total loading.

The trace metals contained in the particulate emissions comprise an appreciable portion of the total, some 12 to 40 percent by weight for charging and pouring, but only a small part (5%) during blowing. The bulk of the trace elements emitted in the fugitives tends to occur in the inhalable range with a very considerable contribution from the fine (less than 2.5 µm) range.

The trace metal emissions were dominated by arsenic and lead which are present in high quantities in the concentrate and carry through to the matte which is processed in the converter. The potential for trace metal fugitive emissions is then greatest during the charging of matte followed by the charging of reverts, scrap, matte skimming, copper pouring, and finally blowing. Because of the greater variability of the trace element content of the feed materials, the content of the emissions during charging is the most variable, followed by slag skimming and then copper pouring.

SECTION 2

PROCESS DESCRIPTION

Copper converting is a batch operation conducted in two stages. Its purpose is to convert copper matte produced by a smelting furnace [a complex mixture of copper sulfide (Cu_2S), ferrous sulfide (FeS), and trace elements] into blister copper. In the first stage, iron removal is accomplished by blowing air through the molten matte to oxidize the ferrous sulfide to ferrous oxides and eliminate sulfur as SO_2. These oxides combine with the silica flux which is added to the molten bath to produce a molten iron silicate slag that is periodically skimmed from the furnace. In the second stage, the air blowing is continued to oxidize the copper sulfides to form blister copper and SO_2. This blister copper contains about 98.5 to 99.3 percent copper, 0.3 percent sulfur, and some dissolved oxygen and trace metal impurities.

2.1 CONVERTER OPERATION

The Peirce-Smith converter tested (designated No. 4) is a horizontal, refractory-lined steel cylinder [4 x 9 meters (13 x 30 feet)] with an opening in the center (called the converter mouth). The converter is mounted on rollers so it can rotate through an arc of about 120 degrees from the vertical. Compressed air or oxygen-enriched air is supplied through a header along the back of the converter and passes through a horizontal row of openings (tuyeres) in the shell into the interior. A typical Peirce-Smith copper converter is illustrated in Figure 1.

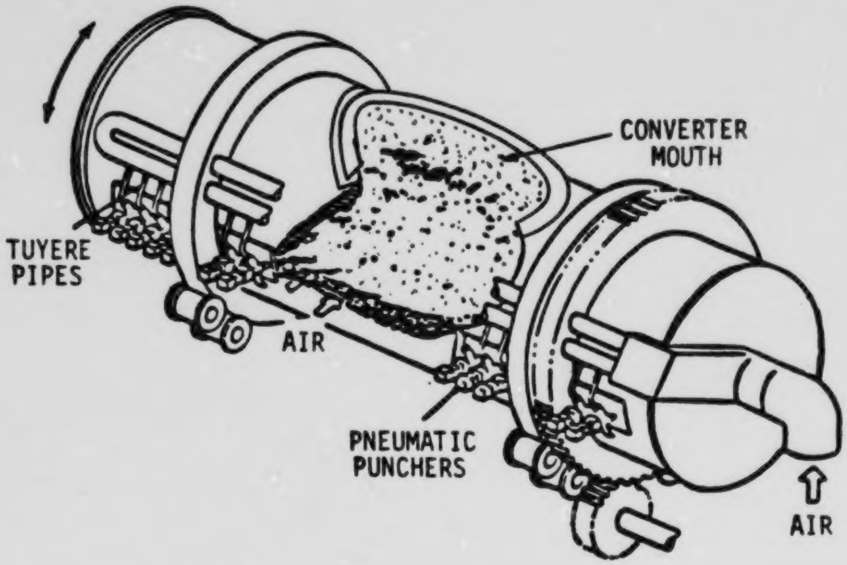

Figure 1. Typical Peirce-Smith primary copper converter.

The copper converting process is a batch operation. The complete cycle is composed of several operations, i.e.: charging of matte, reverts, anode slag, and scrap in various portions; the slag blow; slag skimming; cleanup blow; the finish blow; and finally the pouring of blister copper which is subsequently transferred to the anode furnace for processing to anode copper. During the blowing portion of this cycle, the off-gas is rich in SO_2. This gas is captured by a primary hood which covers the mouth of the converter during blowing (Figure 2).

Molten matte is charged through the converter mouth by ladles carried by overhead cranes. During charging, the converter is rotated to bring the converter mouth to an angle of about 60 degrees from the vertical (as shown in Figure 3). The

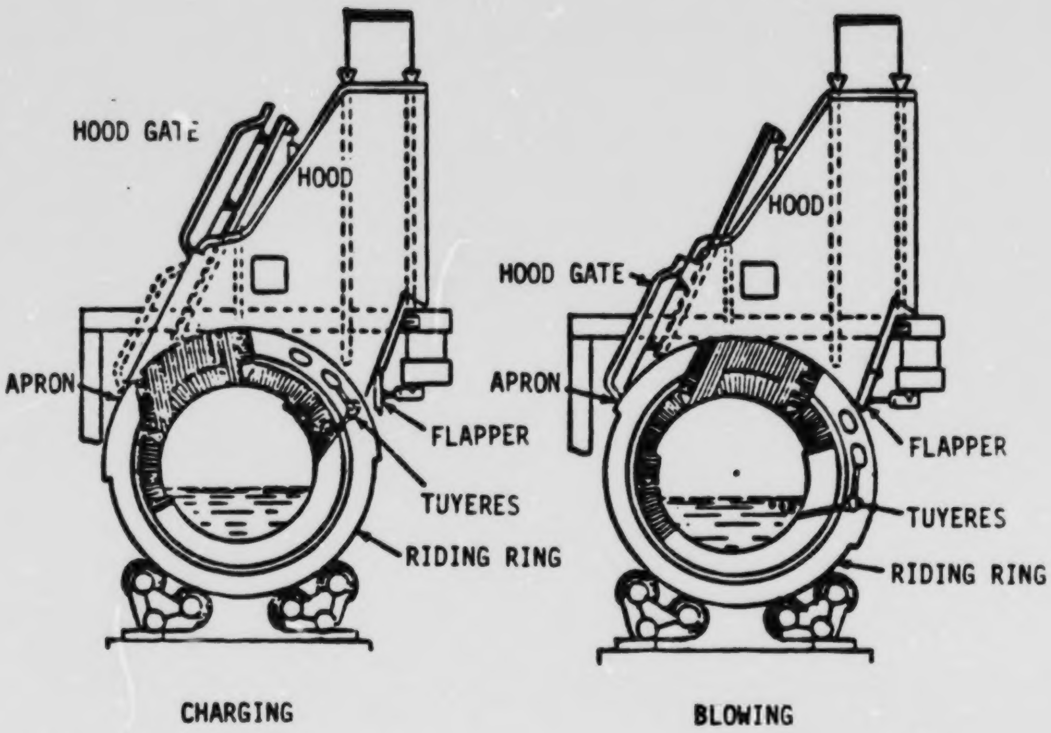

Figure 2. Converter with primary hood.

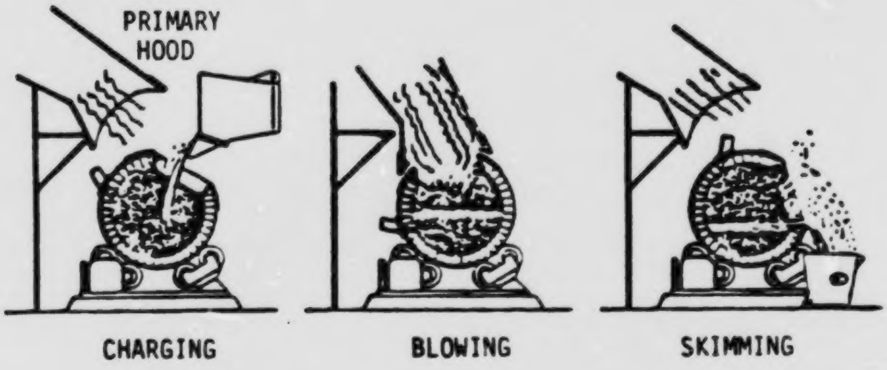

Figure 3. Copper converter operation.

ladles of matte, which are poured through the mouth of the converter, fill it about halfway. Silica fluxing materials are also charged through chutes and conveyor belts into the side of the converter. When the converter is in the charging position, the tuyeres are above the level of the matte. After charging, air or oxygen-enriched air is supplied under pressure to the tuyere line, and blowing commences. The converter is then rotated, which swings the mouth to the vertical and submerges the tuyeres to a depth of 6 to 24 inches below the surface of the matte. The primary hood is then lowered over the mouth of the converter. Emissions generated during blowing are captured by the primary hood and are then routed to the SO_2 recovery plant. The primary hood operates only while air is being blown through the converter tuyeres.

The blowing continues until a substantial layer of slag has been formed in the converter. The primary hood is raised and the converter is again rotated, which swings the mouth through an arc of about 120 degrees from the vertical and raises the tuyere line above the surface of the molten bath. The air supply to the tuyere line is shut off, and the blowing is discontinued. Slag is skimmed or poured into a ladle, and is recycled to the reverberatory furnace for recovery of entrained copper matte. The converter is then returned to the charging position, and fresh matte, fluxing materials, and cold supplements (such as smelter reverts) are added to bring the converter charge back to the working level. The converter is rotated again to the vertical position, the primary hood lowered, and blowing is resumed.

This process is repeated until a charge of copper sulfide (white metal) accumulates in the converter and fills it to the working level. At this stage, the copper blow or finish blow begins. During this portion of the converter operating cycle, the copper sulfide is oxidized and forms SO_2 and blister copper. On completion of the copper blow, the converter contains only metallic copper (blister). The converter is rotated to the pouring or skimming position and the blister copper is poured into ladles for transfer to the anode furnace. The emptied converter is then charged with fresh matte and fluxing materials, and the converting cycle is repeated.

The copper converting process is autogenous; sufficient heat is produced by the oxidation of sulfur to maintain the necessary operating temperature of 1200° to 1260°C (2200° to 2300°F). Consequently, no fuel or other source of heat energy is required. More heat is released within the converter during the slag blow than during the copper blow. The oxidation of one pound of ferrous sulfide according to the following reaction releases about 2742 kJ (2600 Btu):

$$2FeS + 3O_2 + SiO_2 \rightarrow 2FeO \cdot SiO_2 + 2SO_2$$

while the oxidation of one pound of cupric sulfide according to the following reaction releases only about 633 kJ (600 Btu):

$$Cu_2S + O_2 \rightarrow 2Cu + SO_2$$

Thus, the amount of heat released during a slag blow is more than sufficient to keep the bath in a molten state and compensate for heat losses. Converter operators must control the converter temperature to prevent damage to the refractory lining during the slag blow. Smelter reverts and copper scrap are charged to the converters to lower the converter temperature generated by the excessive heat being released.

2.2 CONVERTER EMISSIONS

As gases laden with dust and fumes escape from the converter mouth, they are captured by a large gas collection system (primary hooding system). Room air enters this system through a gap between the hood and converter and water is sprayed into the duct to cool the gases. The total process gas stream passes through a series of cyclones and two fans and is then divided and sent to one of two gas cleaning systems consisting of electrostatic precipitators, spray chambers, and packed and open scrubbing towers. The gases are then ducted either to an SO_2 recovery plant or to a single-contact sulfuric acid plant.

When the converter is rolled out for skimming and charging, the gate on the primary hood (see Figure 2) is moved up and away from the mouth to provide clearance for the overhead crane and ladle. The injection of blowing air continues until the molten bath level is below the tuyeres to prevent the matte from entering the tuyeres and causing them to freeze. Significant amounts of off-gases from the hot bath escape the primary hood system during this period. (When the blowing air is turned off, the primary hood draft also shuts off.) These emissions (fugitive emissions) usually are greater when cold material such as scrap is charged. Before the converter is rolled back to the blowing position, the air is turned on again, which causes the resumption of significant emissions.

The most significant fugitive emissions from a converter are generated during the converter roll-out and roll-in modes, charging (including cold additions), slag skimming, and blister copper pouring. These emissions consist primarily of particulate matter and sulfur dioxide (SO_2). Fumes present in the gases include particulate oxides of arsenic, antimony, and lead, metallic sulfates, and sulfur trioxide (SO_3). At the ASARCO plant, the fugitive emissions are captured by an air curtain hooding system which is described below.

2.3 AIR CURTAIN HOODING SYSTEM

An air curtain is a horizontal moving "sheet" of air that extends across an open space and decreases the passage of gases on one side of the curtain to the other side. The air curtain is created by blowing compressed air through a slot or nozzle. The objective is to achieve absolutely uniform and parallel movement of the air sheet with little or no turbulence. On the opposite side of the space, the moving air sheet is captured by a suction plenum and air exhaust system.

Figures 4 and 5 illustrate the air curtain as applied to the No. 4 Converter. The curtain directs fumes rising from the

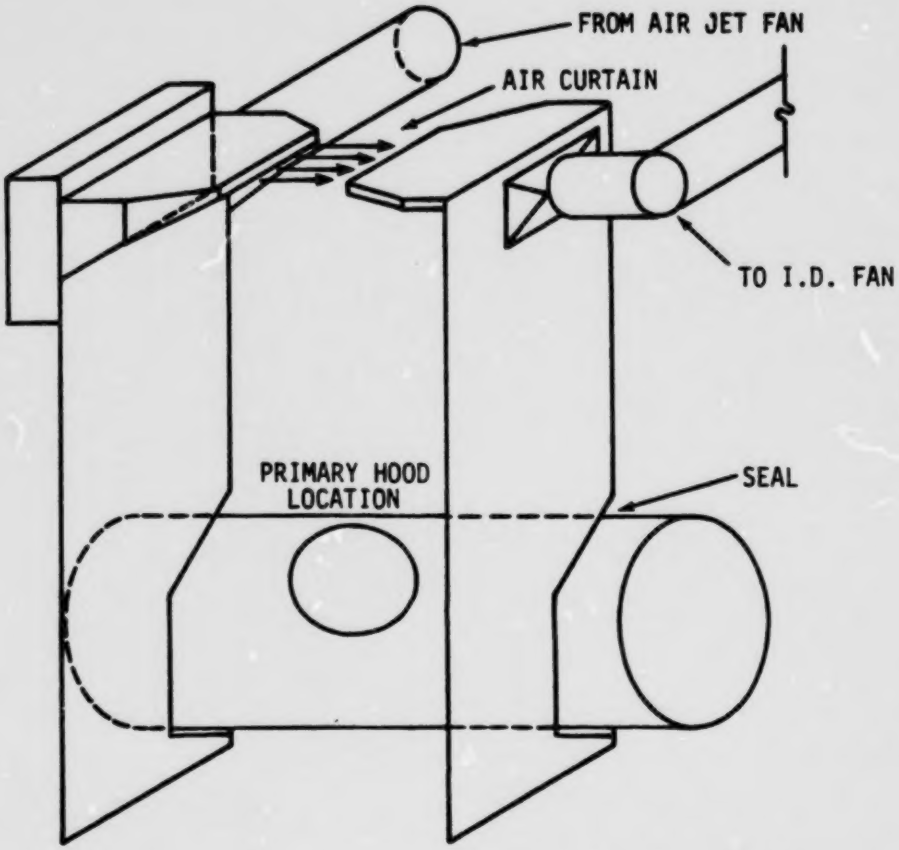

Figure 4. Converter air curtain/secondary hooding system (no scale).

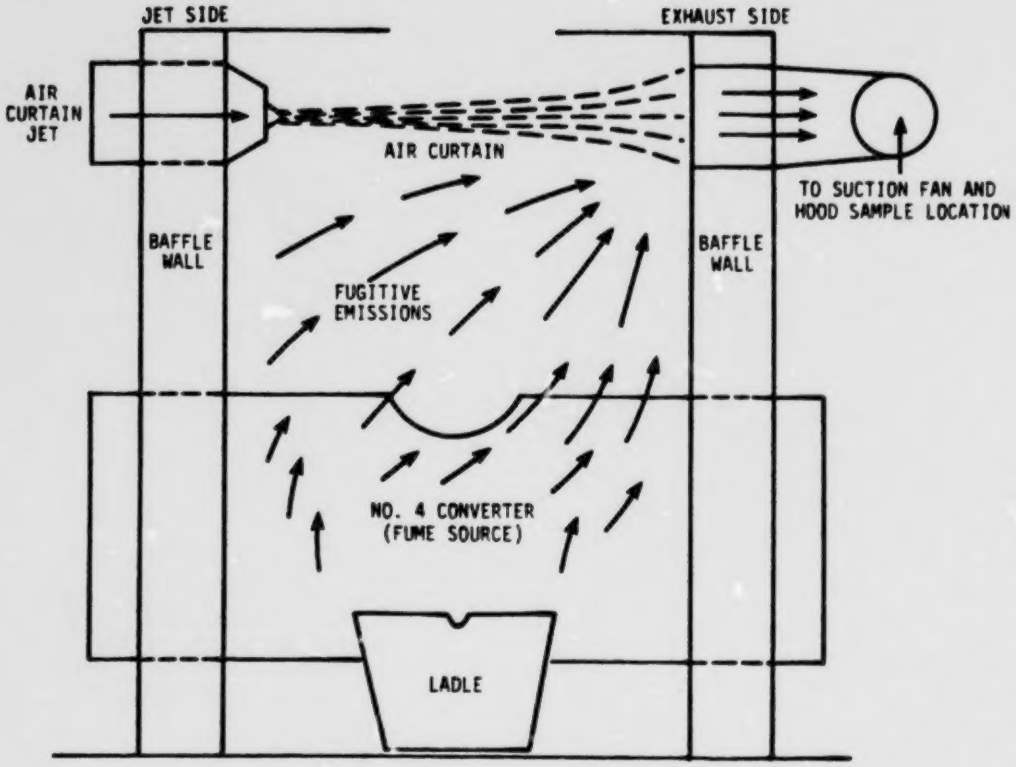

Figure 5. Air curtain control system.

source into the suction plenum. Room air is also pulled into the curtain from both above and below. Because most fumes cannot penetrate the curtain, they are collected by the suction plenum. The collected emissions then pass through a suction fan, an electrostatic precipitator for particulate removal, and finally are released to the atmosphere through the main stack.

Air volume control for the system is regulated automatically by dampers in the air curtain jet, the 1.5-m (5-ft) exhaust duct, and the induced-draft fan. The dampers are manually set for a predetermined exhaust-side flow and, when placed in the automatic control position, are activated by movement of the primary hood and converter. When the primary hood is lifted and the converter is rolled out, the system switches to a high flow condition to control the heavy amount of fugitive emissions generated during roll-out activities (matte charging, slag skimming, cold additions, and copper pouring). At the completion of the converter roll-out activities, the converter is rolled in and the primary hood is retracted over the converter mouth. At this point, the system switches to a lower flow condition because fugitive emissions are much lower during the blowing and idling modes.

SECTION 3

PROCESS OPERATION AND TEST LOG

This section summarizes converter operations relative to specific testing activities conducted from January 18 through 22, 1983.

The Test Plan for this project called for the evaluation of a total of four complete converter cycles and certain segments of each cycle. Production curtailments due to poor meteorological conditions and operational problems with the reverberatory furnace and sulfur dioxide recovery plant precluded obtaining data for four complete cycles. Instead, three separate cycle segments were evaluated, as shown in Table 1. Tables 2 and 3 summarize specific sample events and the segments of each converter cycle sampled.

Table 1 shows sequential converter operations from the initial matte charge through the copper finish blow. A complete cycle (from the initial matte charge through the copper pour) normally takes about 12 hours. Because of the previously mentioned production curtailments, however, converter cycles were frequently interrupted and seldom completed within the 12-hour time frame during the period of testing activities.

As Table 1 shows, each converter cycle tested followed the same basic format: each cycle began with the matte being charged, followed by a series of slag blows, slag skims, and material additions. This pattern was continuous through the cleanup blow. The only difference between individual converter cycles was the variation in the quantity and type (quality) of the materials charged to the converter. This variation affected the amount of slag produced, which is a function of the purity of the material charged. It also altered the number of blows required to remove

TABLE 1. CONVERTER CYCLE AND TESTS CONDUCTED

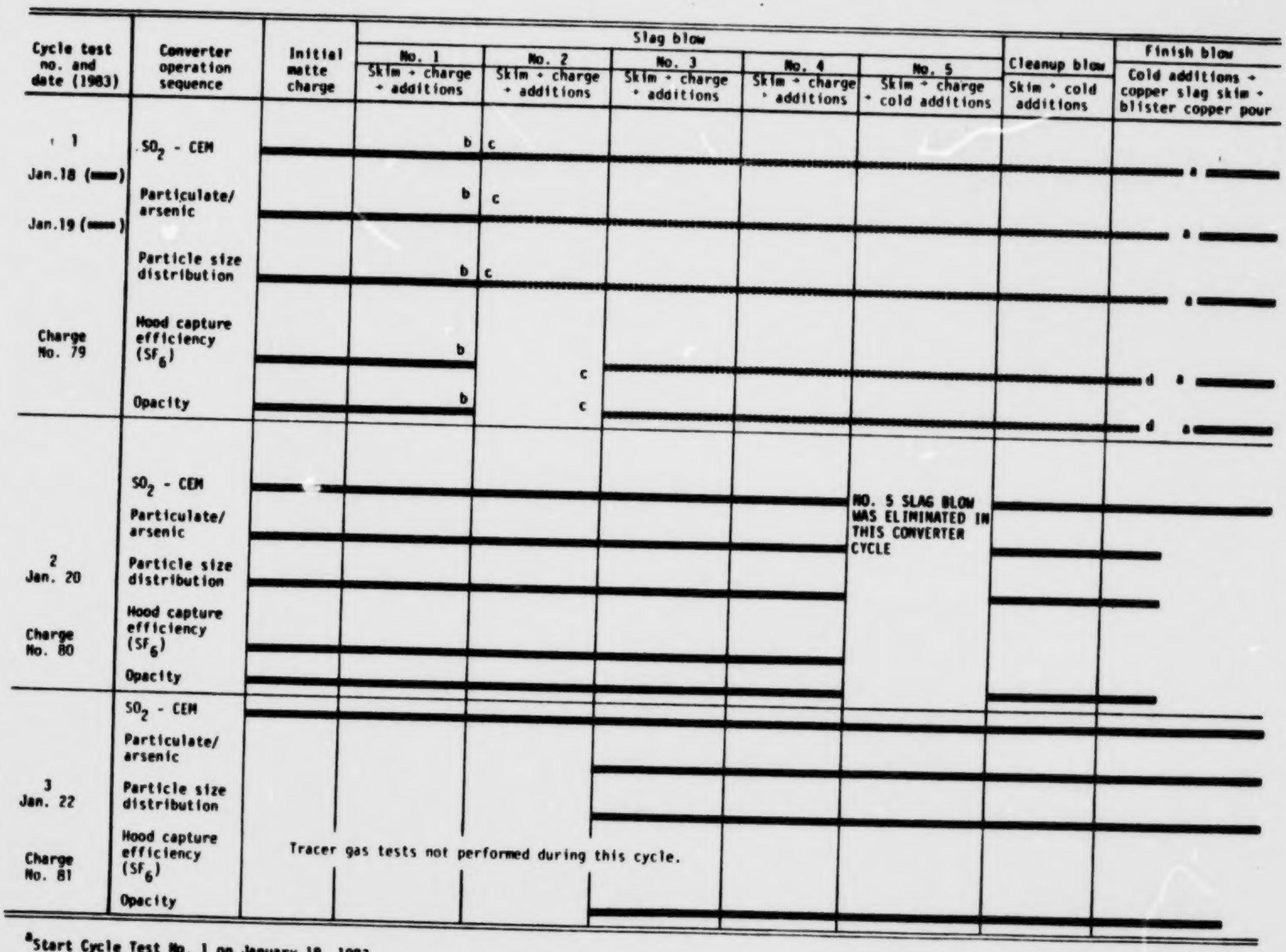

[a] Start Cycle Test No. 1 on January 18, 1983.

[b] End Cycle Test No. 1 on January 18, 1983.

[c] Start Cycle Test No. 1 on January 19, 1983.

[d] End Cycle Test No. 1 on January 19, 1983.

TABLE 2. SAMPLE MATRIX

Sample train type	Run No.	Cycle Test No.	Date (1983)	Segments sampled during the converter cycle							
				Matte charge, No. of ladles tested	Cold additions, No. of ladles tested	Anode and copper slag addition, No. of ladles tested	Slag skim, No. of ladles tested	Slag blows tested	Cleanup blows tested	Finish blows tested	Copper pour, No. of ladles tested
Particulate/arsenic (continuous sampling train)	PATC-1	1	1/18 1/19	14	8	4.50	10.75	4	1	1	10
	PATC-2	2	1/20	14	10[a]	0	9.75	4	1	1	
	PATC-3	3	1/22	4	14[b]	0	7.25	3	1	1	9
Particulate/arsenic specific mode sampling train)	PASM-1	1	1/18 1/19	14	7	4.50	10.75				10
	PASM-2	2	1/20	14	10[a]	0	9.75				
	PASM-3	3	1/22	0	0	0	7.25	0	0	0	0
Andersen Mark III impactor (charging mode)	PSMC-1	1	1/18 1/19	14	1	4.90					
	PSMC-2	1	1/19	2	7						
	PSMC-3	2	1/20	10	4						
	PSMC-4	2	1/20	4	6[a]						
	PSMC-5	3	1/22	4	12[b]						
Andersen Mark III impactor (skimming mode)	PSSS-1	1	1/18 1/19				10.75				10
	PSSS-2	2	1/20				9.25				
	PSSS-3	3	1/22				7.25				
Andersen Mark III impactor with 15-μm precutter (blowing mode)	PSB-1	1	1/18 1/19					4	1	1	
	PSB-2	2	1/20					2			
	PSB-3	2	1/20					1	1	1	
	PSB-4	3	1/22					1	1	1	
SO_2 Continuous monitor		All	1/14- 1/22	Continuous for 1/14 through 1/22							
Secondary hood capture efficiency SF_6 tracer gas		Preliminaries and 1-2	1/14 1/17 1/18- 1/20	X	X	X	X	X	X	X	X
Opacity using a transmissometer		1-3	1/18- 1/22	X	X	X	X	X	X	X	X

[a] Four of the cold additions were blocks of blister.

[b] Seven of the cold additions were blocks of blister.

Reproduced from
best available copy.

TABLE 3. TEST LOG

Cycle Test No.	Date (1983)	Time (24-h)	Converter event	SO_2-CEM	Particulate/ arsenic PATC	Particulate/ arsenic PASM	Particle size distribution			Hood capture efficiency (SF_6)	Opacity
							Blowing	Charging	Skimming		
1	1/18	0802	Copper finish blow	X	X		X				X
		0810	Cold addition (ladle)	X	X					X	X
		0813-0907	Copper finish blow	X	X		X			X	X
		0908-0916	Copper slag skim (1½ ladles)	X	X	X			X	X	X
		0923-1046	Idle	X							X
		1047-1110	Copper finish blow	X	X					X	X
		1111-1212	Blister copper pour (10 ladles)	X	X	X			X	X	X
		1237-1250	Matte charge (3 ladles)	X	X	X		X		X	X
		1254-1259	Copper slag addition (1 ladle)	X	X	X		X		X	X
		1301-1302	Matte charge (1 ladle)	X	X	X		X		X	X
		1306	Anode slag addition (1 ladle)	X	X	X		X		X	X
		1315-1327	Matte charge (2 ladles)	X	X	X		X		X	X
		1341	Copper slag addition (1 ladle)	X	X	X		X		X	X
		1342-1510	Idle	X							X
		1511	Cold addition, shell slag (1 ladle)	X							X
		1513-1545	No. 1 slag blow	X	X		X			X	X
		1545-1558	Slag skim (3 ladles)	X	X	X			X	X	X
		1616-1622	Matte charge (3 ladles)	X	X	X		X		X	X
		1627	Converter on idle until 1/19/83								
1	1/19	0726-0729	Cold addition (1 ladle)		X						X
		0730-0809	No. 2 slag blow	X	X		X				X
		0810-0833	Slag skim (3 ladles)	X	X	X			X		X
		0834-0838	Matte charge (2 ladles)	X	X	X		X			X
		0839-0844	Cold addition, shell slag (2 ladles)	X	X	X		X			X
		0845-0915	No. 3 slag blow	X	X		X				X
		0916-0934	Slag skim (2 ladles)	X	X	X			X	X	X
		0935-0937	Matte charge (1 ladle)	X	X	X		X		X	X
		0938-0941	Cold addition (1 ladle)	X	X	X		X		X	X
		0942-0944	Matte charge (1 ladle)	X	X	X		X		X	X
		0945-1009	No. 4 slag blow	X	X		X			X	X
		1010-1013	Slag skim (1 ladle)	X	X	X			X	X	X
		1014-1029	Cleanup blow	X	X		X			X	X
		1030-1036	Slag skim (1 ladle)	X	X	X			X	X	X
		1037-1126	Idle	X							X
		1127-1135	Cold addition, scrap (2 ladles)	X	X	X		X		X	X
		1143-1229	Copper finish blow	X	X		X			X	X
		1230-1235	Cold addition (2 ladles)	X	X	X		X		X	X
		1236-1316	Copper finish blow	X	X		X			X	X
		1317-1321	Cold addition, scrap (2 ladles)	X	X	X		X		X	X
		1322-1400	Copper finish blow	X	X		X				X
			End Test No. 1								

TABLE 3 (continued)

Cycle Test No.	Date (1983)	Time (24-h)	Converter event	SO_2-CEM	Particulate/ arsenic PATC	Particulate/ arsenic PASM	Particle size distribution			Hood capture efficiency (SF_6)	Opacity
							Blowing	Charging	Skimming		
2	1/20	0820-0947	Matte charge (6 ladles)	X	X	X		X		X	X
		0948-1001	Cold addition, shell slag (2 ladles)	X	X	X		X		X	X
		1002-1003	Matte charge (1 ladle)	X	X	X		X		X	X
		1014-1049	No. 1 slag blow	X	X		X			X	X
		1050-1108	Slag skim (2½ ladles)	X	X	X			X	X	X
		1111-1116	Matte charge (3 ladles)	X	X	X		X		X	X
		1117-1119	Cold addition, shell slag (2 ladles)	X	X	X		X		X	X
		1120-1125	No. 2 slag blow	X	X		X			X	X
		1126-1350	Idle	X							X
		1351-1424	No. 2 slag blow (continued)	X	X		X			X	X
		1425-1447	Slag skim (3 ladles)	X	X	X			X	X	X
		1448-1454	Matte charge (2 ladles)	X	X	X		X		X	X
		1455-1459	Cold addition, shell slag (2 ladles)	X	X	X		X		X	X
		1500-1536	No. 3 slag blow	X	X					X	X
		1537-1553	Slag skim (2 ladles)	X	X	X			X	X	X
		1554-1614	Matte charge (2 ladles)	X	X	X		X		X	X
		1615-1654	No. 4 slag blow	X	X		X			X	X
		1655-1707	Slag skim (2 ladles)	X	X	X			X	X	X
		1708-1732	Idle	X							X
		1733-1755	Cleanup blow	X	X		X				X
		1756-1809	Slag skim (1 ladle)	X	X	X					X
		1810-1814	Cold addition, blister copper (4 blocks)	X	X	X		X			X
		1815-1835	Copper finish blow	X	X		X				X
		1836-1922	Idle	X							X
		1923-2001	Copper finish blow	X	X		X				X
			End Test No. 2								
3	1/22	0907-0911	Cold addition, shell slag (2 ladles)	X	X						X
		0912-0951	No. 3 slag blow	X	X						X
		0952-1009	Slag skim (2½ ladles)	X	X	X			X		X
		1010-1042	Idle	X							X
		1043-1049	Matte charge (2 ladles)	X	X			X			X
		1050-1055	Cold addition, shell slag (2 ladles)	X	X			X			X
		1056-1131	No. 4 slag blow	X	X						X
		1132-1136	Idle	X							X
		1137-1204	Slag skim (3 ladles)	X	X	X			X		X
		1205-1209	Matte charge (2 ladles)	X	X			X			X
		1210-1601	Idle	X							X
		1602-1621	No. 5 slag blow	X	X		X				X
		1622-1630	Slag skim (2 ladles)	X	X	X			X		X
		1631-1700	Idle	X							X
		1701-1715	Cleanup blow	X	X		X				X
		1716-1725	Slag blow (1 ladle)	X	X	X			X		X
		1726-1734	Cold addition, blister copper (5 blocks)	X	X			X			X
		1735-1824	Copper finish blow	X	X		X				X
		1827-1830	Cold addition, scrap wood (1 ladle)	X	X			X			X

TABLE 3 (continued)

Cycle Test No.	Date (1983)	Time (24-h)	Converter event	SO_x-CEM	Particulate/ arsenic PATC	Particulate/ arsenic PASM	Particle size distribution			Hood capture efficiency (SF_6)	Opacity
							Blowing	Charging	Skimming		
		1831-1834	Cold addition, blister copper (2 blocks)	X	X			X			X
		1835-1900	Idle	X							X
		1901-1930	Copper finish blow	X	X		X				X
		1931-2001	Idle	X							X
		2002-2032	Copper finish blow	X	X		X				X
		2033-2034	Cold addition	X	X			X			X
		2035-2109	Copper finish blow	X	X		X				X
		2110-2114	Slag skim	X	X						X
		2115-2116	Cold addition, metal powder and wood (1 ladle)	X	X			X			X
		2117-2207	Copper finish blow	X	X		X				
		2208-2214	Cu slag skim	X	X						
		2215-2302	Idle	X							
		2303-2338	Blister copper pour (9 ladles)	X	X						
			End of Test No. 3								

the slag and, consequently, the length of the converter cycle. During the first and third converter cycles tested, five slag blows were required to make the material in the converter pure enough for the cleanup blow; whereas it took only four slag blows during the second converter cycle tested.

The sulfur dioxide continuous emissions monitoring system (SO_2-CEM) was in operation throughout each of the three cycles evaluated. In fact, the SO_2-CEM commenced sample data collection on January 14 and provided a continuous SO_2 emission characterization for the No. 4 Converter through January 22. The manual emission tests (particulate/arsenic, particle size distribution, tracer capture efficiency, transmissometer and visual observations) were performed during specific converter operations, as shown in Table 1.

Tests for particle size distribution were performed with Andersen Mark III in-stack particle size impactors. Size distribution samples were collected during the converter charging mode (matte and other additions), skimming mode (slag and blister pour), and blowing mode (slag, cleanup, and finish). Table 2 shows the variation in the number of charges, pours, or blows tested during each particle size run. Particle size samples were obtained by compositing samples over several separate charge, pour, or blow periods in order to obtain sufficient loadings on the individual impactor stages.

The preliminary tracer recovery efficiency tests were performed on January 14 and 17. The preliminary runs were designed to provide data relative to tracer recovery efficiency as a function of tracer injection location. These data are summarized in Section 4 of this report. As shown in Tables 1 and 3, the tracer recovery efficiency tests were conducted during most of the operating modes of the first two converter cycles tested. No tracer tests were performed on January 22. On January 20 between 10:15 and 11:30 a.m., the primary hood damper system malfunctioned. During this period, massive emissions escaped the primary hood during the blow mode on several occasions. Opacity measurements were obtained with a transmissometer during the manual emission tests, as shown. Observations of visible emissions were made by the two observers throughout the test period.

Tests for filterable particulate and arsenic were performed with two separate, yet identical, sample trains. One train (designated PATC) was run for the duration of each cycle tested to provide a composite of all emissions over the entire cycle, and the second train (designated PASM) was run only during operations when the converter was in a rolled out, or open, position to provide a composite of emissions occurring during such activities as charging, slag skimming, and copper pouring. For cycle Test No. 3, the PASM particulate/arsenic sample train was run during slag skimming only in an effort to further characterize skimming emissions.

SECTION 4

AIR CURTAIN CAPTURE EFFICIENCY

The primary objective of the test program was to obtain an estimate of the overall capture or collection efficiency of the air curtain control system and its efficiency during specific converter operational modes.

Because no absolute measurement procedure was available for quantification of hood collection efficiency, several techniques were used to estimate this efficiency. These techniques included 1) a tracer mass balance, 2) observation of visible emissions, and 3) opacity measurements with a transmissometer. This section describes the techniques used to quantify the air curtain collection efficiency and presents the test results. Example calculations are given in Appendix A. Field and analytical data are presented in Appendix B. A detailed description of the sample and analytical techniques is presented in Appendix D and the logs of visible emissions observations are presented in Appendix H.

4.1 TRACER GAS MASS BALANCE

4.1.1 Principle

A suitable tracer was quantitatively injected at various points within the air curtain control area. By combining the measurements of the tracer concentration at the air curtain exhaust sampling point with flow rate measurements, it was possible to calculate the amount of tracer passing the sampling point (i.e., the amount collected by the air curtain and suction plenum). The tracer recovery efficiency was then calculated from the amount injected and the amount captured on a mass-flow basis.

Sulfur hexafluoride (SF_6) was used as the tracer. This colorless, odorless, tasteless gas is not flammable, is nontoxic, and is extremely inert. It is also stable up to a temperature of 500°C (932°F). The minimum detection limit for SF_6 (using a gas chromatograph with electron capture detector) is 5 parts per trillion. The SF_6 background level in ambient air is in the 10^{-14} range.*

The SF_6 was injected into the control of the air curtain at a constant rate. Maintenance of a constant pressure on a limiting orifice ensured that a constant injection flow rate was achieved. The limiting orifice was calibrated before and after each sustained injection by using a 0 to 10 cubic centimeter (cc) scale bubble meter. Injection rates were 30 to 50 cc/min. Also, the temperature at each injection point was monitored during each SF_6 injection to ensure that decomposition did not occur.

Single point samples of the air curtain hood flue gas were collected at a downstream sampling location by pulling a constant rate at a point of average velocity in the exhaust duct into a leak-free, 15-liter Tedlar bag. The sample bags were taken to the onsite laboratory for immediate analysis by a Perkin-Elmer Model 3920 gas chromatograph equipped with a Ni-63 electron capture detector and a Valco gas sampling valve with a 1-ml sampling loop.

For each injection calculation, the average of the SF_6 injection rate in cc/min determined before and after each sustained injection was used. The concentration of SF_6 at the air curtain hood sample location combined with the average gas flow measurements in cc/min units yields the SF_6 mass flow rate at the sample location. The air curtain capture efficiency for each injection point was then calculated as follows:

$$E = 1 - \left(\frac{Q_i - Q_m}{Q_i}\right)$$

---

*J. E. Lovelock, Nature, pp. 230-379 (1971).

where:

E = SF_6 capture efficiency

Q_i = SF_6 injection rate into air curtain control area in cc/min

Q_m = SF_6 mass flow rate at sample location, cc/min; where Q_m = SF_6 concentration (part/part volume/volume) x average volumetric flow rate (cc/min)

In an effort to define the accuracy of this method, the following procedure was developed for determining relative error. The definition for the term "percent error" as used here is defined as follows. An associated or assumed error of ±10 percent represents a standard deviation of ±3 σ's (standard deviation units).

The equation for calculating the tracer recovery efficiency (E) is:

$$E = \left[1 - \left(\frac{Q_i - Q_m}{Q_i}\right)\right] 100 \tag{1}$$

where:

Q_i = amount of the tracer substance injected into the air stream (cc/min)

Q_m = amount of the tracer substance measured (cc/min)

Equation 1 can also be expressed as:

$$E = \left(\frac{Q_m}{Q_i}\right) \times 10^2 \tag{2}$$

The relative error of the recovery efficiency [RE(E)] is expressed as:

$$RE(E) = \left[\frac{Var(E)}{E^2}\right]^{1/2} \tag{3}$$

where:

Var(E) = variance of E and

$$\mathrm{Var}(E) = \frac{1}{Q_i^2}\left[\frac{Q_m}{Q_i^2}\,\mathrm{Var}(Q_i) + \mathrm{Var}(Q_m)\right] \quad (4)$$

$$\mathrm{RE}(E) = \left[\frac{\mathrm{Var}(Q_i)}{Q_i^2} + \frac{\mathrm{Var}(Q_m)}{Q_m^2}\right] \quad (5)$$

From Equation 1,

Q_i = the amount of SF_6 injected (6)

and $Q_m = C\ F$ (7)

C = ppb, concentration of tracer measured at downstream sample location

F = cc/min, mass flow rate at collection point

Using proper calibration and sample techniques, it is assumed that the error in the SF_6 injection rate is ±5 percent. It is further assumed that the error in the SF_6 concentration measurement and in the gas flow measurement (F) (using EPA Method 2*) is ±10 percent.

Based on average data values obtained during the tracer study, typical values used in this calculation would be:

Q_i = 45.00 cc/min SF_6

$RE(Q_i)$ = ±5 percent

and

F = 126,230 acfm = 3.58×10^9 cc/min

C = 1.2×10^{-8} part/part SF_6

Q_m = 42.96 cc/min

RE(c) = ±10 percent

RE(f) = ±10 percent

---

*The EPA Program for the Standardization of Stationary Source Emission Test Methodology, A Review, EPA-600/4-76-044.

Equations 4 and 5 become

$$\mathrm{Var}(Q_i) = Q_i^2 \left[\frac{RE(Q_i)}{3}\right]^2 \tag{8}$$

$$\mathrm{Var}(Q_m) = C^2 \left[\frac{RE(f)F}{3}\right]^2 + F^2 \left[\frac{RE(c)C}{3}\right]^2 \tag{9}$$

For the typical values used here, the relative error of the recovery efficiency is determined as follows:

$$\mathrm{Var}(Q_i) = (45)^2 \left[\frac{0.05}{3}\right]^2$$

$$= 0.56$$

$$\mathrm{Var}(Q_m) = (1.2)^2 \left[\frac{(0.10)(35.8)}{3}\right]^2 + (35.8)^2 \left[\frac{(0.10)(1.2)}{3}\right]^2$$

$$= 4.10$$

$$RE(E) = \left[\frac{0.56}{(45)^2} + \left(\frac{4.10}{(35.8)^2}\right)\right]^{1/2}$$

$$= \pm 0.059$$

$$= \pm 5.9\%$$

Because the error of the measurements is assumed to represent the interval equivalent to 3 standard deviations, the relative error in tracer recovery efficiency measurements would be approximately ±18 percent (i.e., 3 x 5.9%).* Tracer recovery data reported in the following sections are subject to the ±18 percent error limits.

4.1.2 Preliminary Method Evaluation

Before tracer gas tests could be performed on the air curtain hooding system, it was necessary to evaluate available sample and analytical methodologies relative to this program. Literature searches were made to ascertain the compatibility of the use of sulfur hexafluoride as a tracer in previous studies with the planned application on the air curtain hooding system.

---

*Bennett, C.A., and N.L. Franklin, Statistical Analysis in Chemistry and the Chemical Industry, John Wiley & Sons, Inc., 1954.

The GC-ECD was assembled specifically for SF_6 analysis according to referenced procedures.* A series of calibration runs was made to evaluate instrument response and accuracy. These preliminary runs compared favorably with available analytical data.* An evaluation also was performed to determine if tracer losses occurred in the Tedlar bags used to collect the actual flue gas samples. A known concentration of sulfur hexafluoride was placed in sample bags and analyzed after a 24-hour period. No loss of sulfur hexafluoride was observed. The sample bags were then purged with nitrogen and analyzed for residual sulfur hexafluoride to evaluate the effects of reusing sample bags for multiple sample collection. In each case, the sulfur hexafluoride tracer concentration was below the minimum detection limit (5×10^{-12}) of the analytical method.

4.1.3 Tracer Method Feasibility Tests

In December 1982 PEDCo performed a series of tracer gas tests on the converter air curtain secondary hood to evaluate the feasibility of the tracer gas method relative to establishing a reproducible data base for tracer recovery efficiency and to evaluate the most practical means of obtaining the desired data.

Initially, a series of tests were performed in which SF_6 was quantitatively injected directly into the secondary hood exhaust duct downstream of the suction plenum. Flue gas samples were collected at the secondary hood test location and the combined tracer concentration measured at the sample location and flue gas flow measurements yielded the mass flow of tracer at the sample location. Tracer recovery efficiencies were then calculated as described in Subsection 4.1.1. These data were used to quantify inherent measurement biases and establish the most practical means for sampling in the exhaust duct.

---

*Improvements in the Determination of Sulfur Hexafluoride for Use as a Meteorological Tracer. Analytical Chemistry, Vol. 44, No. 4, April 1972; and SF_6 Tracer Gas Analysis of Mine Ventilation Systems, Technology News, No. 143, May 1982.

At the completion of these tests, the tracer was quantitatively injected directly into the area above the No. 4 converter to establish the effective hood control area and to evaluate measurement techniques for the planned manual test program in January 1983.

In summary, the December 1982 tracer test data indicated that the methodology as applied to the air curtain hood system provided a feasible means of estimating air curtain capture efficiency. The suitability of sulfur hexafluoride as the tracer gas was also verified. The following sections detail the December 1982 test activities.

To establish the tracer recovery efficiency and to account for any inherent measurement biases, the tracer was quantitatively injected directly into the air curtain secondary hood exhaust duct downstream of the secondary hood suction plenum. Flue gas samples were collected at the secondary hood exhaust sample location approximately 76 meters (250 feet) downstream from the injection point. The combined tracer concentration measured at the sample location and the flue gas flow measurements yielded the mass flow rate of tracer at the sample location. Collection efficiencies were then calculated by comparing the amount of tracer injected per minute and the mass flow rate of the tracer passing the sampling location.

Test Runs 1 through 4 (Table 4) were trial runs designed to establish the injection rate and subsequent tracer concentration measurable by the GC-ECD and an exponential dilution calibration curve. As shown in Table 4, the tracer injection rate was increased for each of the first four tests until the measured concentration was in the proper range. For these four tests, two samples were collected simultaneously at two points of average velocity in the duct. For tests 5T through 14T integrated samples were collected by traversing the cross-sectional area of the duct. Gas flow rates reported for these runs are actual flow rates measured during the collection of each sample. Recovery efficiencies ranged from 74 to 94 percent for the integrated samples, and the average tracer recovery efficiency was 84 percent.

TABLE 4. SUMMARY OF PRELIMINARY TRACER RECOVERY EFFICIENCY DATA

Sample I.D.	Date (1982)	Measured[a] gas flow rate, cc/min	SF_6[b] concentration, v/v	Average SF_6[c] injection rate, cc/min	SF_6[d] mass flow rate, cc/min	Recovery[e] efficiency, %
1A&B	12/9	2.92×10^{9}	-	2.87	-	-
2A&B	12/9	2.92×10^{9}	-	3.47	-	-
3A&B	12/9	2.92×10^{9}	-	10.07	-	-
4A&B	12/9	2.92×10^{9}	3.09×10^{-9}	10.14	9.02	89
PR-5T	12/10	2.91×10^{9}	8.02×10^{-9}	24.91	23.34	94
PR-6T	12/10	2.89×10^{9}	6.98×10^{-9}	24.91	20.17	81
PR-7T	12/10	3.02×10^{9}	6.88×10^{-9}	24.91	20.78	83
PR-8T	12/10	3.03×10^{9}	6.99×10^{-9}	24.91	21.18	85
PT-9T	12/10	3.01×10^{9}	9.12×10^{-9}	30.91	27.45	89
PT-10T	12/10	2.96×10^{9}	8.95×10^{-9}	30.91	26.49	86
PT-11T	12/10	2.96×10^{9}	9.34×10^{-9}	30.91	27.65	89
PT-12T	12/10	2.94×10^{9}	8.84×10^{-9}	30.91	25.99	84
PT-13T	12/11	2.65×10^{9}	8.81×10^{-9}	30.21	23.35	77
PT-14T	12/11	2.60×10^{9}	8.55×10^{-9}	30.21	22.23	74

Runs 1 through 4 A&B were collected at two separate points of average velocity in the duct. For Runs 1 through 3 the SF_6 concentration was at the minimum detectable limit. Runs PR-5T through PR-14T were collected as integrated samples by traversing the cross-sectional area of the stack.

[a] Measured gas flow rate (secondary exhaust duct): acfm x 28,320 = cc/min.

[b] SF_6 concentration (parts per part; volume per volume)

[c] SF_6 injection rate determined by bubble meter calibration before and after each injection. The difference ranged from 0.06 to 0.14 cc/min for Tests 1 through 4 and 0.06 to 2.58 cc/min for Tests 5T through 14T.

[d] SF_6 mass flow rate = gas flow rate (cc/min) x SF_6 concentration (v/v) = cc/min SF_6.

[e] Recovery efficiency =

$$100 - \left(\frac{SF_6 \text{ injected} - SF_6 \text{ measured}}{SF_6 \text{ injected}}\right) \times 100$$

Note: Tracer recovery efficiencies are subject to a ±18 percent relative error as described in Subsection 4.1.2.

Before the single point recovery tests were performed, flue gas samples were collected at each of the 12 sample points (EPA Reference Method 1) to define the SF_6 concentration profile in the exhaust duct. Figure 6 presents the SF_6 concentration profile.

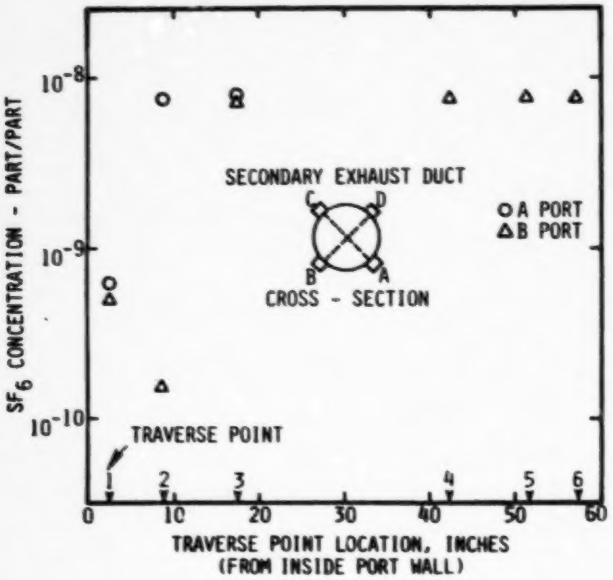

Figure 6. SF_6 concentration profile.

Negative pressure at the sample location causes air inleakage and dilution near the sample port. This dilution caused distortion of the SF_6 concentration at Test Points 1 and 2 (both sample ports), which explains the lower recovery efficiencies on the integrated samples (Table 4). The remaining points showed uniform SF_6 concentration distribution.

Table 5 summarizes the results of samples collected at a single point in the secondary hood exhaust duct. During these tests, the tracer was injected into the air curtain exhaust duct downstream of the secondary hood suction plenum. The tracer recovery efficiency ranged from 79 to 97 percent, and the average recovery efficiency was 89 percent. Single point sampling was desirable because more samples could be collected in a given amount of time. Also, the amount of test equipment required at the sample location to make other manual tests prohibited the collection of integrated gas samples. The gas flow rates reported in Table 5 and subsequent calculations represent average values obtained for each flow mode.

TABLE 5. SUMMARY OF SINGLE POINT TRACER RECOVERY EFFICIENCY TESTS

Sample I.D.	Date (1982)	Average gas flow rate, cc/min	SF_6 concentration, v/v	SF_6 injection rate, cc/min	SF_6 mass flow rate, cc/min	Recovery efficiency, %
PRSP-1[a]	12/11	2.92×10^9	9.89×10^{-9}	30.21	28.89	96
PRSP-2[a]	12/11	2.92×10^9	1.00×10^{-8}	30.21	29.20	97
PRSP-3[a]	12/11	2.92×10^9	9.67×10^{-9}	30.21	28.24	93
PRSP-4[a]	12/11	2.92×10^9	9.74×10^{-9}	30.21	28.44	94
PRSP-5[b]	12/11	4.12×10^9	5.55×10^{-9}	28.94	22.87	79
PRSP-6[b]	12/11	4.12×10^9	5.77×10^{-9}	28.94	23.77	82
PRSP-7[b]	12/11	4.12×10^9	5.75×10^{-9}	28.94	23.69	82
PRSP-8[c]	12/11	2.05×10^9	1.24×10^{-8}	28.94	25.42	88
PRSP-9[c]	12/11	2.05×10^9	1.25×10^{-8}	28.94	25.63	89
PRSP-10[c]	12/11	2.05×10^9	1.26×10^{-8}	28.94	25.83	89
Total				294.48	261.98	
Average				29.45	26.20	89

[a] A medium air flow.

[b] A high air flow.

[c] A low air flow.

Note: SF_6 recovery efficiencies are subject to a ±18 percent relative error as described in Subsection 4.1.2.

Air volume for the air curtain control system is regulated by a series of dampers activated by limiting switches during movement of the converter and primary hood. For the December 1982 tests, three separate damper settings and subsequent exhaust gas volumes were used in the operation of the air curtain system. Table 5 presents the average volumetric flow rates measured by

EPA Reference Methods 1 and 2* at the air curtain hood exhaust test location. Velocity measurements were made for each flow mode to determine an average volumetric flow rate for each setting. Volumetric flows were calculated in actual cubic meters per minute and cubic feet per minute and then converted to cubic centimeters per minute for the tracer mass flow calculations. Stack gas moisture content was less than 1 percent by volume as determined using wet bulb-dry bulb techniques.

Table 6 presents a summary of tracer recovery efficiency at the air curtain suction plenum. Injections were made directly into the suction plenum, and six gas samples were collected at a single point in the duct. Recovery efficiencies ranged from 91 to 97 percent and averaged 94 percent.

TABLE 6. SUMMARY OF TRACER RECOVERY EFFICIENCY AT AIR CURTAIN SUCTION INLET

Sample I.D.	Date (1982)	Average gas flow[a] rate, cc/min	SF_6 concentration, v/v	SF_6 injection rate, cc/min	SF_6 mass flow rate, cc/min	Recovery efficiency, %
AC-1	12/11	2.92×10^9	9.95×10^{-9}	30.92	29.05	94
AC-2	12/11	2.92×10^9	9.68×10^{-9}	30.92	28.27	91
AC-3	12/11	2.92×10^9	9.93×10^{-9}	30.92	28.99	94
AC-4	12/11	2.92×10^9	1.00×10^{-8}	30.92	29.20	94
AC-5	12/11	2.92×10^9	1.03×10^{-8}	30.92	30.08	97
AC-6	12/11	2.92×10^9	1.01×10^{-8}	30.92	29.49	95
Average				30.92	29.18	94

[a] Average gas flow rate at medium flow setting.

Note: SF_6 recovery efficiencies are subject to a ±18 percent relative error as described in Subsection 4.1.2.

---

*Stack gas composition was ambient; 20.9% oxygen, 0.0% carbon dioxide, with the balance being nitrogen.

The tracer recovery efficiency data presented in Tables 4 through 6 indicated that collection efficiencies were reproducible and comparable regardless of the sample collection technique (single point versus multi-point sample collection) used. As noted previously, single point sample collection was desirable based on the number of samples which could be collected in a short amount of time. Average recovery efficiencies ranging from 84 to 94 percent indicate a measurement bias (to the low side) was prevalent for these samples. However, considering the ±18 percent relative error associated with the measurement technique, the data do provide a good estimation of tracer collection efficiency.

Based on the recovery test data presented in Tables 4 through 6, preparations were made to begin injections into the area immediately above the No. 4 converter. As shown in Figures 7 and 8, sample ports were located in access doors on both sides of the air curtain wall so that a sample matrix could be constructed immediately above the No. 4 converter. Starting on the curtain exhaust side, injections were made at four sample points, placed at approximately 0.6-m (2-foot) intervals, in each of the ports designated in Figure 8. Sustained injections were made in each port, and bubble meter calibrations of the injection system were performed before and after each injection. At each injection point the temperature was recorded to preclude possible tracer decomposition. Temperatures within the measurement area (Figure 7) ranged from 13°C (55°F) to 315°C (600°F) and averaged value of 37°C (96°F). Based on the temperatures measured in the control area, thermal decomposition of the tracer did not occur.

A single sample was collected at the exhaust duct sample location for each injection point. The velocity head was recorded for each sample collected, and based on the converter operational mode and fan damper setting, the average gas flow rate determined for that damper setting was used in the collection efficiency calculations. A similar procedure was used on the jet side of the curtain, except that two points (Nos. 5 and 6) were used to complete a six-point cross-sectional traverse.

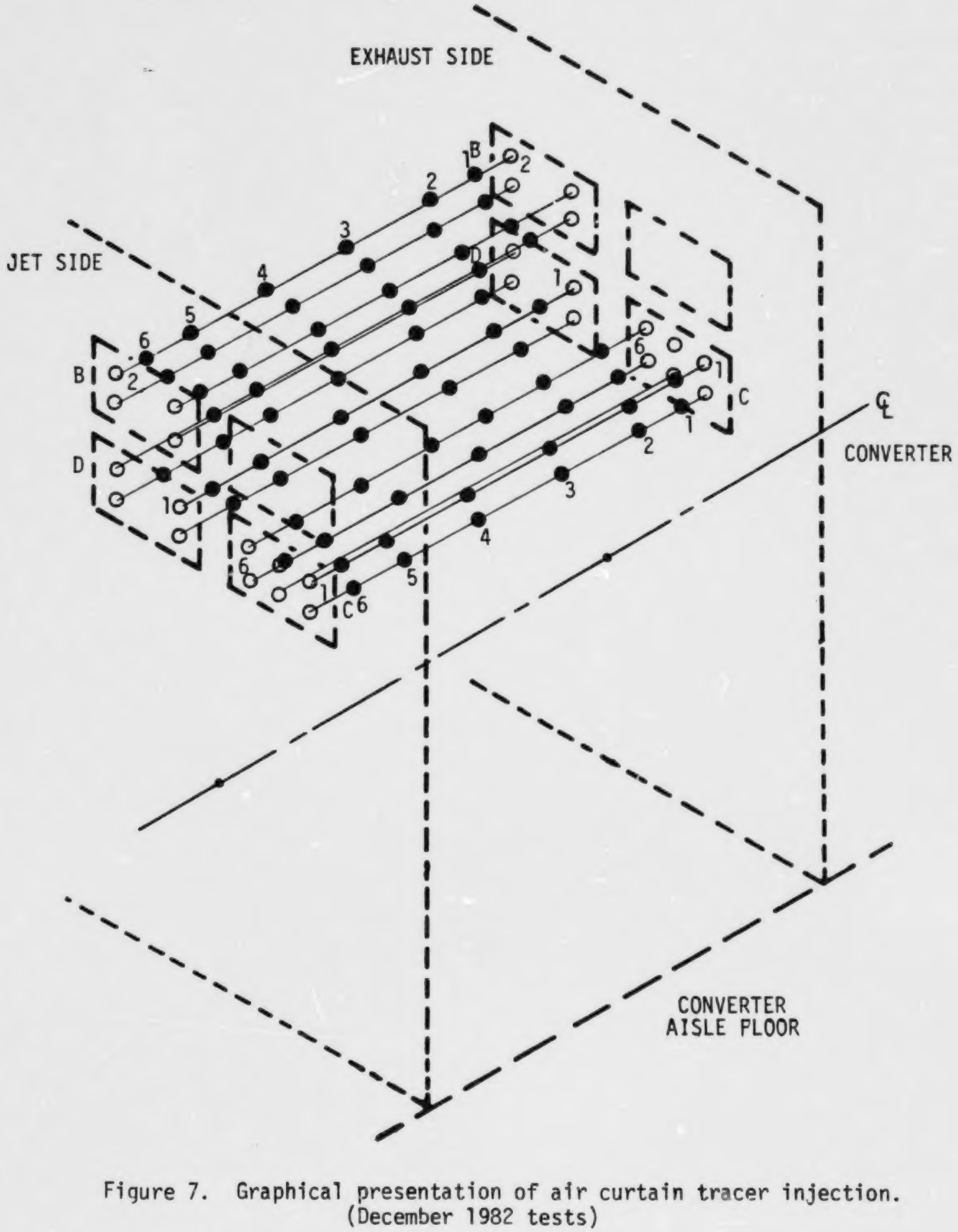

Figure 7. Graphical presentation of air curtain tracer injection. (December 1982 tests)

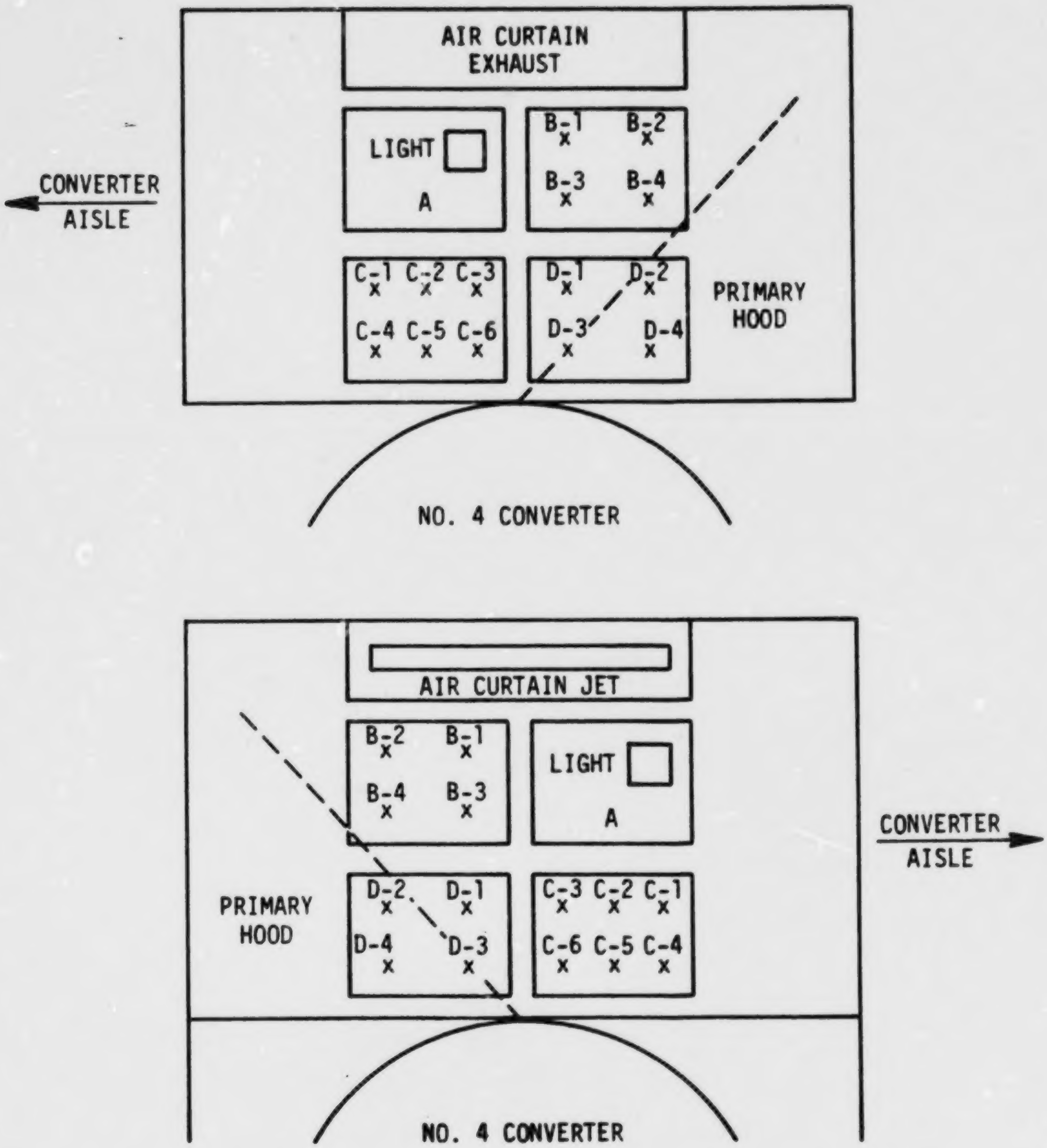

Figure 8. Injection point matrix used for preliminary tracer gas tests.

The results of the air curtain sample matrix tests are summarized in Table 7 for tracer injection in the exhaust side and Table 8 for sample injection on the jet side of the matrix.

A summary of the tracer recovery efficiencies and corresponding converter operation modes is presented in Table 9. No attempt was made to evaluate recovery efficiencies at the same sample point for the various converter modes. Also, several matrix points (Port D4, Points 1-6) were not evaluated because they were inaccessible. Matrix points C1-2, C5-2, C5-5, and D1-5 were evaluated during a change in converter operation, which resulted in fluctuating volumetric flow rates and inaccurate tracer mass flow calculations. These data are not included with the reported results.

A total of 76 SF_6 injections were made in the three-dimensional matrix previously described. A summary of the results by sample port, relative position within the matrix area, and converter operating mode is given in Table 10 . Tracer recovery efficiencies ranged from 73 to 113 percent, and the overall average was 87 percent. After a review of these data, it was decided that the number of injection points in the matrix could be reduced for the January 1983 test effort.

TABLE 7. SUMMARY OF TRACER RECOVERY TEST DATA ON EXHAUST SIDE

Sample I.D.	Date (1982)	Average gas flow[a] rate, cc/min	SF_6 concentration, v/v	SF_6 injection rate, cc/min	SF_6 mass flow rate, cc/min	Recovery efficiency, %
A (Light)	12/12	2.92×10^9	9.67×10^{-9}	30.72	28.24	92
B1-1	12/12	2.92×10^9	9.12×10^{-9}	32.17	26.63	83
B1-2	12/12	2.92×10^9	9.17×10^{-9}	32.17	26.78	83
B1-3	12/12	2.92×10^9	9.14×10^{-9}	32.17	26.69	83
B1-4	12/12	2.92×10^9	8.90×10^{-9}	32.17	25.99	81
B2-1	12/12	4.12×10^9	6.49×10^{-9}	31.96	26.74	84
B2-2	12/12	4.12×10^9	6.17×10^{-9}	31.96	25.42	80
B2-3	12/12	4.12×10^9	6.26×10^{-9}	31.96	25.79	81
B2-4	12/12	4.12×10^9	6.33×10^{-9}	31.96	26.08	82
B3-1	12/12	4.12×10^9	6.24×10^{-9}	31.43	25.71	82
B3-2	12/12	4.12×10^9	6.35×10^{-9}	31.43	26.16	83
B3-3	12/12	4.12×10^9	6.29×10^{-9}	31.43	25.91	82
B3-4	12/12	4.12×10^9	6.04×10^{-9}	31.43	24.88	79
B4-1	12/12	2.92×10^9	9.33×10^{-9}	31.08	27.24	88
B4-2	12/12	2.92×10^9	9.62×10^{-9}	31.08	28.09	90

(continued)

TABLE 7 (continued)

Sample I.D.	Date (1982)	Average gas flow[a] rate, cc/min	SF_6 concentration, v/v	SF_6 injection rate, cc/min	SF_6 mass flow rate, cc/min	Recovery efficiency, %
B4-3	12/12	4.12×10^9	7.46×10^{-9}	31.08	30.74	99
B4-4	12/12	4.12×10^9	6.26×10^{-9}	31.08	25.79	83
C1-1	12/12	4.12×10^9	7.43×10^{-9}	34.01	30.61	90
C1-3	12/12	2.92×10^9	9.73×10^{-9}	34.01	28.41	84
C1-4	12/12	2.92×10^9	9.63×10^{-9}	34.01	28.82	85
C2-1	12/12	2.92×10^9	8.50×10^{-9}	32.47	24.82	76
C2-2	12/12	2.92×10^9	8.53×10^{-9}	32.47	24.91	77
C2-3	12/12	2.92×10^9	8.45×10^{-9}	32.47	24.67	76
C2-4	12/12	2.92×10^9	8.58×10^{-9}	32.47	25.05	77
C3-1	12/12	2.92×10^9	8.26×10^{-9}	32.33	24.12	75
C3-2	12/12	2.92×10^9	8.09×10^{-9}	32.33	23.62	73
C3-3	12/12	4.12×10^9	7.47×10^{-9}	32.33	30.78	95
C3-4	12/12	4.12×10^9	5.94×10^{-9}	32.33	24.47	76
C4-1	12/12	4.12×10^9	6.46×10^{-9}	31.55	26.62	84
C4-2	12/12	4.12×10^9	6.55×10^{-9}	31.55	26.99	86
C4-3	12/12	4.12×10^9	6.68×10^{-9}	31.55	27.52	87
C4-4	12/12	2.92×10^9	9.92×10^{-9}	31.55	28.97	92
C5-1	12/12	4.12×10^9	8.22×10^{-9}	30.68	33.87	110
C5-3	12/12	2.92×10^9	9.48×10^{-9}	30.68	27.68	90
C5-4	12/12	2.92×10^9	9.96×10^{-9}	30.68	29.08	95
C6-1	12/12	4.12×10^9	7.76×10^{-9}	30.72	31.97	104
C6-2	12/12	2.92×10^9	9.60×10^{-9}	30.72	28.03	91
C6-3	12/12	2.92×10^9	1.03×10^{-8}	30.72	30.08	98
C6-4	12/12	2.92×10^9	9.46×10^{-9}	30.72	27.62	90
D1-1	12/12	2.92×10^9	9.20×10^{-9}	32.00	26.86	84
D1-2	12/12	4.12×10^9	7.06×10^{-9}	32.00	29.09	91
D1-3	12/12	2.92×10^9	8.62×10^{-9}	32.00	25.17	79
D1-4	12/12	2.92×10^9	8.15×10^{-9}	32.00	23.80	74
D2-1	12/12	2.92×10^9	8.55×10^{-9}	31.94	24.97	78
D2-2	12/12	2.92×10^9	8.79×10^{-9}	31.94	25.67	80
D2-3	12/12	2.92×10^9	8.57×10^{-9}	31.94	25.02	78
D2-4	12/12	4.12×10^9	7.04×10^{-9}	31.94	29.00	91
D3-1	12/12	4.12×10^9	6.29×10^{-9}	31.47	25.91	82
D3-2	12/12	4.12×10^9	6.23×10^{-9}	31.47	25.67	82
D3-3	12/12	4.12×10^9	6.32×10^{-9}	31.47	26.04	83
D3-4	12/12	4.12×10^9	6.32×10^{-9}	31.47	26.04	83

[a] Secondary exhaust duct gas flow rate in cubic centimeters per minute. Values represent average measured flow rates (EPA Methods 1 and 2) for each of three separate damper settings.

Note: Tracer recovery efficiencies are subject to a ±18 percent relative error as described in Subsection 4.1.2.

TABLE 8. SUMMARY OF TRACER RECOVERY TEST DATA ON JET SIDE

Sample I.D.	Date (1982)	Average gas flow rate, cc/min	SF_6 concentration, v/v	SF_6 injection rate, cc/min	Uncorrected SF_6 mass flow rate, cc/min	Recovery efficiency, %
A (Light)	12/13	2.92×10^9	1.05×10^{-8}	31.10	30.66	99
C1-5	12/13	4.12×10^9	6.46×10^{-9}	29.89	26.62	89
C1-6	12/13	4.12×10^9	6.51×10^{-9}	29.89	26.82	90
C2-5	12/13	2.92×10^9	9.89×10^{-9}	30.38	28.88	95
C2-6	12/13	2.92×10^9	7.78×10^{-9}	30.38	22.72	75
C3-5	12/13	2.92×10^9	9.70×10^{-9}	30.45	28.32	93
C3-6	12/13	2.05×10^9	1.08×10^{-8}	30.45	22.14	73
C4-5	12/13	2.92×10^9	9.52×10^{-9}	30.50	27.80	91
C4-6	12/13	2.92×10^9	8.12×10^{-9}	30.50	23.71	78
C5-6	12/13	2.92×10^9	8.63×10^{-9}	30.54	25.20	83
C6-5	12/13	2.92×10^9	9.75×10^{-9}	30.41	28.47	94
C6-6	12/13	2.92×10^9	8.51×10^{-9}	30.41	24.85	82
D1-6	12/13	2.92×10^9	1.00×10^{-8}	30.30	29.20	96
D3-5	12/13	2.92×10^9	9.86×10^{-9}	30.56	28.79	94
D3-6	12/13	4.12×10^9	8.37×10^{-9}	30.56	34.48	113
B1-5	12/13	2.92×10^9	9.68×10^{-9}	31.04	28.27	91
B1-6	12/13	2.92×10^9	8.50×10^{-9}	31.04	24.82	80
B2-5	12/13	2.92×10^9	1.00×10^{-8}	31.10	29.20	94
B2-6	12/13	2.92×10^9	9.42×10^{-9}	31.10	27.51	88
B3-5	12/13	2.05×10^9	1.26×10^{-8}	31.01	25.83	83
B3-6	12/13	2.92×10^9	1.03×10^{-8}	31.01	30.08	97
B4-5	12/13	2.92×10^9	1.06×10^{-8}	31.10	30.95	99
B4-6	12/13	2.92×10^9	8.90×10^{-9}	31.10	25.99	84

Note: Tracer recovery efficiencies are subject to a ±18 percent relative error as described in Subsection 4.1.2.

TABLE 9. SUMMARY OF MATRIX AREA TRACER RECOVERY EFFICIENCY DATA

Sample I.D.	Recovery efficiency, %	Converter mode
A (light)	92	Blowing
	99	Blowing
B1-1	83	Blowing
B1-2	83	Blowing
B1-3	83	Blowing
B1-4	81	Blowing
B1-5	91	Blowing
B1-6	80	Blowing
B2-1	84	Slag skimming
B2-2	80	Idle
B2-3	81	Idle
B2-4	82	Idle
B2-5	94	Blowing
B2-6	88	Blowing
B3-1	82	Idle
B3-2	83	Idle
B3-3	82	Idle
B3-4	79	Blister copper pour
B3-5	83	Silica charge
B3-6	97	Blowing
B4-1	88	Blowing
B4-2	90	Blowing
B4-3	99	Copper pour
B4-4	83	Primary hood up
B4-5	99	Blowing
B4-6	84	Blowing
C1-1	90	Slag skim
C1-3	84	Blowing
C1-4	85	Blowing
C1-5	89	Matte charge
C1-6	90	Cold dope charge
C2-1	76	Blowing
C2-2	77	Blowing
C2-3	76	Blowing
C2-4	77	Blowing
C2-5	95	Blowing
C2-6	75	Blowing
C3-1	75	Blowing
C3-2	73	Blowing
C3-3	95	Blowing and skimming slag
C3-4	76	Skimming slag
C3-5	93	Blowing
C3-6	73	Silica charge
D1-2	84	Blowing
D1-2	91	Skimming slag
D1-3	79	Blowing
D1-4	74	Blowing
D1-5	110	Skimming slag
D1-6	96	Blowing
D2-1	78	Blowing
D2-2	80	Blowing
D2-3	78	Blowing
D2-4	91	Skimming slag
C4-1	84	Matte charge
C4-2	86	Matte charge
C4-3	87	Matte charge
C4-4	92	Blowing
C4-5	91	Blowing
C4-6	78	Blowing
C5-1	110	Matte charge
C5-3	90	Blowing
C5-4	95	Blowing
C5-5	96	Matte charge
C5-6	83	Blowing
C6-1	104	Matte charge
C6-2	91	Blowing
C6-3	98	Blowing
C6-4	90	Blowing
C6-5	94	Blowing
C6-6	82	Blowing
D3-1	82	Idle
D3-2	82	Idle
D3-3	83	Idle
D3-4	83	Idle
D3-5	94	Blowing
D3-6	113	Skimming slag

Note: Tracer recovery efficiencies are subject to a ±18 percent relative error as described in Subsection 4.1.2.

TABLE 10. COLLECTION EFFICIENCY OF SF_6 WITHIN THE AIR CURTAIN MATRIX AREA (DECEMBER 1982)

Port	Position						Average
	1 Exhaust	2	3	4	5	6 Jet	
B-1	83	83	83	81	91	80	83.5
B-2	84	80	81	82	94	88	84.8
B-3	82	83	82	79	83	97	84.3
B-4	88	90	99	83	99	84	90.5
Average	84.2	84.0	86.2	81.2	91.8	87.2	85.8
C-1	90	92	84	85	89	90	88.3
C-2	76	77	76	77	95	75	79.3
C-3	75	73	95	76	93	73	80.3
C-4	84	86	87	92	91	78	80.8
C-5	110	99	90	95	96	83	95.5
C-6	104	91	98	90	94	82	93.2
Average	89.8	86.3	88.3	85.8	93.0	80.2	87.2
D-1	84	91	79	74	110	96	89.0
D-2	78	80	78	91	-	-	81.8
D-3	82	82	83	83	94	113	89.5
Average	81.3	84.3	79.7	82.7	102	104.5	86.7
Grand average	86.2	85.2	85.2	83.7	94.1	86.8	86.8

Note: SF_6 recovery efficiencies are subject to a ±18 percent relative error as described in Subsection 4.1.2.

4.1.4 Estimated Air Curtain Hood Capture Efficiency Using a Tracer Gas

Based on the December 1982 field work, the following conclusions were drawn relative to achieving an estimation of air curtain capture efficiency.

1. The tracer gas methodology provided a feasible means of estimating air curtain capture efficiency,
2. The suitability of sulfur hexafluoride as the tracer gas was verified, and
3. The air curtain control volume was established.

This section summarizes results from the January 1983 test program in which additional tracer recovery tests were conducted in the upper and lower portions of the air curtain control volume. The objective in performing tracer recovery tests in the lower portion of the control volume was to evaluate the effectiveness of the secondary hood in controlling emissions below the converter mouth and near the front edge of the baffle walls. Also, this data would indicate if thermal buoyancy or lift increased collection efficiency during specific converter roll-out modes. These data, in conjunction with visual observations and the transmissometer opacity data, were then used to estimate hood capture efficiency; overall and for specific converter operating modes.

Prior to the start of the test program, air flow measurements were performed in the air curtain hood exhaust duct at the sampling plane according to procedures described in EPA Methods 1 and 2. These measurements were used to establish baseline volumetric flow data for the automatic damper system associated with the air curtain control system.

Before the evaluation test program was started, ASARCO personnel made adjustments to the damper settings in an effort to optimize volumetric flow for the test program. The flow patterns established during the December 1982 preliminary tests were changed as follows: 1) the high flow mode was reduced to 3540 actual m^3/min (126,230 acfm), 2) the medium flow mode was eliminated, and 3) the low flow mode was set at 2124 actual m^3/min (75,500 acfm). In practice, the low flow condition was used for blowing and idling, and the high flow condition was used for converter roll-out activities, i.e., charging and skimming.

Table 11 summarizes the volumetric flow data obtained at the air curtain exhaust sample location. No further adjustments were made to the suction fan setting during the sampling period. The average values for each flow condition were used in all tracer gas mass balance calculations, depending on converter operational mode at the time of tracer sample collection. The average volumetric flow rate for the low flow condition was 2124 actual m^3/min (75,505 acfm) with an average static pressure of -5.3 mmHg (-2.86 in.H_2O). The average volumetric flow rate for the high flow condition was 3552 actual m^3/min (126,230 acfm) with an average static pressure of -15.6 mmHg (-8.38 in.H_2O). Based on previous data, moisture content of the gas stream was estimated to be 1 percent and the dry molecular weight was estimated to be 28.84 (ambient) for calculation purposes. This value was verified by wet bulb/dry bulb measurements and an Orsat gas analyzer for gas composition (oxygen and carbon dioxide). The flue gas static pressure was measured using a 0-36 in. water manometer. The static pressure was closely monitored throughout the test series to ensure that the volumetric flow did not change significantly. As the data in Table 11 show, the static pressures monitored during the manual field tests compared favorably with those measured during the volumetric flow determinations. The data also show that no significant change occurred in the volumetric flow during the test series.

Figures 9 and 10 present profiles of the air curtain exhaust duct velocity for each flow mode. Average values (by traverse point) for measurements made during a given flow mode were used to construct these profiles. The tracer samples were collected at Sample Point 3 in both ports. A PEDCo representative (in the converter building) coordinated the sample activities and the monitoring of velocity pressures at the sample collection point.

TABLE 11. SUMMARY OF VOLUMETRIC FLOW DATA

Run No.	Date (1983)	Flow condition[a]	Volumetric flow rate[b] Actual m³/min (acfm)	Volumetric flow rate[b] Standard dNm³/min (dscfm)	Static pressure[c], mmHg (in.H_2O)	Flue gas temperature, °C (°F)	Gas composition[d] O_2	Gas composition[d] CO_2	Moisture content, % (% by volume)	Static pressure[f] monitored during manual emission tests, mmHg (in.H_2O)
V-6	1/12	Low	2115 (75,182)	2125 (75,527)	- 5.6 (-3.00)	14 (57)	20.9	0.0	~1.0 (0.76)	- 4.5 (-2.4)
V-7	1/12	Low	2075 (73,748)	2083 (74,040)	- 5.6 (-3.00)	14 (57)				
V-8	1/12	Low	2122 (75,427)	2132 (75,757)	- 5.0 (-2.70)	14 (57)				- 5.2 (-2.8)
V-9	1/12	Low	2179 (77,452)	2187 (77,716)	- 5.0 (-2.70)	14.4 (58)				- 4.7 (-2.5)
V-10	1/12	Low	2144 (76,194)	2150 (76,429)	- 5.0 (-2.70)	14.4 (58)				-
V-11	1/13	Low	2138 (75,977)	2175 (77,311)	- 5.6 (-3.00)	15 (59)				- 5.6 (-3.0)
V-17	1/13	Low	2121 (75,410)	2171 (77,156)	- 5.2 (-2.80)	13 (56)				-
V-18	1/13	Low	2084 (74,406)	2141 (76,086)	- 5.4 (-2.90)	13 (56)				- 5.4 (-2.9)
V-19	1/13	Low	2105 (74,797)	2153 (76,504)	- 5.6 (-3.00)	13 (56)				- 5.6 (-3.0)
V-20	1/13	Low	2084 (74,051)	2130 (75,686)	- 5.4 (-2.90)	14 (57)				- 5.0 (-2.7)
V-21	1/13	Low	2155 (76,589)	2202 (78,274)	- 5.2 (-2.80)	14 (57)				-
V-22	1/14	Low	2188 (77,768)	2244 (79,752)	- 5.6 (-3.00)	11 (52)				- 5.2 (-2.8)
V-23	1/18	Low	2099 (74,616)	2097 (74,535)	- 4.7 (-2.50)	11.7 (53)				- 4.7 (-2.5)
V-24	1/19	Low	2123 (75,446)	2089 (74,249)	- 5.6 (-3.00)	16 (61)				-
Average		Low	2124 (75,505)	2149 (76,359)	- 5.3 (-2.86)	14 (57)	20.9	0.0	<1.0	- 5.10 (-2.73)
V-12	1/13	High	3530 (125,475)	3577 (127,124)	-15.7 (-8.40)	12 (54)	20.9	0.0	~1.0 (0.76)	-15.9 (-8.5)
V-13	1/13	High	3577 (127,123)	3620 (128,658)	-15.5 (-8.30)	12.8 (55)				-16.8 (-9.0)
V-14	1/13	High	3521 (125,148)	3569 (126,855)	-15.3 (-8.20)	12 (54)				-15.7 (-8.4)
V-15	1/13	High	3621 (128,685)	3671 (130,482)	-15.7 (-8.40)	12 (54)				-15.5 (-8.3)
V-16	1/13	High	3526 (125,322)	3577 (127,134)	-15.3 (-8.20)	12 (54)				-15.7 (-8.4)
V-17	1/13	High	3535 (125,624)	3413 (121,288)	-16.4 (-8.80)	17 (63)				-15.7 (-8.4)
Average		High	3552 (126,230)	3571 (126,924)	-15.6 (-8.38)	13 (56)	20.9	0.0	<1.0	-15.9 (-8.5)

[a] Flow condition related to converter mode. Low - all blowing modes, converter hold and idle; High - matte charge, slag skim, cold additions, copper pouring, and occasionally for converter idle.

[b] Volumetric flow rate in actual cubic meters per minute (actual m³/min) and actual cubic feet per minute (acfm) at stack conditions using 1 percent moisture by volume and 28.84 dry molecular weight. Also, dry normal cubic meters per minute (dNm³/min) and dry standard cubic feet per minute (dscfm) at 20°C (68°F) and 760 mmHg (29.92 in.Hg) and zero percent moisture.

[c] Static pressure obtained using a 0-36 in.H_2O water manometer.

[d] Gas compostion as determined using a Fyrite gas analyzer and an Orsat gas analyzer as described in EPA Reference Method 3.

[e] Moisture content as determined using wet bulb-dry bulb techniques. Value in parentheses is average measured percent moisture from the manual emission tests for particulate. Average wet bulb temperature: 12°C (54°F); average dry bulb temperature: 14°C (58°F).

[f] Static pressure as monitored during SF_6 sample collection and manual emission tests, 1/18 through 1/22, 1983. Data represent values recorded on the SF_6 sample collection data sheets - Appendix B.

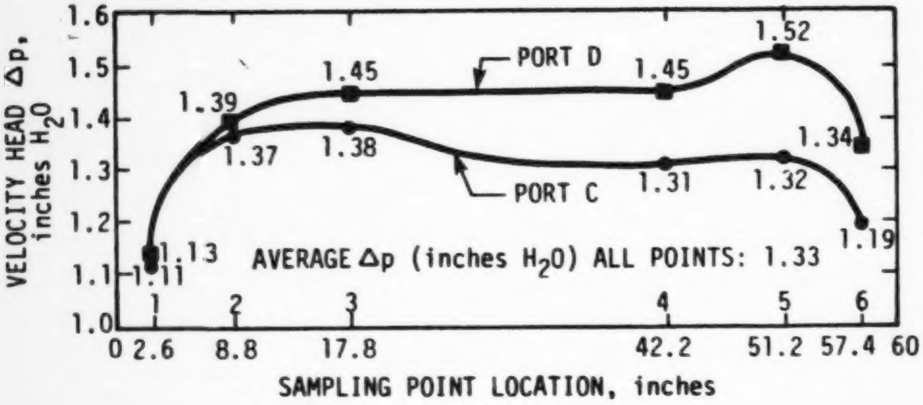

Figure 9. Velocity profile for low flow condition.

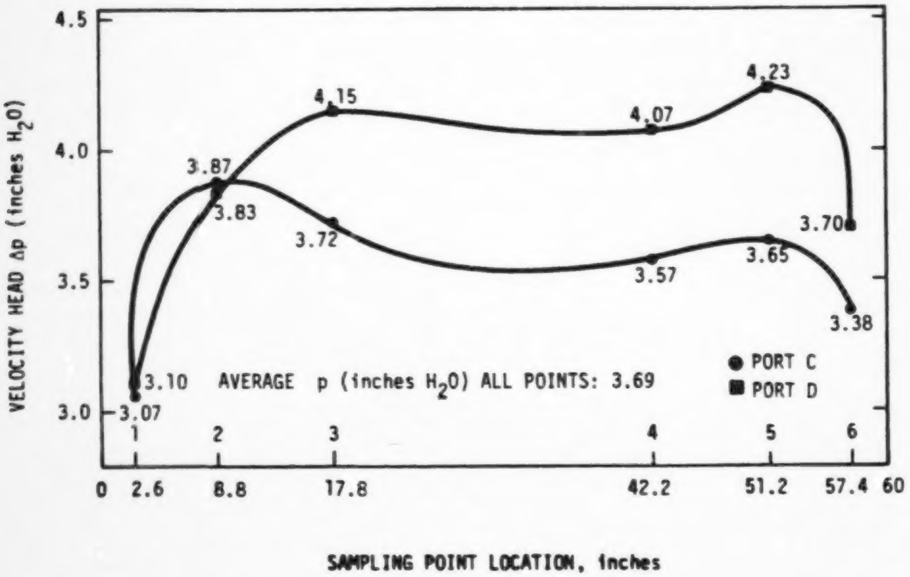

Figure 10. Velocity profile for high flow condition.

Figure 11 shows the tracer injection locations used during this manual test program. Tracer injection locations were varied to establish tracer recovery efficiency by characterizing the effective capture volume of the system. A sample matrix (described in Subsection 4.1.3) was used to locate multiple injection points within the upper control volume. Sample ports in adjacent access doors on both sides of the converter baffle walls were used to construct the sample injection matrix (Figure 12). The results of this sampling were used to characterize the tracer recovery efficiency of the air curtain hood system in the area immediately above the converter. Several single point injections were performed in the lower portion of the control volume (Figure 11) to further characterize the effective capture volume of the hooding system, particularly during converter roll-out activities. The results from these injections would indicate if the secondary hood was effective in controlling the area below the converter mouth and near the front edge of the baffle walls. Also this data would indicate if thermal lift increased the collection efficiency during converter roll-out.

The planned matrix tests called for injection of tracer at 16 points in a three-dimensional configuration above the top of the converter. The matrix injections were to be made through Ports B-2, C-1, C-6, and D-1 at four positions each. The matrix design provided for three injections at each injection point on each of two days, for a total of 96 test points. The resulting data were to be evaluated on site. Based on this evaluation, the number of injection points within the sample matrix were to be increased or reduced according to the statistical differences between injection location and converter operational mode for similar injection points. As noted previously, process operational problems made it impossible to complete the test series as planned, and several changes had to be made to compensate for the inconsistent process operation.

On January 14, 1983, recovery efficiencies for 45 of 48 planned tests were determined. The measured recovery efficiencies

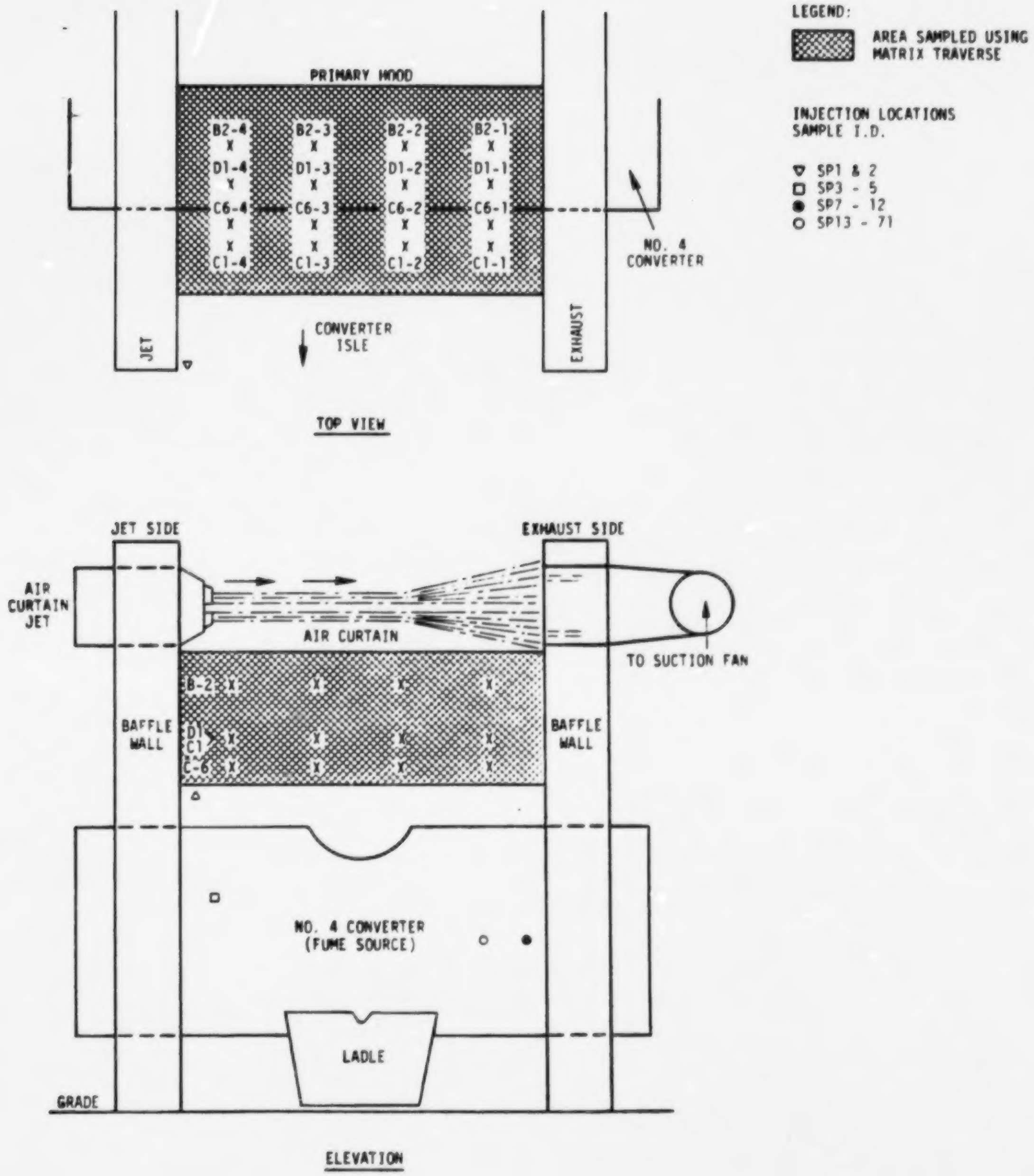

Figure 11. SF_6 injection locations.

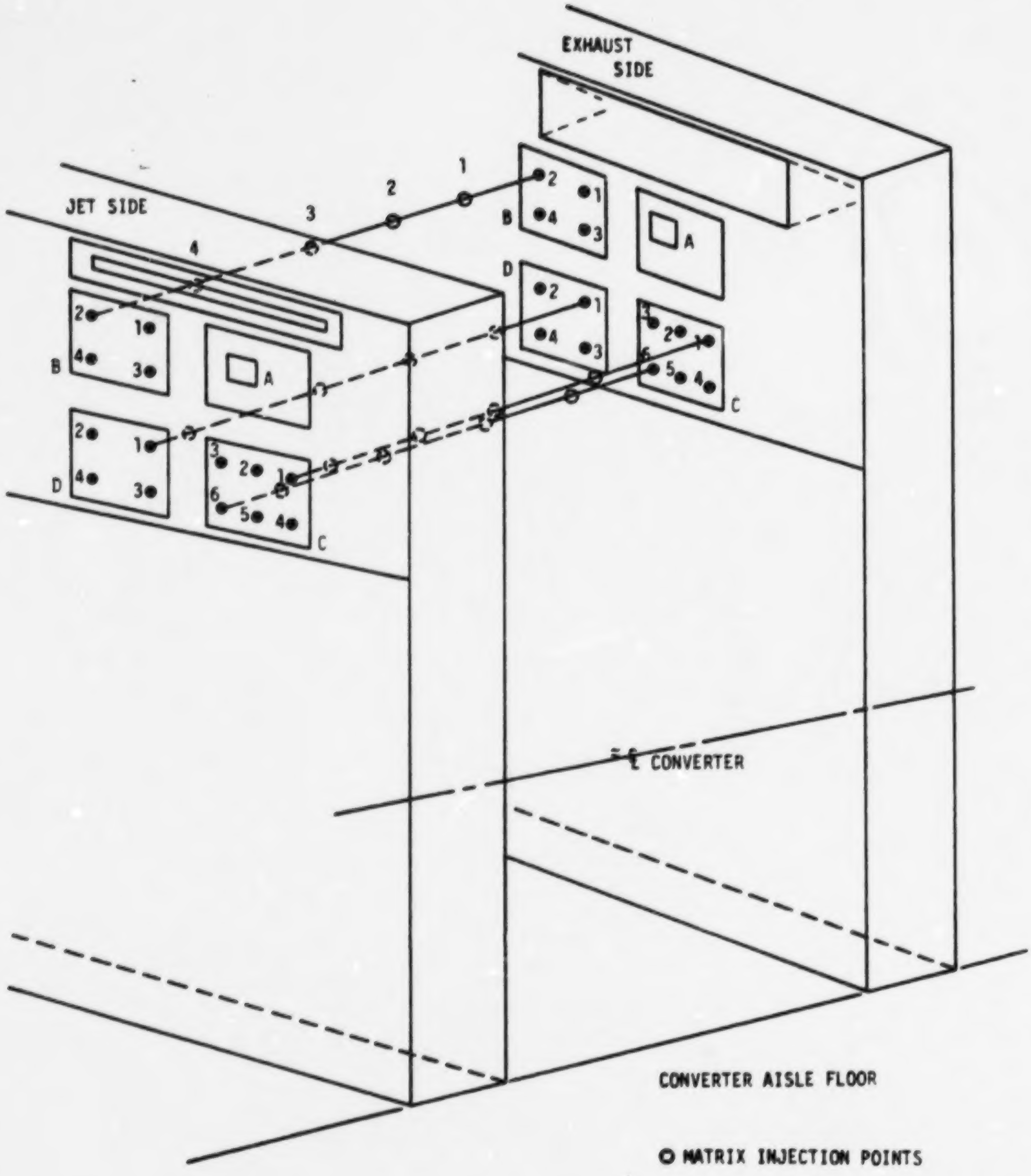

Figure 12. Tracer injection matrix.

are presented in Table 12. Average recovery efficiencies for individual releases varied from 69 to 119 percent, and the overall average efficiency for the 45 tests was 94 percent. The port through which the releases of the tracer substance were made did not have any effect on the average recovery efficiency. The average recovery efficiency of all releases made through a given port ranged from 93.0 percent for Port C-6 to 95.4 percent for Port C-1. This difference was not statistically significant. The variability between the average recovery efficiency of the replicates made at a given position (between the jet side and the exhaust side) was statistically significant. The greatest difference occurred at Port D-1, where the average recovery efficiency ranged from 83.3 to 105.7 percent. The recovery efficiencies for Positions 1 and 2 (near the exhaust side) were approximately 96.6 percent and were generally higher than those for Positions 3 and 4 (near the jet side) which were approximately 91.6 percent.

Average tracer recovery efficiencies for the various converter-operating modes are also presented. With the exception of cold additions, the average recovery efficiency was not affected by the operating mode of the converter; averages varied from 92.8 percent during blowing to 95.0 percent during slag skimming.

The remaining test series of 48 injections were performed on January 17, 18, and 19. The results of these tests are summarized in Table 13. For this series of tests, the tracer recovery efficiency varied from 65 to 119 percent and the overall average was 96.0 percent. The port through which the tracer releases were made had no effect on the average tracer recovery efficiency of the air curtain hood. The average efficiency varied from 94.5 percent at Port C-6 to 98.0 percent at Port B-2. For positions within the matrix, the average recovery efficiency varied from 80.7 percent at Position 4, Port D-1, to 106 percent at Position 2, Port D-1. Recovery efficiencies were consistently higher for Positions 1 and 2 (near the exhaust side) than for Positions 3

TABLE 12. TRACER RECOVERY EFFICIENCY WITHIN THE AIR CURTAIN CONTROL (MATRIX) AREA (JANUARY 14, 1983)

	Position				
	Exhaust		Jet		
Port	1	2	3	4	Average
B-2	97	102	94	97	97.5
B-2	89	95	89	96	92.2
B-2	94	97	79	94	91.0
Average	93.3	98.0	87.3	85.7	93.6
C-1	97	93	-	94	94.7
C-1	95	105	95	91	96.5
C-1	97	95	97	90	94.8
Average	96.3	97.7	96.0	91.7	95.4
C-6	95	94	-	93	94.0
C-6	101	93	96	81	92.8
C-6	94	97	89	90	92.5
Average	96.7	94.7	92.5	88.0	93.0
D-1	91	105	98	91	96.2
D-1	89	119	-	90	99.3
D-1	93	93	98	69	88.2
Average	91.0	105.7	98.0	83.3	94.2
Grand average					94.0

Note: SF_6 recovery efficiencies are subject to a ±18 percent relative error as described in Subsection 4.1.2.

TABLE 13. SF_6 COLLECTION EFFICIENCY WITHIN THE CONTROL (MATRIX) AREA (JANUARY 17, 18, 19, 1983)

		Position				
		Exhaust		Jet		
Port	Test date (1983)	1	2	3	4	Average
B-2	1/17	103	99	95	93	97.5
B-2	1/18	95	107.5	81	87	92.6
B-2	1/19	101	103	119	92	103.8
Average		99.7	103.2	98.3	90.7	98.0
C-1	1/17	105	103	99	93	100.0
C-1	1/18	95	96	84	91	91.5
C-1	1/19	99	103	104	69	93.8
Average		99.7	100.7	95.7	84.3	95.1
C-6	1/17	104	102	101	81	97.0
C-6	1/18	93	106.5	95	79	93.4
C-6	1/19	96	99	93	95	93.2
Average		97.7	102.5	96.3	81.7	94.5
D-1	1/17	106	106	96	65	93.2
D-1	1/18	101	111	92	88	98.0
D-1	1/19	106	97	89	89	98.2
Average		104.3	106.0	95.0	80.7	96.5
Overall average						96.0

Note: SF_6 recovery efficiencies are subject to a ±18 percent relative error as described in Subsection 4.1.2.

and 4 (near the jet side). Figures 13 and 14 present these data graphically.

Again, operating mode had no adverse effect on the recovery efficiency measured for the air curtain hood by the tracer method. Average collection efficiencies varied from 88.5 percent during copper pouring to 96.7 during cold additions.

In summary, the results of the tracer recovery efficiency data within the upper portion of the air curtain control area indicate that, on the average, at least 90 percent of the gases and particulate matter entering this area is likely to be captured by the air curtain hooding system. Both the December and January matrix test results verify this conclusion. As indicated, the converter operating mode had no adverse effect on the SF_6 control area collection efficiency. Table 14 shows a summary of the tracer recovery efficiency for the upper control volume.

TABLE 14. SUMMARY OF TRACER RECOVERY EFFICIENCY FOR UPPER CONTROL VOLUME

Converter cycle	Blow	Slag skim	Matte charge	Cold add	Idle	Copper pour
Number of injections	19 27	9 7	7 6	3 3	7 4	- 4
Mean, %	92.8 96.7	95.0 94.3	93.1 94.2	102.0 96.7	93.4 100.0	- 88.5
Standard deviation, %	8.47 10.06	4.87 8.08	3.13 9.54	14.7 20.4	3.6 11.4	- 9.6

The first number in each pair is the result of Test 1 and the second of Test 2.

The pertinent data for each sample injection and resulting recovery are presented in Tables 15 through 18. Since injections were made within the upper portion of the air curtain control area, these data would not account for spillage outside the upper control area during the injection and would not necessarily

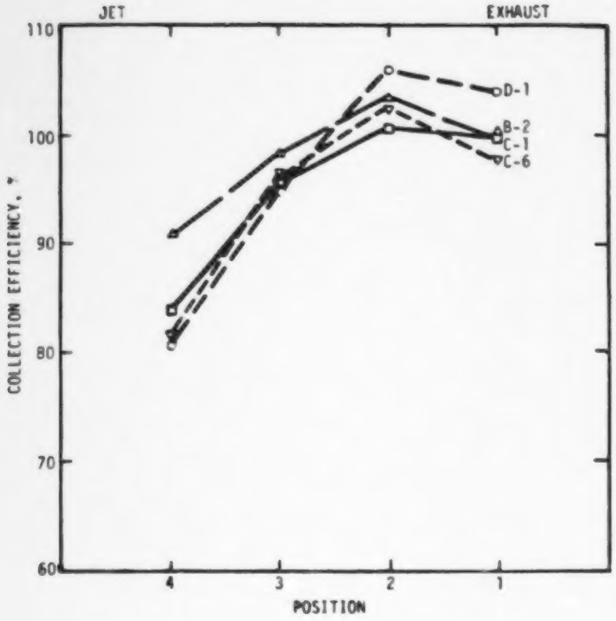

Figure 13. Comparison of hood collection efficiency and matrix port injection.

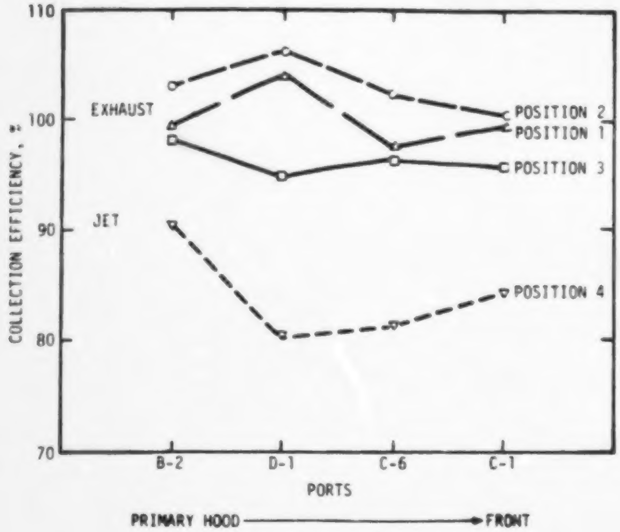

Figure 14. Comparison of hood collection efficiency and matrix point injection.

TABLE 15. SUMMARY OF MATRIX INJECTION TEST DATA, 1/14/83

Sample I.D. and time	Date (1983)	Average gas flow rate, cc/min x 10^9	SF_6 concentration in v/v	SF_6 injection rate, cc/min	SF_6 mass flow, cc/min	Recovery efficiency, %
C6-4 16:05	1/14	3.58 (cold addition)	1.20×10^{-8}	46.02	42.96	93
C6-3 16:15	1/14	2.14 (blow)	-	45.24	-	Sample void
C1-3 16:25	1/14	2.14 (blow)	-	45.62	-	Sample void
B2-3 16:33	1/14	2.14 (blow)	2.03×10^{-8}	46.34	43.44	94
D1-3 16:44	1/14	3.58 (slag skim)	1.26×10^{-8}	46.16	45.11	98
B2-4 16:55	1/14	3.58 (matte charge)	1.24×10^{-8}	45.86	44.39	97
D1-4 17:02	1/14	2.14 (idle)	1.91×10^{-8}	45.07	40.87	91
C1-4 17:11	1/14	3.58 (cold addition)	1.17×10^{-8}	44.52	41.89	94
C6-3 17:18	1/14	3.58 (matte charge)	1.18×10^{-8}	44.16	42.24	96
C1-4 17:27	1/14	3.58 (matte charge)	1.12×10^{-8}	44.27	40.10	91
C6-4 17:35	1/14	2.14 (blow)	1.71×10^{-8}	45.14	36.59	81
D1-3 17:47	1/14	2.14 (blow)	-	45.28	-	Sample void
B2-3 17:58	1/14	3.58 (slag skim)	1.08×10^{-8}	43.42	38.66	89
C1-3 18:10	1/14	3.58 (slag skim)	1.26×10^{-8}	47.72	45.11	95
D1-4 18:16	1/14	3.58 (matte charge)	1.26×10^{-8}	49.88	45.11	90
B2-4 18:23	1/14	3.58 (matte charge)	1.36×10^{-8}	50.59	48.69	96
C6-3 18:30	1/14	3.58 (matte charge)	1.27×10^{-8}	51.30	45.47	89
C6-4 18:36	1/14	2.14 (idle)	2.21×10^{-8}	52.50	47.29	90
D1-3 18:45	1/14	2.14 (idle)	2.30×10^{-8}	49.82	49.22	98
C1-3 18:53	1/14	2.14 (blow)	2.27×10^{-8}	49.94	48.58	97
B2-3 19:01	1/14	2.14 (blow)	1.84×10^{-8}	50.02	39.38	79
C1-4 19:07	1/14	2.14 (blow)	2.12×10^{-8}	50.34	45.37	90
B2-4 19:15	1/14	2.14 (blow)	2.21×10^{-8}	50.46	47.29	94
D1-4 19:22	1/14	2.14 (blow)	1.62×10^{-8}	50.36	34.67	69

(continued)

TABLE 15 (continued)

Sample I.D. and time	Date (1983)	Average gas flow rate, cc/min x 10^9	SF_6 concentration in v/v	SF_6 injection rate, cc/min	SF_6 mass flow, cc/min	Recovery efficiency, %
B2-1 19:50	1/14	2.14 (blow)	2.18×10^{-8}	48.02	46.65	97
C6-2 19:56	1/14	2.14 (blow)	2.14×10^{-8}	48.02	45.80	95
D1-1 20:02	1/14	2.14 (blow)	2.04×10^{-8}	48.02	43.66	91
C1-1 20:10	1/14	2.14 (blow)	2.18×10^{-8}	48.02	46.65	97
B2-2 20:18	1/14	2.14 (blow)	2.29×10^{-8}	48.04	49.01	102
D1-2 20:25	1/14	3.58 (slag skim)	1.41×10^{-8}	48.04	50.48	105
C6-1 21:01	1/14	3.58 (slag skim)	1.26×10^{-8}	48.04	45.11	94
C1-2 21:10	1/14	3.58 (slag skim)	1.25×10^{-8}	48.04	44.75	93
B2-2 21:18	1/14	3.58 (matte charge)	1.29×10^{-8}	48.37	46.18	95
D1-2 21:25	1/14	3.58 (cold addition)	1.61×10^{-8}	48.37	57.64	119
C6-1 21:31	1/14	2.14 (blow)	2.28×10^{-8}	48.37	48.79	101
C1-2 21:37	1/14	2.14 (blow)	2.37×10^{-8}	48.37	50.72	105
C1-1 21:45	1/14	2.14 (blow)	2.15×10^{-8}	48.26	46.01	95
B2-1 21:51	1/14	3.58 (slag skim)	1.20×10^{-8}	48.26	42.96	89
C6-2 21:56	1/14	3.58 (slag skim)	1.25×10^{-8}	48.26	44.75	93
D1-1 22:01	1/14	2.14 (idle)	2.00×10^{-8}	48.26	42.80	89
C1-1 22:10	1/14	2.14 (idle)	2.11×10^{-8}	46.69	45.15	97
B2-2 22:16	1/14	3.58 (slag skim)	1.27×10^{-8}	46.69	45.47	97
C1-2 22:22	1/14	3.58 (slag skim)	1.24×10^{-8}	46.69	44.39	95
B2-1 22:27	1/14	3.58 (matte charge)	1.22×10^{-8}	46.69	43.68	94
C6-2 22:33	1/14	2.14 (blow)	2.12×10^{-8}	46.95	45.37	97
D1-1 22:46	1/14	2.14 (blow)	2.04×10^{-8}	46.95	43.66	93
D1-2 22:54	1/14	2.14 (blow)	2.04×10^{-8}	46.95	43.66	93
C6-1 22:59	1/14	2.14 (blow)	2.06×10^{-8}	46.95	44.08	94

Note: SF_6 recovery efficiencies are subject to a ±18 percent relative error as described in Subsection 4.1.2.

TABLE 16. SUMMARY OF MATRIX INJEXTION TEST DATA, 1/17/83

Sample I.D. and Time	Date (1983)	Average gas flow rate, cc/min x 10^9 (converter mode)	SF_6 concentration in v/v	SF_6 injection rate, cc/min	SF_6 mass flow, cc/min	Recovery efficiency, %
B2-1 10:15	1/17	2.14 (line blow)	2.13×10^{-8}	48.77	50.08	103
B2-2 10:17	1/17	2.14 (line blow)	2.27×10^{-8}	48.77	48.58	99
C1-1 10:20	1/17	2.14 (line blow)	2.39×10^{-8}	48.77	51.15	105
C1-2 10:23	1/17	2.14 (line blow)	2.35×10^{-8}	48.77	50.29	103
C6-1 10:31	1/17	2.14 (line blow)	2.39×10^{-8}	48.96	51.15	104
C6-2 10:33	1/17	2.14 (line blow)	2.33×10^{-8}	48.96	49.86	102
D1-1 10:36	1/17	2.14 (line blow)	2.42×10^{-8}	48.96	51.79	106
D1-2 10:40	1/17	2.14 (line blow)	2.42×10^{-8}	48.96	51.79	106
B2-3 11:13	1/17	2.14 (line blow)	2.08×10^{-8}	46.97	44.51	95
B2-4 11:15	1/17	2.14 (line blow)	2.05×10^{-8}	46.97	43.87	93
C1-3 11:18	1/17	2.14 (line blow)	2.17×10^{-8}	46.97	46.44	99
C1-4 11:21	1/17	2.14 (line blow)	2.05×10^{-8}	46.97	43.87	93
C6-3 11:30	1/17	3.58 (matte charge)	1.32×10^{-8}	46.68	47.26	101
C6-4 11:32	1/17	3.58 (matte charge)	1.06×10^{-8}	46.68	37.95	81
D1-3 11:34	1/17	2.14 (line blow)	2.10×10^{-8}	46.68	44.94	96
D1-4 11:36	1/17	2.14 (line blow)	1.41×10^{-8}	46.68	30.17	65

TABLE 17. SUMMARY OF MATRIX INJECTION TEST DATA, 1/18/83

Sample I.D. and Time	Date (1983)	Average gas flow rate, cc/min x 10^9 (converter mode)	SF_6 concentration in v/v	SF_6 injection rate, cc/min	SF_6 mass flow, cc/min	Recovery efficiency, %
B2-3 09:14	1/18	3.58 (slag skim)	1.07×10^{-8}	47.12	38.31	81
B2-4 09:18	1/18	3.58 (slag skim)	1.15×10^{-8}	47.12	41.17	87
C1-3 09:21	1/18	2.14 (idle)	1.85×10^{-8}	47.12	39.59	84
C1-4 11:12	1/18	3.58 (slag skim)	1.20×10^{-8}	47.42	42.96	91
C6-3 11:15	1/18	3.58 (copper pour)	1.26×10^{-8}	47.42	45.11	95
C6-4 11:18	1/18	3.58 (copper pour)	1.05×10^{-8}	47.42	37.59	79
D1-3 11:21	1/18	3.58 (copper pour)	1.22×10^{-8}	47.42	43.68	92
D1-4 11:24	1/18	3.58 (copper pour)	1.17×10^{-8}	47.42	41.89	88
B2-1 12:54	1/18	2.14 (copper slag charge)	2.12×10^{-8}	49.23	45.37	92
B2-2 12:56	1/18	3.58 (copper slag charge)	1.54×10^{-8}	49.23	55.13	112
C1-1 12:59	1/18	3.58 (copper slag charge)	1.27×10^{-8}	49.23	45.47	92
C1-2 13:00	1/18	2.14 (matte charge)	2.00×10^{-8}	49.23	42.80	87
C6-1 13:04	1/18	2.14 (matte charge)	2.10×10^{-8}	49.23	44.94	91
C6-2 13:09	1/18	3.58 (matte charge)	1.44×10^{-8}	49.23	51.55	105
D1-1 13:30	1/18	3.58 (matte charge)	1.96×10^{-8}	49.23	70.17	143
D1-2 13:46	1/18	3.58 (matte charge)	1.88×10^{-8}	49.23	67.30	137
B2-1 15:37	1/18	2.14 (idle)	1.33×10^{-8}	48.82	47.61	98
B2-2 15:40	1/18	3.58 (slag skim)	1.41×10^{-8}	48.82	50.48	103
C1-1 15:42	1/18	3.58 (slag skim)	1.33×10^{-8}	48.82	47.61	98
C1-2 15:59	1/18	3.58 (slag skim)	1.43×10^{-8}	48.82	51.19	105
C6-1 16:04	1/18	3.58 (slag skim)	1.30×10^{-8}	48.82	46.54	95
C6-2 16:07	1/18	3.58 (matte charge)	1.47×10^{-8}	48.82	52.63	108
D1-1 16:11	1/18	3.58 (matte charge)	1.37×10^{-8}	48.82	49.05	101
D1-2 16:14	1/18	3.58 (matte charge)	1.51×10^{-8}	48.82	54.06	111

TABLE 18. SUMMARY OF MATRIX INJECTION TEST DATA, 1/19/83

Sample I.D. and Time	Date (1983)	Average gas flow rate, cc/min x 10^9 (converter mode)	SF_6 concentration in v/v	SF_6 injection rate, cc/min	SF_6 mass flow, cc/min	Recovery efficiency, %
D1-1 12:24	1/19	2.14 (blow)	2.39×10^{-8}	48.16	51.15	106
D1-2 12:27	1/19	2.14 (blow)	2.26×10^{-8}	48.16	48.36	101
C6-1 12:20	1/19	2.14 (blow)	2.17×10^{-8}	48.16	46.44	96
C6-2 12:22	1/19	2.14 (blow)	2.22×10^{-8}	48.16	47.51	99
C1-1 12:11	1/19	2.14 (blow)	2.23×10^{-8}	48.35	47.72	99
C1-2 12:15	1/19	2.14 (blow)	2.32×10^{-8}	48.35	49.65	103
B2-1 12:06	1/19	2.14 (blow)	2.28×10^{-8}	48.35	48.79	101
B2-2 12:08	1/19	2.14 (blow)	2.32×10^{-8}	48.35	49.65	103
B2-3 13:18	1/19	3.58 (cold addition)	1.58×10^{-8}	47.70	56.56	119
B2-4 13:19	1/19	3.58 (cold addition)	1.23×10^{-8}	47.70	44.03	92
C1-3 13:21	1/19	3.58 (hood up - idle)	1.39×10^{-8}	47.70	49.76	104
C1-4 13:23	1/19	2.14 (blow)	1.53×10^{-8}	47.70	32.74	69
C6-3 13:28	1/19	2.14 (blow)	2.07×10^{-8}	47.86	44.30	93
C6-4 18:30	1/19	2.14 (blow)	1.89×10^{-8}	47.86	40.45	85
D1-3 13:33	1/19	2.14 (blow)	2.18×10^{-8}	47.86	46.65	97
D1-4 13:25	1/19	3.58 (hood up)	1.19×10^{-8}	47.86	42.60	89

correspond to an overall visual assessment of hood capture effectiveness. Data relating visual assessment of hood capture effectiveness to tracer recovery efficiencies are presented in Subsection 4.3 of this report.

In an effort to characterize the effective capture area of the air curtain hooding system, several tests were performed in the lower portion of the air curtain control area (Figure 11). Sustained injections of tracer were made on January 18, 19, and 20 at the designated locations. The results of these tests are summarized in Table 19.

TABLE 19. SUMMARY OF TRACER RECOVERY EFFICIENCY FOR LOWER CONTROL VOLUME

Test	Number of releases	Collection efficiency, %		
		Mean	Standard deviation	Range
Converter mode				
Blowing	6	33.0	5.0	27-42
Matte charge	17	61.8	27.6	35-91
Slag skimming	28	84.0	18.4	52-128
Cold addition	6	61.5	18.3	49-76
Idle	8	53.8	22.7	30-95
Copper pour	4	80.8	16.9	61-98

Tests SP-1 and SP-2, which were performed on January 18, involved the release of the tracer material at a point along the baffle wall on the jet side of the air curtain hood. These tests were conducted during slag skimming and the average recovery efficiency measured was 94.5 percent, which is comparable to that reported for the releases on the three-dimensional matrix in the space above the converter.

Tests SP-3 to SP-5, also performed on January 18, involved the release of the tracer material at a location slightly above the ladle near the jet side of the hood. The average recovery efficiency was 64.3 percent.

On January 19, Tests SP-7 through SP-12 were performed with release of the tracer material at a location slightly above the ladle and very close to the wall on the exhaust side. Tests SP-7 through SP-10 were conducted during slag skimming; the recovery efficiency measured for the four tests ranged from 52 to 79 percent and the overall average recovery efficiency was 63.5 percent. Tests SP-11 and SP-12 were run during matte charging and the average recovery efficiency was 68.5 percent.

Tests SP-13 through SP-19 also were performed on January 19. In these tests the tracer material was also released at a location slightly above the ladle, but farther from the wall on the exhaust side. The recovery efficiency measured for the seven tests ranged from 30 to 89 percent, and the overall average was 58.7 percent. It should be noted that the samples for Tests SP-14, SP-15, and SP-16 (which had collection efficiencies of 32, 33, and 30 percent, respectively) were collected during the blowing mode. These values would be expected because the hooding system was in the low flow mode and there was no thermal lift to enhance the collection efficiency.

The final series of tests (SP-20 through SP-73) were performed on January 20. In these tests the tracer was released very near the ladle on the exhaust side of the hooding system. Recovery efficiencies, which were determined for 53 releases of the tracer material, ranged from 27 to 128 percent, with an overall average of 70 percent. The efficiencies varied from 38 percent for the 6 tests performed during blowing to 84 percent for the 28 tests performed during slag skimming. The difference between average efficiencies for the several operating modes is statistically significant.

The special injection tests were designed to characterize hood capture effectiveness in the lower portion of the air curtain control volume. The data clearly show the effects of increased exhaust side air volume and thermal lift from hot gases during converter roll-out modes. Also, the data indicate that determination of tracer recovery from the lower portion of the control volume is heavily dependent on injection locations and converter operation. For example, tests performed during the blowing mode, which is conducted with the primary hood closed and little heat escape, ranged from 27 to 42 percent, compared with 84 percent during slag skimming, 61.8 percent during matte charging, 61.5 percent for cold additions, and 81 percent for blister copper pouring. The tracer recovery efficiencies measured during the slag skimming and copper pour activities are higher because of the position of the SF_6 injection probe and the additional thermal lift. The ladles used during these operating modes were placed on the ground immediately in front of the converter while slag or blister copper was being discharged from the converter, and the injection probe was located above and to the left of the ladle. During the matte charging and cold addition operating modes, the probe was actually below the ladle because an overhead crane has to raise the filled ladles to charge the material to the converter.

In summary, the special point injection tests indicate that thermal lift plays a significant role in increased collection efficiencies in the lower portion of the control volume. Also, the lower tracer collection efficiencies for the various converter roll-out modes could be indicative of the observed fume spillage outside of the lower control volume.

The pertinent data for these sample injection tests and resulting recovery efficiencies are presented in Table 20.

4.2 OPACITY

The opacity of emissions escaping the air curtain were monitored and recorded by use of a double-pass transmissometer coupled with a strip-chart recorder. A detailed description of the instrumentation and test methodology are presented in Section 7 and Appendix D. The instrument was placed in operation at the start of each test period and operated continuously throughout the converter cycle. Table 21 summarizes the opacity of emissions escaping the air curtain slot during the test program, and Figure 15 shows the average opacity of emissions from each operation during the cycle when the converter was rolled out.

TABLE 20. SUMMARY OF SAMPLE AND ANALYTICAL DATA FOR SPECIAL INJECTION POINT TESTS

Sample I.D. and Time	Date (1983)	Average gas flow rate, cc/min x 10^3 (converter mode)	SF_6 concentration in v/v	SF_6 injection rate, cc/min	SF_6 mass flow, cc/min	Recovery efficiency, %
SP-1 11:30	1/18	3.58 (copper pour)	1.19×10^{-8}	46.92	42.60	91
SP-2 11:34	1/18	3.58 (copper pour)	1.29×10^{-8}	46.92	46.18	98
SP-3 11:37	1/18	3.58 (copper pour)	9.58×10^{-9}	46.92	34.30	73
SP-4 11:40	1/18	3.58 (copper pour)	7.94×10^{-9}	46.92	28.43	61
SP-5 12:00	1/18	2.14 (idle)	1.36×10^{-8}	49.06	29.10	59
SP-7 09:18	1/19	3.58 (slag skim)	7.14×10^{-9}	49.03	25.56	52
SP-8 09:20	1/19	3.58 (slag skim)	8.22×10^{-9}	49.03	29.43	60
SP-9 09:23	1/19	3.58 (slag skim)	8.68×10^{-9}	49.03	31.07	63
SP-10 09:27	1/19	3.58 (slag skim)	1.08×10^{-8}	49.03	38.66	79
SP-11 09:30	1/19	3.58 (matte charge)	8.56×10^{-9}	49.03	30.64	62
SP-12 09:32	1/19	3.58 (matte charge)	1.03×10^{-8}	49.03	36.87	75
SP-13 09:43	1/19	3.58 (matte charge)	9.52×10^{-9}	48.18	34.08	71
SP-14 10:22	1/19	2.14 (blow)	7.17×10^{-9}	48.18	15.34	32
SP-15 10:24	1/19	2.14 (blow)	7.45×10^{-9}	48.18	15.94	33
SP-16 10:27	1/19	2.14 (blow)	6.85×10^{-9}	48.18	14.66	30
SP-17 10:31	1/19	3.58 (slag skim)	1.20×10^{-8}	48.18	42.96	89
SP-18 10:33	1/19	3.58 (slag skim)	9.94×10^{-9}	48.18	35.59	74
SP-19 10:35	1/19	3.58 (slag skim)	1.10×10^{-9}	48.18	39.38	82
SP-20 08:26	1/20	3.58 (matte charge)	6.3×10^{-10}	48.25	2.26	5[a]
SP-21 08:28	1/20	3.58 (matte charge)	5.32×10^{-9}	48.25	19.05	40
SP-22 08:30	1/20	3.58 (matte charge)	7.20×10^{-9}	48.25	25.78	53
SP-23 08:32	1/20	3.58 (matte charge)	6.85×10^{-9}	48.25	24.52	51
SP-24 08:34	1/20	3.58 (idle)	6.16×10^{-9}	48.25	22.05	46
SP-25 08:36	1/20	3.58 (idle)	7.04×10^{-9}	48.25	25.20	52
SP-26 08:38	1/20	3.58 (matte charge)	6.77×10^{-9}	48.25	24.24	50

TABLE 20 (continued)

Sample I.D. and Time	Date (1983)	Average gas flow rate, cc/min x 10^9 (converter mode)	SF_6 concentration in v/v	SF_6 injection rate, cc/min	SF_6 mass flow, cc/min	Recovery efficiency, %
SP-27 09:28	1/20	3.58 (matte charge)	1.07×10^{-8}	48.25	38.31	79
SP-28 09:49	1/20	3.58 (cold addition)	6.87×10^{-9}	48.25	24.59	51
SP-29 09:53	1/20	3.58 (cold addition)	6.59×10^{-9}	48.25	23.59	49
SP-30 10:02	1/20	3.58 (matte charge)	4.68×10^{-9}	48.25	16.75	35
SP-31 10:33	1/20	2.14 (blow)	7.57×10^{-9}	47.62	16.20	34
SP-32 10:36	1/20	2.14 (blow)	6.08×10^{-9}	47.62	13.01	27
SP-33 10:38	1/20	2.14 (blow)	9.44×10^{-9}	47.62	20.20	42
SP-34 10:48	1/20	3.58 (slag skim)	9.25×10^{-9}	47.62	33.20	70
SP-35 10:55	1/20	3.58 (slag skim)	8.28×10^{-9}	47.62	29.64	62
SP-36 11:00	1/20	3.58 (slag skim)	1.16×10^{-8}	47.62	41.53	87
SP-37 11:02	1/20	3.58 (slag skim)	1.21×10^{-8}	47.62	43.32	91
SP-38 11:04	1/20	3.58 (idle)	5.28×10^{-9}	47.62	18.90	40
SP-39 11:08	1/20	3.58 (idle)	4.18×10^{-9}	47.62	14.96	31
SP-40 11:09	1/20	3.58 (idle)	4.06×10^{-9}	47.62	14.53	30
SP-41 11:11	1/20	3.58 (matte charge)	9.58×10^{-9}	47.62	34.30	72
SP-42 11:14	1/20	3.58 (matte charge)	9.86×10^{-9}	47.62	35.30	74
SP-43 11:16	1/20	3.58 (cold addition)	7.29×10^{-9}	47.62	26.03	55
SP-44 14:25	1/20	3.58 (slag skim)	1.17×10^{-8}	47.17	41.89	89
SP-46 14:33	1/20	3.58 (slag skim)	1.69×10^{-8}	47.17	60.50	128
SP-47 14:35	1/20	3.58 (slag skim)	1.11×10^{-8}	47.17	39.74	84
SP-48 14:37	1/20	3.58 (slag skim)	1.02×10^{-8}	47.17	36.52	77
SP-49 14:39	1/20	3.58 (slag skim)	1.23×10^{-8}	47.17	44.03	93
SP-50 14:42	1/20	3.58 (slag skim)	1.54×10^{-8}	47.17	55.13	117
SP-51 14:45	1/20	3.58 (slag skim)	9.76×10^{-9}	47.17	34.94	74
SP-52 14:47	1/20	3.58 (matte charge)	1.20×10^{-8}	47.17	42.96	91

TABLE 20 (continued)

Sample I.D. and Time	Date (1983)	Average gas flow rate, cc/min x 10^3 (converter mode)	SF_6 concentration in v/v	SF_6 injection rate, cc/min	SF_6 mass flow, cc/min	Recovery efficiency, %
SP-53 14:48	1/20	3.58 (matte charge)	1.20×10^{-8}	47.17	42.96	91
SP-54 14:50	1/20	3.58 (matte charge)	1.01×10^{-8}	47.17	36.16	77
SP-55 14:52	1/20	3.58 (matte charge)	1.09×10^{-8}	47.17	39.02	83
SP-56 14:55	1/20	3.58 (cold addition)	9.19×10^{-9}	47.17	32.90	70
SP-57 14:56	1/20	3.58 (cold addition)	1.0×10^{-8}	47.17	35.80	76
SP-58 14:58	1/20	3.58 (cold addition)	8.94×10^{-9}	47.17	32.00	68
SP-59 15:00	1/20	3.58 (roll in)	9.10×10^{-9}	47.17	32.58	69
SP-60 15:38	1/20	3.58 (slag skim)	1.26×10^{-8}	47.17	45.11	96
SP-61 15:40	1/20	3.58 (slag skim)	1.02×10^{-8}	47.17	36.52	77
SP-62 15:42	1/20	3.58 (slag skim)	9.16×10^{-9}	47.17	32.79	70
SP-63 15:44	1/20	3.58 (slag skim)	1.07×10^{-8}	47.17	38.31	81
SP-64 15:46	1/20	3.58 (slag skim)	1.34×10^{-8}	47.17	47.97	102
SP-65 15:47	1/20	3.58 (slag skim)	9.55×10^{-9}	47.17	34.19	72
SP-66 15:48	1/20	3.58 (slag skim)	9.31×10^{-9}	47.17	33.33	71
SP-67 15:50	1/20	3.58 (idle)	1.02×10^{-8}	47.17	36.52	77
SP-68 15:52	1/20	3.58 (matte charge)	1.02×10^{-8}	47.17	36.52	77
SP-69 15:54	1/20	3.58 (matte charge)	1.04×10^{-8}	47.17	37.23	79
SP-70 16:55	1/20	3.58 (slag skim)	1.15×10^{-8}	47.17	41.17	87
SP-71 16:57	1/20	3.58 (slag skim)	1.36×10^{-8}	47.17	48.69	103
SP-72 17:03	1/20	3.58 (slag skim)	1.62×10^{-8}	47.17	57.99	123
SP-73 17:05	1/20	3.58 (idle)	1.25×10^{-8}	47.17	44.75	95

[a] Excluded from average.

TABLE 21. SUMMARY OF OPACITY OF EMISSIONS ESCAPING AIR CURTAIN

Converter operation	Number of operations observed	Opacity, %		
		Average	Low	High
Cold addition charge (reverts and cold dope)	14	21	5	54
Matte charge	25	14	5	34
Scrap copper charge	5	18	9	28
Blister copper charge (imperfect anodes)	4	9	9	9
Slag skimming	31	18	2	50
Blister copper pour	9	9	5	17
Total	88			

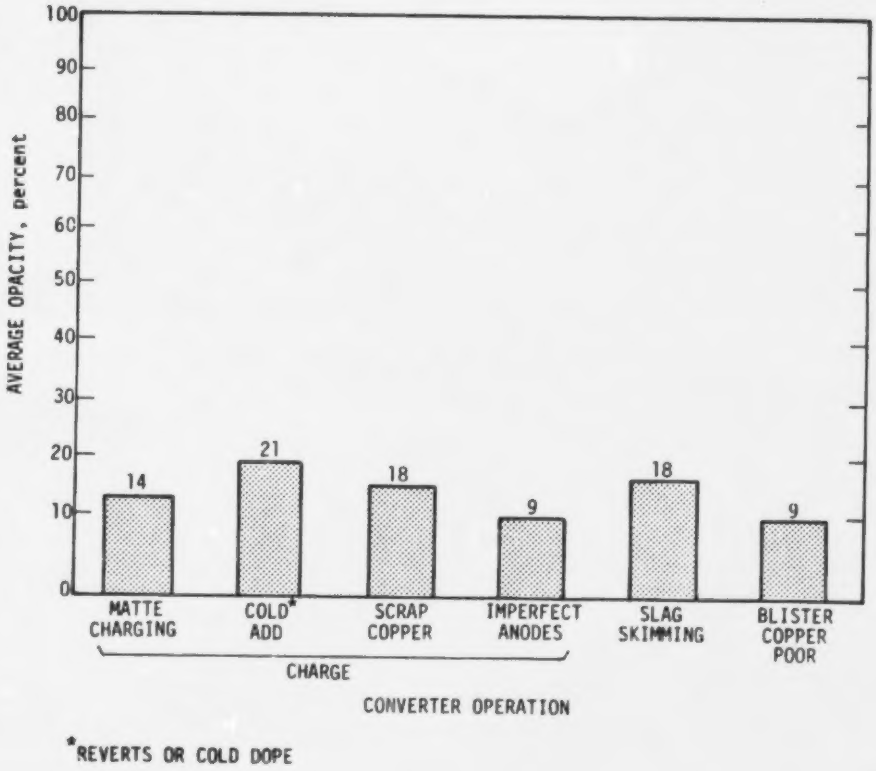

Figure 15. Average opacity vs. converter operation.

A total of 86 converter operations that generate fugitive emissions were monitored during the test program. Average opacities ranged from 9 percent during blister copper pouring to 21 percent during cold addition charging. Emissions from converter operations controlled by the primary hood (slag blowing and finish blowing) showed zero percent opacity from the air curtain. Because the air curtain was in operation during the entire testing program, there was no opportunity to evaluate fugitive emissions when the air curtain was not operating.

Two major problems were encountered during opacity monitoring. The first problem involved the strip-chart recorder, which was equipped with a capillary inking system. This system did not ink properly in the dusty environment of the smelter. Recorder chart speed was also restricted to 1 inch per hour, which resulted in poor resolution and the inability to separate events that occurred within short time intervals. Every effort was made to minimize the effect of these problems on data quality. To provide better resolution and to separate close-occurring events, the operator manually advance the strip chart. On Saturday, January 22, 1983, a dual-speed strip chart recorder was found and used during that test run. This recorder had chart speeds of 6 and 30 inches per hour. The faster speeds improved resolution and allowed events to be recorded on a real-time basis. The capillary ink system on the recorder was cleaned and flushed as frequently as practical.

The second problem involved blinding of the transmissometer by the crane block and cables as the crane moved in and out while servicing the converter. The instrument was mounted at the top of the secondary hood in a position that appeared to minimize the crane cables' interference with the measurement beam. This mounting arrangement proved to be satisfactory during most of the test program; however, on January 22 the second shift crane operator positioned the crane block so that the transmissometer beam was blocked during most of the charging and slagging operations that occurred between 3:30 p.m. and 9:30 p.m.

4.3 VISUAL OBSERVATIONS

Throughout the test program, Mr. Alfred Vervaert of the U.S. EPA and Mr. James Nolan of the Puget Sound Air Pollution Control Authority (PSAPCA) visually observed the hood's performance. In general, hood performance was characterized by estimating overall hood capture effectiveness and the location, approximate opacity, duration, and significance of any visible emissions observed. As shown in the observation logs, lighting and background conditions within the converter building made absolute opacity readings very difficult. Typed copies of the observation logs are in Appendix H. A summary of the visual estimation of hood capture efficiencies by converter event is presented in Table 22.

TABLE 22. SUMMARY OF VISUAL OBSERVATIONS OF HOOD CAPTURE EFFECTIVENESS BY CONVERTER EVENT

Converter event	Observer No. 1[a]		Observer No. 2[b]	
	No. of events observed[c]	Estimated hood capture efficiency,[d] %	No. of events observed[c]	Estimated hood capture efficiency[d], %
Roll-in Roll-out	21	77	20	76
Blow-hold	14	96	5	90
Matte-charge	42	94	33	91
Slag skim	34	78	30	82
Copper pour	12	92	12	85
Other additions	42	95	26	85

[a] Observer No. 1 was Mr. A.E. Vervart of the U.S. EPA.

[b] Observer No. 2 was Mr. J. Nolan of the PSAPCA.

[c] From observation logs (Appendix H). Represents number of recorded observations per event.

[d] Represents average value for the number of recorded events.

The estimated secondary hood capture efficiency as visually determined by two independent observers are comparable for each converter event. The largest discrepancy occurred during additions (other than copper matte) where average estimated capture efficiencies were 95 percent (Observer No. 1) and 85 percent (Observer No. 2). Average estimated capture efficiencies were equal to or greater than 85 percent for the following converter events: blow-hold, matte charging, copper pouring, and other additions (copper scrap, blister copper, etc.). These data compare favorably with the tracer recovery efficiencies measured in the control area for similar operating modes. Converter roll-in and roll-out events were characterized by average estimated capture efficiencies of 77 percent (Observer No. 1) and 76 percent (Observer No. 2). Slag skimming operations showed average capture efficiencies of 78 percent (Observer No. 1) and 82 percent (Observer No. 2).

Visual emissions observation revealed that converter and crane operations introduce significant variability in overall hood capture efficiency particularly for skimming operations. For example, as visually determined, hood capture effectiveness increased considerably (greater than 90 percent) during skimming operations when the overhead crane operator held the receiving ladle next to the converter while the converter was slowly rotated to the discharge position. In contrast, when the receiving ladle was placed on the ground during skimming operations and the slag discharge rate was rapid, considerable fumes spilled into the converter aisle. Converter and overhead crane operations were inconsistent throughout the entire test program.

Observations of visual emissions to estimate hood capture efficiency were made by assessing the overall capture effectiveness during specific operating modes. The duration and intensity of fugitive emissions generated were highly variable often lasting only seconds as recorded by the observers. Since these observations were overall assessments, that is, the entire converter-secondary hood area, they would not necessarily correspond to tracer gas recovery data for a given converter mode. For example and as noted previously, when the receiving ladle was placed on the ground during skimming operations and the slag discharge rate was rapid, considerable fumes spilled into the converter aisle. Tracer recovery tests performed in the upper control volume during such an event would not account for this spillage and would probably show a greater recovery efficiency than an overall visual assessment. For this reason, visual observation must be used in conjunction with the tracer to quantify capture effectiveness.

Data from the test program substantiates this fact as the average tracer recovery efficiency in the upper control area averaged over 90 percent during skimming operations compared to average visual assessments of 78 and 82 percent. In contrast, tracer recovery efficiencies from the special injection point tests during skimming operations averaged 84 percent.

In summary, the visual observation and tracer recovery data indicate that the fugitive emission capture effectiveness of the secondary hood is greater than 90 percent. The capture effectiveness during converter roll-in and roll-out and slag skimming operations is more variable than other converter modes since fugitive emissions generated during these events are more dependent upon converter and crane operations. It was observed that careful operation of the converter and ladle during the discharge of slag and blister copper could minimize the occurrence of fume "spillage" and provide capture efficiencies of 90 percent or greater.

Thermal lift plays a significant role in increased collection efficiencies for fumes generated in the lower portion of the control area. Also, the lower tracer recovery efficiencies for the various converter roll-out modes are indicative of fume spillage outside the control area.

It is believed that no practical correlation can be made between opacities recorded by the observers and the transmissometer. The transmissometer was mounted perpendicular to the longitudinal axis of the slot, whereas position of the visual observers was such that their view was parallel to the longitudinal axis of the slot, which resulted in a considerably longer path length through the escaping emissions. The apparent opacity increases as the path length through the emissions increases. Also, when positioned in front of the converter, the overhead crane interfered with visual observations above the slot area.

The observation logs, given in Table 23, describe the location, duration, and approximate opacity of escaping emissions and estimated hood capture efficiency for the three cycles evaluated.

TABLE 23. SUMMARY OF VISUAL OBSERVATIONS LOGS BY EVENT

			Observer 1				Observer 2			
Event	Date (1983)	Approximate time, h	Location of escaping emissions	Appoximate duration of emissions	Approximate opacity of escaping emissions	Approximate hood capture efficiency	Location of escaping emissions	Approximate duration of emissions	Approximate opacity of escaping emissions	Approximate hood capture efficiency
Cu pour	1/18	0915	Pour	1 min.	Moderate	≥95	Out front under sheet metal	Small puffs	10-20	>90
		1109	Pour	4 min.	Moderate	>95	Top right	3 min.	5-10	>90
		1112					Front		5-10	
		1115		1 min.	Moderate-heavy; 10	>95				>90
		1116	1° hood			100				
		1122	Out front	5 sec.		>95	Out front below sheet metal		5-10	~90
		1128	Upper right front of hood		Moderate-heavy; 20	90	Top right		10-20 cont; 35 large puffs	80
		1131	Front right		Heavy; 30	80	Slot/right front		5-10/40-50	70
		1137	Front right	15 sec.	Moderate-heavy	80	Front	15 sec.	60/10	~80
		1142	Front		30	80-90	Right front		10-20	80-90
		1146			Moderate	>95	Front		≤5	>90
		1200		10 sec.	Light-moderate	100	Left front	1 min.	15-20	80-90
		1204			Light-moderate	>95	Front		50	90
		1210			Light-moderate		Bottom front		20	70-80
Blow and hold	1/18	0805					Slot		10	
		0835					None			
		0900	None				None			
		0940[a]	None				None			
		1100	None				None			
		1510	None				None			
	1/19	0722[a]	None							
		0729			Little or none				Very little	
		0744[a]	None				2° hood-left rear	4 min.	5-10	
		0745	None							
		0757	None				2° hood-left rear	2 min.	5-10	
		0823[a]	Mouth		Light	100				
		0842	None				None			
		0854	1° hood	5 sec.	Very light	100				
		0856	1° hood	Slight puffing						
		0900					2° hood-left rear			
		0902	None							
		0907					None			
		0940	None				None			
		0945	1° hood		Light					
		1000	None				None			
		1238	None				2° hood-left rear	22 min.	20-40	
		1330	None				2° hood-left rear	≥25 min.	20-40	
		1356	1° hood		Light	100				
		1358	1° hood		Moderate	100				

(continued)

TABLE 23 (continued)

Event	Date (1983)	Approx-imate time, h	Observer 1				Observer 2			
			Location of escaping emissions	Appoximate duration of emissions	Approximate opacity of escaping emissions	Approximate hood capture efficiency	Location of escaping emissions	Approximate duration of emissions	Approximate opacity of escaping emissions	Approximate hood capture efficiency
Blow and hold (cont'd)	1/20	1000	1° hood	2 min.	Heavy	95	Slot	30 sec.	30	
		1003	1° hood		Moderate-heavy	95	Slot		5-10	90
		1012	1° hood		Very dense, 80	> 95	SiO_2 charge door	22 min.	Quite a bit	90
		1015	1° hood		Heavy	95				
		1018	1° hood		Heavy	95				90
		1043	All part 1° hood and converter		Extremely heavy	> 95	1° hood		100	90
		1500	Upper middle of opening	< 5 min.	Heavy; 20	95	None			
		1730			Moderate	100	None			
		1815		5 sec.	Heavy; 20-30	90	Top		Small amount	
	1/22	0910		10-15 sec.	Moderate	90	Back of converter			90
Slag skim	1/18	0911			Moderate-heavy	95	Front under sheet metal	Small puffs	10-20	>90
		1544		5 sec.	Heavy; 60	<60	Front of 2° hood	1 min.	100	50-70
		1547								90
		1552		30 sec.		<60	Right part 2° hood		60-80	90
		1554								
		1558	Front	60 sec.	> 30	<60	Front of hood	2 min.	80	50-70
	1/19	0807	Front		Light	<70	Front/some puff through slot		Heavy;60-80	50-70
			Mouth			100				
		0815	Pour	2½ min.	Moderate-heavy; 20	85-90	Slot/front right	Small puffs	10-20/20	90
		0823	Front	3 min.		<80-90	--/Front right	--/puffs	Moderate/30	> 90
		0912	Front	1 min.	Heavy-v. heavy; 20-30		Front and slot	1 min.	30-40	70
			Mouth		Light	100				
		0922	Front	3½ min.	Moderate-heavy; 20-30	<80-90	Front		30-40	80-90
		1007	Front		Very heavy	<50-80	Front/slot	Puffs/puffs	40/10-40	90
		1028	Front right	7 min.	Heavy; 20-30		Slot/front	5 min.	20/60	50-90; avg. ~80
	1/20	1045				<80		15 sec.	40	70-90
		1048	Front	3 min.	Moderate-heavy; 20	90	20% of front of hood (lower right)	1½ min-puffs	40	90
		1052	Front	5-10 sec.	Moderate; 30					
			Front	2 min.		70-80; overall 80	Top right right (5-90% of hood area)	2 min.	20	90

(continued)

TABLE 23 (continued)

			Observer 1				Observer 2			
Event	Date (1983)	Approximate time, h	Location of escaping emissions	Appoximate duration of emissions	Approximate opacity of escaping emissions	Approximate hood capture efficiency	Location of escaping emissions	Approximate duration of emissions	Approximate opacity of escaping emissions	Approximate hood capture efficiency
Slag skim (cont'd)	1/20	1058	Front	2 min.	20	80-90; overall 85	Lower right front (30% of 2° hood face)	1½ min.	20-40	80
		1424	Front	<2 min.		70	Front (25% of face)/slot	45 sec.	40-60/20	70
		1432	Front	1½ min.	Moderate-heavy; 20-30	70	Front (25%)/slot	1½ min.	50-60/10	80
		1438	Front	2 min. 45 sec.	Heavy; 10-20	70-80	Right front face (20%)	3 min.	20-30	80-90
		1537	Right front	50 sec.	Heavy Light	70 100	Front (25%)	1 min.	40-50	70-80
		1545	Front	54 sec.	Heavy; 30-40	70	Front (25%)	2 min.	30-40	70-80
		1655	Front		Moderate-heavy; 20	80-90	Slot/face (20%)	1½ min. puffs	40/60-80	80
		1703			Heavy; 20-30	80	Slot/face (50%)	3½ min.	20/40	80-90
Slag skim (cont'd)	1/22	0959		45 sec.	Moderate-heavy	95	Right front	50 sec. puffs	40	>90
		1002		1 min. 45 sec.	20; moderate-heavy	95		1 min. 45 sec.		>90
		1012		45 sec.	Moderate-heavy; 20	90	Slot	2 min. 45 sec. (slight puffs)	10-20	>90
		1137			Heavy	70-80	Slot/front	30 sec. puffs	40-50/40	80-90
		1140	Right front		Heavy; <20	70-90	Front/slot	1½ min. puffs	20/10	90
		1145		2 min. 43 sec.	Moderate-heavy; <20	80-95; overall 90	Front	3 min. puffs	20	>90
		1153		3 min. 53 sec.	Moderate-heavy; 10-20-30	80-95; overall 90	Front	4 min. puffs	40	>90
		1622		2 min	Heavy; 20	80				
		1628	Mouth		Moderate	90				
		1630		2 min. 10 sec.	Heavy; 20-40	70				
		1718		3 min. 35 sec.	Heavy; 20	80-90; overall 85				
Other additions										
Blister Cu-ladle,	1/18	0921			Moderate-heavy	>95	Front	Small puffs		
Cu slag		1243	Behind 2° hood; SiO_2 chg. chute	15 min.	40-50	>90	Top of hood		80	80-90

(continued)

TABLE 23 (continued)

Event	Date (1983)	Approximate time, h	Observer 1				Observer 2			
			Location of escaping emissions	Appoximate duration of emissions	Approximate opacity of escaping emissions	Approximate hood capture efficiency	Location of escaping emissions	Approximate duration of emissions	Approximate opacity of escaping emissions	Approximate hood capture efficiency
Anode slag		1305		3 min.	10-20	90->95	Slot		20-30;upto 80	>90
--		1311	1° hood		Moderate-light; <5	90				100
Cu slag		1344		1 min.		95	Slot		30-40	>90
--		1348				100				
Scrap		1509					Front and top of hood	Short duration	100	~25
Shell slag		1511						½ min.	100	~25
SiO_2		1514	1° hood-mid-pt.		Light		1° hood		60-70	Effectively controlled
SiO_2		1515	1° hood	5 sec.	30					
SiO_2		1517								
--		1520					Top left rear of 2° hood		10-20	
--		1521	Behind 2° hood		20					
--		1522	1° hood	2 sec.		>95				
--		1524					Left top rear of 2° hood		5-10	
--		1525	1° hood			100	Left rear of of 2° hood		20-30	
--		1530					Left rear of of 2° hood		10-20	
Shell slag	1/19	0725				100				
SiO_2		0731	1° hood		Light	100				
--		0744	None				Left rear of of 2° hood		5-10	

(continued)

TABLE 23 (continued)

Event	Date (1983)	Approx-imate time, h	Observer 1				Observer 2			
			Location of escaping emissions	Appoximate duration of emissions	Approximate opac-ity of escaping emissions	Approximate hood capture efficiency	Location of escaping emissions	Approximate duration of emissions	Approximate opac-ity of escaping emissions	Approximate hood capture efficiency
SiO_2		0755								
--		0757	None				Rear left of 2° hood		5-10	
Shell slag		0836	Right front	2 sec	20	85-85; overall 90	Front	Puffs	40-60	>90
Shell slag		0840				100				≥95
Shell slag		0936			60	40-95; overall 85	Slot and top of front		80-100	50-60
2 scrap charges		1127-1135								
Scrap		1229		30 sec.	60-70	70-80	Slot	1 puff	40	>90
--						90-95				
Scrap		1235	Slot	15-20 sec.	50-60		Slot	1 puff	30-40	>90
Scrap		1316		1 min.	20	>90	Slot	5 sec. 1 min.	60 5-10	>90
Scrap-large piece		1317				>90	Slot	5 sec. 1 min.	60 5-10	>90
Scrap		1410					Slot	Puff		>90
Shell slag	1/20	0947	Rear right		40	95	Rear of slot/ top right front of 2° hood	40 sec/ puffs	40-100/10	80
Shell slag		0952		28 sec.	60	>95 even-tually	Right side of slot	30 sec.	40-60	80
SiO_2		1008	1° hood		Heavy	95	1° hood		Heavy	>90

(continued)

TABLE 23 (continued)

			Observer 1				Observer 2			
Event	Date (1983)	Approx-imate time, h	Location of escaping emissions	Appoximate duration of emissions	Approximate opac-ity of escaping emissions	Approximate hood capture efficiency	Location of escaping emissions	Approximate duration of emissions	Approximate opac-ity of escaping emissions	Approximate hood capture efficiency
SiO_2		1011	1° hood		80	>95	1° hood		Very heavy	>90
Shell slag		1117		20 sec.		100		20 sec.		>90
Shell slag		1118		20 sec.		100		15 sec.		>90
Shell slag		1454		3 sec.	30-40	>95	Slot	Puffs	20	>90
Shell slag		1457				>95				100
SiO_2		1505								
Blister Cu block		1808				95				
Blister Cu block		1810				>95				
Blister Cu block		1812				>95				
Blister Cu block		1814				100				
Shell slag	1/22	0907	Upper right front	2 sec.	30	90-95; overall 95	Right front face/slot	1 puff/puffs	60/50	>90
Shell slag		0911				100				100
Shell slag		1051	Upper right rear	10 sec.		>95		20 sec.		100
Shell slag		1055				100		15 sec.		100
SiO_2		1605	None							

(continued)

TABLE 23 (continued)

			Observer 1				Observer 2			
Event	Date (1983)	Approx-imate time, h	Location of escaping emissions	Appoximate duration of emissions	Approximate opac-ity of escaping emissions	Approximate hood capture efficiency	Location of escaping emissions	Approximate duration of emissions	Approximate opac-ity of escaping emissions	Approximate hood capture efficiency
SiO_2		1705	None							
Blister Cu block		1726		5 sec.		100				
Blister Cu block		1738		5 sec.		100				
Blister Cu block		1731		5 sec.		100				
Blister Cu block		1733		5 sec.		100				
Blister Cu block		1735		5 sec.		100				
Cu spills		1827				95				
Blister Cu block		1832	Top			90				
Blister Bu block		1834				95				
Powdered scrap		2033				80 prior to fire				
Powdered scrap		2116				Undeter-minable				
Matte charge	1/18	1237	Ladle	5 min.	Heavy-v. heavy V. light	>95 100	Front	Small puffs	5	>90
		1240		30 sec.	Heavy-v. heavy	>95	Front/top		5/5-10	>95
		1300		10 sec.			Top		5-10	>90
		1313	Top of hood 1° hood	15 sec.	V. heavy; 30 Moderate; <10	>95 95	Slot/front	--/few puffs	20/10-20	>90
		1325[a]	Mouth		Light	>95				

(continued)

TABLE 23 (continued)

Event	Date (1983)	Approx-imate time, h	Observer 1				Observer 2			
			Location of escaping emissions	Appoximate duration of emissions	Approximate opacity of escaping emissions	Approximate hood capture efficiency	Location of escaping emissions	Approximate duration of emissions	Approximate opacity of escaping emissions	Approximate hood capture efficiency
Matte charge (cont'd)	1/18	1327	1° hood	30 sec.	V. heavy; <20	>95 >95	Slot		10-20	>95
		1335[a]	1° hood (mid-pt)			Nearly 100				
		1340	Top	30 sec.	Heavy	>95	Slot		15-20	>90
		1616		10 sec.	Heavy	95	Top right front	20 sec.	40	80-90
		1618	Mouth	1-2 sec.	20	>90 100				>90
		1621	Front		Heavy; 20-30	>80	Right front of hood	30 sec.	40-60	80-90
	1/19	0830		30 sec.	Heavy	>95		30 sec.		>95
		0834		30 sec.	<20	>95		30 sec.		>90
		0932	Mouth	15 sec.	Light	95 100		10 sec.		>90
		0939		18 sec.		>95		15 sec.		>95
	1/20	0822			Heavy	<50				
				45 sec.		90%	Top 10% of face/ slot	Puff/1½ min	4-60/50	80
			Mouth		Moderate	100				>95
		0833	Mouth		Moderate	100				
		0840		20 sec.	15	>90	Slot	Puff	10-20	>90 >90
		0854		20 sec.	Moderate-heavy	95		15 sec.		>90
		0855								>95
		0909	Above air jet	5 sec.	>20	<90; range 85-95	Slot	15 sec.	10-20	>90

(continued)

TABLE 23 (continued)

Event	Date (1983)	Approx-imate time, h	Observer 1				Observer 2			
			Location of escaping emissions	Appoximate duration of emissions	Approximate opacity of escaping emissions	Approximate hood capture efficiency	Location of escaping emissions	Approximate duration of emissions	Approximate opacity of escaping emissions	Approximate hood capture efficiency
Matte charge (cont'd)	1/20	0911								>95
		0915				>95				
		0926	Right rear of hood	Large puffs	30	>90				>90
		0930			Moderate	95				>95
		0944	Right rear			95				>90
		0958	Right rear	Large puffs		95	Slot		10-20	>90
		1110	Right rear	Brief puffing		>95				
		1111				>95				
		1114				>95				
		1449	Ladle	5 sec.		90-95	Slot/front	Puffs	5-10/20	>90
		1452		25 sec.		95		17 sec.		>90
		1554		20 sec.		>95	Slot	Small puffs		>95
		1608		15 sec.		>95		15 sec.		>95
	1/22	1046		20 sec.	20	95	Slot	25 sec. (puffs)	20-40	>90
		1047		20 sec.	20	95	Slot	Small puffs		>90
		1206		20 sec.		100		15 sec.		>90
		1209		15 sec.		>95		20 sec.		>90
Roll-in Roll-out										
In Out	1/18	0805 0906		15 sec.		75 100	Slot	½ min.	<10 20-30 0	~70-80 >90
In Out		1045 1109		12 sec.	Light 30	100 70	None Top	10 sec.	20-30	

(continued)

TABLE 23 (continued)

Event	Date (1983)	Approx-imate time, h	Observer 1				Observer 2			
			Location of escaping emissions	Appoximate duration of emissions	Approximate opac-ity of escaping emissions	Approximate hood capture efficiency	Location of escaping emissions	Approximate duration of emissions	Approximate opac-ity of escaping emissions	Approximate hood capture efficiency
Roll-in Roll-out										
Out		1544		5 sec.	60	<60		1 min.	100	50-70
In	1/19	0729								
Out		0807		5-10 sec.	40-50	<50	Slot (some from front)	30 sec.	50-60	70
In		0842			Moderate-heavy	>95				
Out		0912								50
In		0940								
Out		1007				<50	Slot and top front of hood			50 max.
In				2 sec.		90				
Out		1028			30-40	<50		30 sec.		50
Out		1223	Hood	30 sec.	~20		Front	15 sec.	~20	>90
Out		1312		5 sec.	30		Slot	10 sec.	30	70-80
In		1319				>90				
Out		1408					Slot	10 sec.	40	70
--										>90
In	1/20	1119				>95	1° hood			>90
Out		1129			100					
In/Out		1139								
In/Out		1142								
In/Out		1214								
Out		1424					Slot	20 sec.	60	70-80
Out		1537				Undeter-minable	Top of hood and 2° hood slot	10 sec.		
In		1615				100				
Out		1756						~45 sec.		50-60
In		1815		2 sec.	20-30	90	Top			

(continued)

TABLE 23 (continued)

Event	Date (1983)	Approx-imate time, h	Observer 1				Observer 2			
			Location of escaping emissions	Appoximate duration of emissions	Approximate opacity of escaping emissions	Approximate hood capture efficiency	Location of escaping emissions	Approximate duration of emissions	Approximate opacity of escaping emissions	Approximate hood capture efficiency
Roll-in Roll-out										
In		1915								99
Out		1959	Over top of hood	10 sec.	Light	90				
In	1/22	0913								>90
Out		0952		5 sec.	40-60	60-70				90
In		1057								>90
Out		1138	Right front	10 sec.	20 (pen. 40-60)	70	Top	Large puffs		80
Out		1716				<50				
In		1736				100				
Out		1823								
Out		1931				60				
Out		2115		5 sec.	40	60				

SECTION 5

EMISSION FACTOR DEVELOPMENT

This section summarizes emission test results for sulfur dioxide, filterable particulate, filterable and gaseous arsenic, particle size distribution (inhalable particulate), and trace metals in the exhaust stream of the secondary hood or air curtain system.* Results for each pollutant are reported separately, and where applicable, emission factors have been developed for overall converter operation and specific operational modes (charging, skimming, and blowing). As noted previously, converter production curtailments were caused by stagnant air conditions and process operational problems resulted in frequently interrupted test activity. For these reasons, only three converter cycle segments (Section 3) were evaluated instead of four complete cycles as originally planned. Except for the basic cycle operations normally encountered during the converter process (i.e., matte charges, slag skimming, etc.) specific process operational details, such as the number of ladles of matte charged, the number of ladles skimmed, the number and type of other charges (scrap, copper slag, anode slag, and blister copper), and event duration, varied greatly. Consequently, between-cycle data comparisons are likely to show a degree of variability attributed primarily to process operation.

Appendix A contains example calculations and computer printouts of all the emission results. Appendices B and C present field and laboratory data. Appendix D details the sample and analytical procedures used during this test program, and Appendix E summarizes equipment calibration procedures and results.

---

*No measurements were made in the primary hood exhaust stream which contains the bulk of the converter emissions.

5.1 SULFUR DIOXIDE (SO_2)

The SO_2 continuous emission monitor (CEM) was set up, calibrated, and allowed to stabilize for 24 hours before data collection was begun. The CEM recorded the better part of six converter cycles between January 14 and January 22, 1983. The initial matte charge for Charge 76 took place shortly before the CEM system began sampling. The finish blow and copper pour emissions at the end of Charge 76 were discarded because of the failure of a manometer in the CEM sample interface. The CEM system was returned to service in time to record over 90 percent of the emissions from Charge 77. The hood SO_2 emissions for Charges 78 through 81 were continuously recorded with only minor gaps for daily calibration and maintenance. High concentrations recorded during standby which occurred on January 17 during Cycle 78 and high concentrations which occurred as a result of a primary hood malfunction on January 22 during Charge 80 were not included in the summary of charge or cycle emissions.

At the end of data collection, 200 hours of strip chart recordings were evaluated. The PEDCo operator's logs and notations on the SO_2 strip chart identified individual emission episodes and operating modes. The ASARCO operator's log provided the number of ladles charged and skimmed and the tons of copper produced per charge. Under normal operating conditions, the measured SO_2 emission data appeared on the strip chart as a series of well-defined peaks. Each individual peak was treated as a separate emission event. The maximum SO_2 concentration was calculated from total peak height. The average SO_2 concentration was calculated by dividing peak area by peak duration. Individual SO_2 emission rates were calculated using the average SO_2 concentration of each peak and the exhaust flow rates measured at the air curtain hood test location. These individual emission rates were multiplied by event duration to yield the mass of SO_2 emitted per event.

More than 470 individual data points were reduced and used in the calculation of the overall emission factors presented in Table 24. The results for Charge 76 are not representative because a large portion of the cycle could not be included. The results for Charge 78 include SO_2 emissions for matte charges during the early morning hours of January 18 that are much higher than any other cycle. Based only on the data gathered for Charges 77, 79, 80, and 81, the SO_2 emission factor for one converter cycle is estimated to be approximately 7 pounds of SO_2 per ton of copper produced. The average concentration of SO_2 emitted during normal operation for all six charges was approximately 90 ppm. The cycle and mode SO_2 averages are the sum of the average individual event concentrations times the individual event duration divided by the total duration of events.

Since each peak was integrated from baseline to baseline, the periods between peaks, defined as zero emissions, were not included in the average values. The maximum and minimum emissions throughout each cycle varied greatly, as shown in Table 24, from peaks which exceeded 7000 ppm SO_2 to low level emissions that averaged only 1 ppm SO_2.

The SO_2 emissions within each cycle were evaluated in relation to specific operating modes. Table 25 summarizes the SO_2 emissions that occurred during matte charges. If the data from Charges 76 and 77 are disregarded as incomplete, the average number of matte charges per cycle is 14, and SO_2 emissions averaged 0.53 Kg/Mg (1.16 lb per ton) copper produced. The SO_2 emissions for individual matte charges also varied significantly from maximum concentrations of more than 1530 ppm to a minimum concentration of 30 ppm. The average concentration for all matte charges was approximately 120 ppm SO_2. The SO_2 emissions from slag skimming are summarized in Table 26. The average number of slag skims for each cycle was 10, and the average SO_2 emission rate was 0.36 Kg/Mg (0.8 lb/ton). The maximum slag skim SO_2 emission concentrations did not exceed 572 ppm while the minimum

TABLE 24. SO_2 EMISSION SUMMARY

	Charge No.					
	76[a]	77[b]	78[c]	79	80[d]	81
SO_2, Kg (lb)	174 (384)	390 (859)	849 (1872)	553 (1220)	370 (815)	366 (795)
Copper, Megagrams (tons)	163 (180)	100 (110)	113 (125)	136 (150)	109 (120)	136 (150)
Emission factor, Kg/Megagram (lb/ton)	.97 (2.13)	3.54 (7.81)	6.80 (15.0)	3.69 (8.13)	3.08 (6.79)	2.40 (5.30)
Maximum SO_2[e,f] concentration, ppm	>983	>1330	6690	>7000	1780	1165
Minimum SO_2[g] concentration, ppm	4.0	4.0	29	1.0	2.1	30
Average SO_2[h] concentration, ppm	68	83	112	108	89	77

[a] Incomplete cycle; initial matte charge, finish blow, and copper pour not included.

[b] Incomplete cycle; initial matte charge not included.

[c] High SO_2 emissions during standby; overnight 1/16-1/17 not included.

[d] High SO_2 emissions during primary hood malfunction not included.

[e] SO_2 concentration measured by peak height.

[f] Parts per million, ppm, dry basis.

[g] SO_2 concentration measured by peak height, periods with zero emissions not included.

[h] Time weighted average of operating mode average concentrations.

TABLE 25. SO_2 EMISSION DURING MATTE CHARGES

	Charge No.					
	76	77	78	79	80	81
Number of events	8	7	13	14	13	16
Average duration, min.	4	6	6	4	3	3
Total SO_2, Kg (lb)	27 (59.0)	17 (38.8)	119 (261.3)	39 (85.9)	52 (115.5)	66 (145.1)
Average SO_2/event, Kg (lb)	3.4 (7.4)	2.5 (5.5)	9.1 (20.1)	2.8 (6.1)	4.0 (8.9)	4.1 (9.07)
SO_2/ton Cu, Kg (lb)	0.15 (0.33)	0.16 (0.35)	0.95 (2.09)	0.26 (0.57)	0.45 (1.0)	0.44 (0.97)
Maximum SO_2 concentration, ppm	981	283	1210	805	>1530	728
Minimum SO_2 concentration,[a] ppm	88	56	154	106	122	30
Average SO_2 concentration,[a] ppm	100	53	180	94	168	124

[a] Periods of zero emissions not included.

TABLE 26. SO_2 EMISSION DURING SLAG SKIMS

	Charge No.					
	76	77	78	79	80	81
Number of events	10	7	13	9	10	11
Average duration, min.	6	7	4	4	3	4
Total SO_2, Kg (lb)	35.7 (78.7)	61.3 (135.2)	54.7 (120.6)	31.8 (70.2)	42.5 (93.8)	60.9 (134.2)
Average SO_2/event, Kg (lb)	3.6 (7.9)	8.8 (19.3)	4.2 (9.3)	3.5 (7.8)	4.3 (9.4)	5.5 (12.2)
SO_2/ton Cu, Kg (lb)	0.20 (0.44)	0.56 (1.23)	0.44 (0.96)	0.21 (0.47)	0.35 (0.78)	0.40 (0.89)
Maximum SO_2 concentration, ppm	431	515	572	261	266	358
Minimum SO_2 concentration,[a] ppm	46	166	86	97	112	75
Average SO_2 concentration,[a] ppm	81	141	148	124	148	153

[a] Periods of zero emissions not included.

emission concentrations were 46 ppm SO_2. The average concentration during all slag skims was approximately 133 ppm. Table 27 summarizes average SO_2 emissions during copper pours. The emission episodes from this process were the most uniform, with an average emission factor of 0.30 Kg/Mg (0.67 lb SO_2/ton). The copper pour emissions generally began with one large peak followed by peaks of steadily decreasing size. The maximum peak concentration was 729 ppm SO_2 and the minimum peak concentration was 30 ppm SO_2. The average SO_2 concentration during all copper pour was 75 ppm.

The cold addition mode included all ladles of material charged to the converter except copper matte. Emissions from these charges, which included shell reverts and scrap copper, varied significantly throughout the cycles. An occasional ladle of anode furnace slag was also included in this group, even though it was in a molten state when charged to the converter. These anode slag additions generated the most intense SO_2 emissions episodes, and several peaks were measured at more than 6000 ppm SO_2. The average emission rates shown in Table 28 reflect the wide divergence within this group. The overall cold addition average was 1.2 Kg/Mg (2.65 lb SO_2/ton) copper. The peak emissions concentration during cold additions exceeded the measurement capacity of the SO_2 analyzer, which was approximately 7000 ppm. The minimum peak concentrations were 30 ppm SO_2. The overall average emission concentrations during cold addition was approximately 300 ppm.

Table 29 lists SO_2 emissions during standby, idle, or blow modes. Standby mode included those periods when the converter was on hold due to meteorological production curtailments. Idle mode included periods of maintenance downtime during a production cycle or periods of converter inactivity between production cycles. Emission data collected when the tuyere lines were blowing are included in this summary. Periods when the converter was on hold for more than one hour were considered process upsets and are not included in these data. This group is characterized

TABLE 27. SO_2 EMISSION DURING COPPER POUR

	Charge No.[a]				
	77	78	79	80	81
Number of events	12	14	11	10	11
Average duration, min.	4	4	3	4	4
Total SO_2, Kg (lb)	26.2 (57.8)	37.6 (82.9)	52.1 (114.9)	56.1 (123.7)	25.9 (57.0)
Average SO_2/event, Kg (lb)	2.2 (4.81)	15.2 (6.91)	3.7 (8.21)	5.1 (11.25)	2.6 (5.7)
SO_2/ton Cu, Kg (lb)	0.24 (0.53)	0.30 (0.66)	0.35 (0.77)	0.47 (1.03)	0.17 (0.38)
Maximum SO_2 concentration, ppm	374	729	496	644	243
Minimum SO_2 concentration,[a] ppm	30	55	62	154	90
Average SO_2 concentration,[b] ppm	42	78	116	141	73

[a] No available data from Charge No. 76 copper pour.

[b] Periods of zero emissions not included.

TABLE 28. SO_2 EMISSION DURING COLD ADDITIONS

	Charge No.					
	76	77	78	79	80	81
Number of events	10	10	9	14	10	14
Average duration, min.	4	7	4	5	3	3
Total SO_2, Kg (lb)	45.8 (101.0)	167.7 (369.6)	281.1 (619.8)	337.6 (744.3)	79.2 (174.6)	40.4 (89.0)
Average SO_2/event, Kg (lb)	4.6 (10.1)	16.8 (37.0)	31.3 (68.9)	24.1 (53.2)	7.9 (17.5)	2.9 (6.4)
SO_2/ton Cu, Kg (lb)	0.25 (0.56)	1.5 (3.36)	2.2 (4.96)	2.2 (4.96)	0.66 (1.46)	0.27 (0.59)
Maximum SO_2 concentration, ppm	987	>1330	6690	>7000	1470	486
Minimum SO_2[a] concentration, ppm	82	126	86	36	140	30
Average SO_2[a] concentration, ppm	131	296	536	500	274	99

[a] Periods of zero emissions not included.

TABLE 29. SO_2 EMISSION DURING STANDBY, BLOW, AND IDLE MODES

	Charge No.					
	76	77	78	79	80	81
Number of events	10	14	15	11	11	10
Average duration, min.	18	24	26	31	28	20
Total SO_2, Kg (lb)	5.10 (11.0)	17.6 (38.7)	43.5 (96.0)	1.4 (3.04)	8.3 (18.4)	38.2 (84.16)
Average SO_2/event, Kg (lb)	0.50 (1.1)	1.3 (2.8)	2.9 (6.4)	0.14 (0.3)	0.77 (1.7)	3.8 (8.4)
SO_2/ton Cu, Kg (lb)	0.03 (0.06)	0.16 (0.35)	0.35 (0.77)	.009 (0.02)	0.07 (0.15)	0.25 (0.56)
Maximum SO_2 concentration, ppm	75	107	257	20	260	169
Minimum SO_2 concentration,[a] ppm	4.0	4.0	29	1.0	2.1	118
Average SO_2 concentration,[b] ppm	11	14	41	2.0	20	20

[a] Periods of zero emissions not included.

[b] Periods of zero emissions greater than one hour in duration are not included.

by periods of very low SO_2 emissions that occur when the primary hood is down. Most of the data collected during the blow modes show no detectable SO_2. This is due in part to the high instrument range used to detect the intense emission episodes. The lower detectable limit on the high- and mid-ranges of the SO_2 analyzer were 16 ppm and 2.5 ppm, respectively. On one of the few occasions when the SO_2 analyzer was switched to the low range it showed readings of approximately 1 and 2 ppm SO_2 during the converter blows. This low level could have resulted from residual SO_2 in the system. The distinct peaks with concentrations over 200 ppm that occurred during the blow mode could represent fugitive emissions captured from other nearby converters. The overall average concentrations during the blow mode was less than 20 ppm SO_2.

The emissions recorded during the converter roll-out mode (summarized in Table 30) include all the peaks that immediately precede or follow a converter blow. These emissions are generated when the primary hood is raised or lowered while air is blowing through the tuyere lines. The converter operators are responsible for controlling this aspect; as a result, the converter roll-out emissions range from zero to more than 2000 ppm SO_2. The overall average during this mode was 1.05 Kg SO_2/Mg (2.32 lb SO_2/ton) copper. The overall average concentration during the converter roll-out is approximately 330 ppm SO_2. The data segments that were not included in the data summaries just discussed are listed in Table 31. These include all idle periods of one hour or more in duration, as well as two significant periods of unusually high or sustained emissions that qualified as process upsets.

One of the high emission periods was due to a loss in primary hood draft as a result of operating problems in the chemical plant. This upset which occurred during Charge 80 was characterized by frequent releases of smoke from the primary hood during the blow mode. The SO_2 emissions were very intense and irregular, reaching maximum concentrations of 3420 ppm. The minimum

TABLE 30. SO_2 EMISSION DURING CONVERTER ROLLS

	Charge No.					
	76	77	78	79	80	81
Number of events	10	7	19	12	15	16
Average duration, min.	4	4	3	3	3	5
Total SO_2, Kg (lb)	61 (134.4)	127.8 (281.7)	313.8 (691.8)	92.4 (203.7)	130.9 (288.5)	129.5 (285.4)
Average SO_2/event, Kg (lb)	6.1 (13.4)	14.2 (31.2)	16.5 (36.4)	7.7 (17.0)	8.7 (19.2)	8.1 (17.8)
SO_2/ton Cu, Kg (lb)	0.34 (0.75)	0.90 (1.99)	2.5 (5.53)	0.62 (1.36)	1.09 (2.4)	0.86 (1.9)
Maximum SO_2 concentration, ppm	>983	>727	2300	1010	1780	1170
Minimum SO_2 concentration,[a] ppm	86	143	62	77	18	154
Average SO_2 concentration,[a] ppm	212	399	472	321	320	255

[a] Periods of zero emissions not included.

TABLE 31. SO_2 EMISSION DURING UPSET CONDITIONS[a]

	Charge No.						
	77	78	78	79	80	80	81
Mode	Standby	Standby	Standby	Standby	Standby	Primary hood leak	Standby
Duration, min.	583	568	1032	904	92	82	1902
Total SO_2, Kg (lb)	0.51 (1.12)	176.7 (389.6)	0.0	0.0	0.0	174 (383.7)	0.0
Maximum SO_2 concentration, ppm	30.0	83	0.0	0.0	0.0	3420	0.0
Minimum SO_2 concentration, ppm	-	40	-	-	-	204	-
Average SO_2 concentration, ppm	<1.0	59	0.0	0.0	0.0	889	0.0

---

[a] These values are not included in previous data summaries.

SO_2 concentrations fell to 204 ppm between puffs but the overall average concentration was close to 1000 ppm. The other high emission period occurred during a standby mode during Charge 78. The emissions were characterized by consistent low level emissions. One SO_2 peak did occur during this time reaching a maximum concentration of 128 ppm. The average concentration was approximately 50 ppm and the emission slowly tapered off toward the end of this period to reach the minimum value of 31 ppm. The emission episodes described above occurred during apparent upset conditions. A comparison was made between these two upsets and similar operations which were conducted during the same charge cycle after the upset was corrected. These data are presented in Table 32. The normal operation data chosen for this table was collected on the low range of the analyzer. It is characterized by flat traces which taper towards zero. As seen on Table 29, some peaks did occur during the blow, standby, and idle modes. In general, the periods of operation when the primary hood was down had very low SO_2 emissions which would indicate efficient primary hood operation.

A detailed summary of emissions is given in Appendix B, along with examples of the strip charts. The data reduction methods are included in Appendix D.

5.2 FILTERABLE PARTICULATE EMISSIONS

Table 33 summarizes the flue gas conditions and particulate emissions data collected during the particulate/arsenic test runs. Volumetric flow rates are expressed in cubic meters per second and actual cubic feet per minute at stack conditions. Flow rates corrected to standard conditions [20°C and 760 mm Hg (68°F and 29.92 in.Hg) and zero percent moisture] are expressed as dry normal cubic meters per minute and dry standard cubic feet per minute. Particulate concentrations are reported in milligrams per dry normal cubic meter and grains per dry standard cubic foot. Emission rates are expressed in kilograms per hour and pounds per hour. The product of the concentration and the

TABLE 32. COMPARISON OF SO_2 EMISSION DURING NORMAL AND UPSET PRIMARY HOOD OPERATION

	Charge No.			
	78	79	80	80
Primary hood operation	Upset	Normal	Upset	Normal
Converter mode	Standby	Finish blow and standby	Blow	Blow
Duration, min.	558	92	82	62
Maximum SO_2 concentration, ppm	128	1.7	3420	3.0
Minimum SO_2 concentration, ppm	31	0.6	204	1.0
Average SO_2 concentration, ppm	50	1.2	889	2.0
Total SO_2, lb	352	1.36	383	1.55

TABLE 33. SUMMARY OF FILTERABLE PARTICULATE EMISSIONS DATA

Run No.	Date (1983)	Sampling period	Sampling time, min.	Sample volume		Filterable particulate mass, mg	Filterable particulate concentration		Filterable particulate emission rate	
				dNm^3	dscf		mg/dNm^3	gr/dscf	kg/h	lb/h
						Total cycle				
PATC-1	1/18 1/19	0806-1604 0745-1403	650.0	11.218	396.173	364.9	32.5	0.014	5.2	11.5
PATC-2	1/20	0820-2003	470.0	6.657	235.103	307.5	46.2	0.020	7.3	16.1
PATC-3	1/22	0910-2343	453.0	7.474	263.952	153.6	20.6	0.009	3.2	7.1
Average							33.1	0.014	5.2	11.6
						Specific mode				
PASM-1	1/18 1/19	0909-1625 0830-1322	233.5	3.475	122.709	227.8	65.6	0.029	14.3	31.6
PASM-2	1/20	0820-1832	131.6	1.885	66.565	194.9	103.4	0.045	22.2	49.0
PASM-3	1/22	0955-1930	40.4	0.638	22.536	62.4	97.8	0.043	21.2	46.8
Average							88.9	0.039	19.2	42.5

Run No.	Date (1983)	Flow rate				Temperature		Moisture, %	CO$_2$, %	O$_2$, %	Isokinetics, %
		Standard		Actual							
		dNm^3/min	dscfm	m^3/min	acfm	°C	°F				
					Total cycle						
PATC-1	1/18 1/19	2,680	94,700	2,780	98,000	20	68	0.68	0.0	20.9	103.0
PATC-2	1/20	2,630	92,900	2,690	94,900	21	69	0.77	0.0	20.9	86.2
PATC-3	1/22	2,610	92,100	2,660	94,100	17	63	0.84	0.0	20.9	101.3
Average		2,640	93,200	2,710	95,700	19	67	0.76	0.0	20.9	-
					Specific mode						
PASM-1	1/18 1/19	3,571	126,924	3,552	126,232	27	80	0.71	0.0	20.9	100.0
PASM-2	1/20	3,571	126,924	3,552	126,232	23	74	0.37	0.0	20.9	100.8
PASM-3	1/22	3,571	126,924	3,552	126,232	22	72	1.16	0.0	20.9	102.2
Average		**3,571**	**126,924**	**3,522**	**126,232**	**24**	**75**	**0.75**	**0.0**	**20.9**	**-**

volumetric flow rate is the mass emission rate. For Tests PATC 1-3 (converter Cycle Nos. 79, 80, and 81, respectively), the measured flow rate obtained from traversing the exhaust flue was used in the calculation of mass emission rates. For Tests PASM 1-3, however, the average flow rate obtained from the volumetric flow evaluation of the high flow mode [3571 dNm^3/min (126,924 dscfm)] was used because testing was performed at a single point in the exhaust flue. These data are summarized in Table 11 (Section 4 pg. 48). The filterable particulate fraction represents material collected in the sample probe and on the filter, both of which were heated to approximately 121°C (250°F).

During total cycle testing, the volumetric flow rate (corrected to standard conditions) averaged 2640 dNm^3/min (93,200 dscfm), whereas the actual flow rate averaged 2710 m^3/min (95,700 acfm). The flue gas temperature averaged 19°C (66°F) and the moisture content averaged 0.76 percent; carbon dioxide and oxygen contents were 0.0 and 20.9 percent, respectively. The filterable particulate concentration ranged from 20.6 mg/dNm^3 (0.009 gr/dscf) to 46.2 mg/dNm^3 (0.02 gr/dscf).

For the specific mode tests, the filterable particulate concentration ranged from 65.6 mg/dNm^3 (0.029 gr/dscf) to 103.4 mg/dNm^3 (0.045 gr/dscf). Test PASM-3 was performed only during slag skimming and the measured concentration was 97.8 mg/dNm^3 (0.043 gr/dscf).

The filterable particulate concentration during Test No. PATC-2 was higher than the concentrations measured during the other two tests. At the conclusion of the test, a leak rate of 0.08 ft^3/min was found. The metered sample volume was corrected for this leak rate by multiplying the total sample time in minutes by the leak rate and subtracting the resulting value from the metered volume. Using the leak corrected sample volume, a particulate concentration of 46.2 mg/dNm^3 (0.02 gr/dscf) was calculated and reported in Table 33. Because the leak is believed to have occurred at the port change, correcting the sample volume for only the second port sample would result in a corrected particulate concentration of 0.018 gr/dscf. Particle size distribution results reported in Section 5.4 show the majority of particles to be less than 10 micrometers in diameter; therefore, the nonisokinetic sample condition calculated as a result of the leak correction (Table 33) would not have a significant impact on test results. Also, the loss of primary hood draft resulting from operating problems at the chemical plant occurred during this test run. As noted in Subsection 5.1, this upset was characterized by frequent releases of smoke and fumes from the primary hood during the blow mode. The full cycle sample train was run until the smoke releases totally overwhelmed the secondary hood at which time all sampling was terminated until repairs were completed. Since this condition did not occur during Tests PATC-1 or PATC-3, an increase in emission results for PATC-2 would be expected.

With regard to the development of emission factors, process curtailments and operational inconsistencies make it impractical to develop representative emission factors for the overall cycle on any basis other than a pound particulate per ton copper produced. Table 34 summarizes filterable particulate emission factors for the full-cycle (PATC) and specific-mode (PASM) tests. As discussed previously, Test PATC-2 is probably biased high because of an excessive post-test leak rate and subsequent sample volume correction and the loss of primary hood draft resulting in increased emissions during the blow mode. Also, Test PASM-3 was performed during slag skimming operations only. A total of 7.25 ladles of slag were skimmed from the converter during this test. Based on information supplied by ASARCO, each ladle contains 12 to 15 tons of slag. Therefore, during this test, between 87 and 109 tons of slag were skimmed, which yields an emission factor ranging from 0.29 lb of particulate per ton of slag skimmed to 0.36 lb/ton.

TABLE 34. PARTICULATE EMISSION FACTOR DEVELOPMENT

Converter cycle No.	Test I.D.	Date (1983)	Tons copper produced[a]	Total particulate,[b] lb	Emission factor, lb particulate/ ton copper produced
1	PATC-1	1/18-19	150	124.6	0.83
	PASM-1			123.0	0.82
2	PATC-2	1/20	120	126.0	1.05
	PASM-2			107.5	0.90
3	PATC-3	1/22	150	53.6	0.36
	PASM-3[c]			31.5[c]	0.21[c]

[a] Information obtained from ASARCO converter operation logs.

[b] Product of particulate mass emission rate and time of test.

[c] Slag skimming only.

The particulate emission results indicate that the majority of emissions are generated when the primary hood is raised, i.e., charging and skimming. This is substantiated by visual observations and the relative equality of the full cycle and specific mode emission results; specifically the total particulate and emission factor data presented in Table 34. Also, the results from the third converter cycle test (PATC-3 and PASM-3) clearly show the effects of variable converter cycle operation since the number of matte charges, slag skims, and cold additions were significantly less than the other converter cycle tests (see Section 3).

5.3 FILTERABLE AND GASEOUS ARSENIC

Table 35 summarizes the filterable and gaseous arsenic emissions data for tests conducted by EPA Reference Methods 5 and 108.* Two sampling trains were used to obtain the particulate

---

*40 CFR 60, Appendix A, Reference Method 5, July 1, 1982. Method 108 has been proposed and is in draft form.

TABLE 35. SUMMARY OF FILTERABLE AND GASEOUS ARSENIC EMISSION DATA

Cycle Test No.	Run No.	Date (1983)	Sampling period	Concentration[a]		Mass emission rate[b]	
				Filterable	Gaseous	Filterable	Gaseous
				mg/dNm^3 (gr/dscf)	mg/dNm^3 (gr/dscf)	kg/h (lb/h)	kg/h (lb/h)
1	PATC-1	1/18-19	1/18 909-1625	2.18 (0.0009)	0.28 (0.0001)	0.33 (0.73)	0.04 (0.08)
	PASM-1		1/19 830-1322	4.98 (0.002)	0.86 (0.0004)	0.99 (2.18)	0.20 (0.44)
2	PATC-2	1/20	820-2003	3.89 (0.0017)	5.02 (0.002)	0.61 (1.35)	0.72 (1.59)
	PASM-2			9.01 (0.004)	4.72 (0.002)	1.97 (4.35)	0.99 (2.18)
3	PATC-3	1/22	910-2342	1.35 (0.0006)	0.44 (0.0002)	0.21 (0.47)	0.07 (0.16)
	PASM-3[c]			5.86 (0.003)[c]	0.24 (0.0001)[c]	1.48 (3.26)[c]	0.05 (0.11)[c]

[a] Filterable and gaseous arsenic concentration in milligrams per dry normal cubic meter (mg/dNm^3) and grains per dry standard cubic foot (gr/dscf). Standard conditions: 760 mmHg (29.92 in.Hg), 20°C (68°F), and 0 percent moisture.

[b] Mass emission rate in kilograms per hour (kg/h) and pounds per hour (lb/h) calculated using measured concentrations and volumetric flow rates reported in Table 5-9.

[c] Slag skim only.

and arsenic samples. Sampling was performed for the duration of each converter cycle tested and during specific converter rollout modes: matte charge, slag skim, cold addition, and copper pouring. Analysis for filterable and gaseous arsenic was performed at the completion of the gravimetric particulate determination.

Arsenic concentrations are reported in milligrams per dry normal cubic meter and grains per dry standard cubic foot. Emission rates are expressed in kilograms per hour and pounds per hour. The product of the concentration and the volumetric flow rate is the mass emission rate. For the total cycle tests (designated PATC), the measured flow rate obtained from the sample traverse was used in the calculations. For tests conducted during converter rollout activities (designated PASM), the average flow rate obtained from the volumetric flow evaluation of the high-flow mode was used because these tests were performed at a single point in the duct. Volumetric flow data were summarized earlier in Sections 4 and 5.2.

The filterable arsenic fraction represents material collected in the sample probe and on the filter, both of which were heated to approximately 121°C (250°F). The gaseous arsenic fraction represents material that passed through the heated filter and condensed or was trapped in the impinger section of the sample train, which was maintained at a temperature of 20°C (68°F) or less.

During the total cycle tests, the filterable arsenic concentration ranged from 1.35 mg/dNm^3 (0.0006 gr/dscf) to 3.89 mg/dNm^3 (0.0017 gr/dscf), and the corresponding mass emission rates ranged from 0.21 kg/h (0.47 lb/h) to 0.61 kg/h (1.36 lb/h). Gaseous arsenic concentrations during Tests PATC-1 and PATC-3 were 0.28 mg/dNm^3 (0.0001 gr/dscf) and 0.44 mg/dNm^3 (0.0002 gr/dscf), respectively.

During Test PATC-2, the gaseous arsenic concentration was 5.02 mg/dNm^3 (0.002 gr/dscf). As noted in Subsections 5.1 and 5.2, the loss of draft by the primary hood caused by operational problems at the chemical plant resulted in frequent releases of smoke and fumes from the primary hood. During this period, particularly in the converter blow mode, heavy volumes of smoke escaped the primary hood system, and some of these emissions were captured by the secondary hood. Sampling continued throughout these intermediate upsets, but was finally stopped when the air curtain control system became overwhelmed by continuous and heavy emission discharge from the primary hood. Therefore, it is reasonable to conclude that fugitive emissions generated by the malfunctioning primary hood draft contributed to the higher arsenic concentrations observed during the second cycle test.

During the specific mode tests, filterable arsenic concentrations ranged from 4.98 mg/dNm^3 (0.002 gr/dscf) to 9.01 mg/dNm^3 (0.004 gr/dscf), and corresponding emission rates ranged from 0.99 kg/h (2.18 lb/h) to 1.98 kg/h (4.35 lb/h). Gaseous arsenic concentrations ranged from 0.24 mg/dNm^3 (0.0001 gr/dscf) to 4.72 mg/dNm^3 (0.002 gr/dscf) and the corresponding emission rates ranged from 0.05 kg/h (0.11 lb/h) to 0.99 kg/h (2.18 lb/h).

Table 36 presents total arsenic emission factors on the basis of a pound of arsenic per ton of copper produced. The total arsenic value for each run was calculated by adding the filterable and gaseous fractions (in milligrams), calculating the concentration and mass emission rate (in pounds per hour), and multiplying the mass emission rate by the time of the test (in hours).

Arsenic emission factors for the total cycle tests ranged from 0.03 lb/ton to 0.20 lb/ton.

Arsenic emission factors for specific mode Tests PASM-1 and 2 were 0.07 lb/ton and 0.12 lb/ton, respectively.

For Test PASM-3, which was run only during slag skimming operations, the arsenic emission factor was 0.02 lb/ton of copper produced. During this test, a total of 7.25 ladles of slag were skimmed from the converter. Based on information supplied by ASARCO, each ladle contains 12 to 15 tons of slag. Therefore, between 87 to 109 tons of slag were skimmed, which yields a skimming emission factor of about 0.025 lb of arsenic per ton of slag skimmed.

TABLE 36. DEVELOPMENT OF ARSENIC EMISSION FACTORS

Converter cycle No.	Test I.D.	Date (1983)	Tons copper produced[a]	Total[b] arsenic, lb	Emission factor, lb arsenic/ton copper produced
1	PATC-1	1/18-19	150	9.48	0.06
Charge No. 79	PASM-1			10.80	0.07
2	PATC-2	1/20	120	24.27	0.20
Charge No. 80	PASM-2			14.32	0.12
3	PATC-3	1/22	150	4.78	0.03
Charge No. 81	PASM-3[c]			2.61[c]	0.02[c]

[a] Information obtained from ASARCO converter operation logs.

[b] Total arsenic obtained by adding the filterable and gaseous fractions (in milligrams), calculating the concentration and subsequent mass emission rate (in pounds per hour), and multiplying the mass emission rate by the time of test (in hours).

[c] Slag skimming only.

In summary, the arsenic emission data show that the majority of these emissions are generated when the primary hood is in the raised position. This is substantiated by the relative equality of the total arsenic and emission factor data presented in Table 36; specifically converter cycle Tests 1 and 3. Results from converter cycle Test 2 show the impact of the primary hood malfunction on arsenic emissions. The results from the full cycle sample train, run primarily during the blowing mode, are significantly higher than the specific mode (roll-out activity) sample train. Both the particulate and arsenic emission data indicate that, when functioning properly, the primary hood on the No. 4 converter is very effective in controlling emissions during the blowing mode.

5.4 PARTICLE SIZE RESULTS

Particle size distribution tests were conducted during three different operating modes. One segment of the converter cycle that was tested was the charging mode, which consisted of all additions to the converter (matte charge, cold additions, anode additions, and copper slag additions). Two other segments were also tested--the skimming mode, which consisted of slag skims and the copper pour, and the blowing mode, which included the slag, cleanup, and finish blows.

The particle size distribution tests were conducted at points of average velocity in the duct that exhausts emissions collected by the air curtain hooding system. These tests were conducted simultaneously with the particulate/arsenic tests (at separate sampling points). The particle size distribution results are presented as the actual measured results during each sample run. Inhalable particulate fractions, percentage less than 10 to 2.5 μm, are also presented.

5.4.1 Measured Particle Size Emission Results

Table 37 presents the particulate loading, impactor flow data, and particle size cut points for each particle size run. During the charging mode sample runs, the particulate loading measured on the first filter stage, in the impactor rinse, and on the last four filter stages accounted for most of the particulate collected by the impactor. The sampling rates in all of the particle size runs conducted during the charging mode were within ±4 percent of the isokinetic value. (The isokinetic rate is the ratio of the velocity of the sample gas stream entering the nozzle to the velocity of the stack gas, expressed as a percentage.) Actual impactor performance limited the aerodynamic size ranges that could be determined during the charging mode particle size runs to a maximum diameter of 9.4 μm and a minimum diameter of 0.3 μm.

During the skimming mode, the particulate loading for the three sample runs on the individual impactor filter stages did

TABLE 37. PARTICULATE LOADING AND IMPACTOR FLOW RATE DATA FOR THE PARTICLE SIZE RUNS

Run No.	Date (1983)	Sampling duration	Impactor flow rate, acms (acfm)	Isokin-etics, %	Average stack temperature, °C (°F)	Particulate loading, mg Stage No.								
						Rinse + 0	1	2	3	4	5	6	7	Backup
					Charging mode									
PSMC-1	1/18- 1/19	1236-1623 0835-0845	1.18 (0.693)	104	29 (85)	28.8	8.8	6.5	3.5	5.3	13.4	19.4	17.6	12.6
cutpoint µm						8.9	7.9	5.1	3.3	1.8	0.9	0.7	0.4	<0.4
PSMC-2	1/19	0936-1322	1.16 (0.685)	102	25 (77)	9.6	3.2	1.6	1.3	1.3	2.5	4.3	7.2	7.3
cutpoint µm						8.9	7.8	5.0	3.2	1.7	0.8	0.6	0.3	<0.3
PSMC-3	1/20	0820-1121	1.09 (0.643)	100	28 (83)	13.0	5.3	3.2	2.0	2.1	9.7	10.8	10.5	12.2
cutpoint µm						9.2	8.2	5.3	3.4	1.9	1.0	0.7	0.4	<0.4
PSMC-4	1/20	1450-1838	1.09 (0.644)	102	27 (81)	12.7	6.0	11.4	4.4	3.8	3.0	4.0	4.5	4.4
cutpoint µm						9.2	8.1	5.2	3.3	1.8	0.9	0.6	0.3	<0.3
PSMC-5	1/22	1047-2120	1.05 (0.615)	96	21 (69)	20.4	5.4	4.2	2.4	3.8	8.9	7.2	4.6	4.5
cutpoint µm						9.4	8.3	5.4	3.5	1.9	1.0	0.7	0.4	<0.4
					Skimming mode									
PSSS-1	1/18- 1/19	0907-1606 0812-1039	1.33 (0.785)	112	26 (78)	16.3	8.7	8.3	4.2	5.4	6.6	16.5	18.4	26.7
cutpoint µm						8.3	7.3	4.7	3.0	1.6	0.8	0.5	0.3	<0.3
PSSS-2	1/20	1045-1708	1.20 (0.709)	111	23 (74)	9.3	5.6	8.2	2.2	6.0	7.8	16.0	12.3	6.9
cutpoint µm						8.7	7.7	4.9	3.2	1.7	0.8	0.6	0.3	<0.3
PSSS-3	1/22	0955-1730	1.22 (0.717)	111	24 (75)	7.9	2.8	0.0	1.5	1.8	5.0	13.0	10.4	5.7
cutpoint µm						8.7	7.7	5.0	3.2	1.8	0.9	0.7	0.4	<0.4
					Blowing mode									
PSB-1	1/18- 1/19	0813-1530 0732-1401	0.760 (0.447)	89	18 (64)	67.0	0.3	0.3	0.7	0.6	1.2	2.2	2.6	2.3
cutpoint µm						10.9	9.6	6.2	4.0	2.2	1.1	0.7	0.4	<0.4
PSB-2	1/20	1004-1418	0.822 (0.484)	100	17 (63)	45.7	0.6	0.8	1.3	2.6	8.8	9.7	7.5	3.0
cutpoint µm						10.4	9.2	6.0	3.8	2.1	1.0	0.7	0.4	<0.4
PSB-3	1/20	1616-2000	0.826 (0.486)	105	18 (65)	58.2	0.2	0.0	0.0	0.2	0.3	0.2	0.2	0.6
cutpoint µm						10.4	9.2	6.0	3.8	2.1	1.0	0.7	0.4	<0.4
PSB-4	1/22	1607-2211	0.829 (0.488)	99	17 (63)	31.4	0.0	0.5	0.3	0.2	0.3	0.8	0.8	0.8
cutpoint µm						10.4	9.2	5.9	3.8	2.1	1.0	0.7	0.4	<0.4

not follow a distinguishable pattern. The sampling rates of all of the particle size runs conducted during the skimming mode were within 12 percent of the isokinetic value. The aerodynamic size ranges determined for these particle size runs varied from a maximum diameter of 8.7 μm to a minimum diameter of 0.3 μm.

During the blowing mode sample runs, the particulate loading measured on the first filter stage and the impactor rinse (which included the material collected in the cyclone precutter) accounted for an average of 83 percent of the total particulate loading during the four sample runs. The sampling rates of all of the particle size runs conducted during the blowing mode were within ±11 percent of the isokinetic value. Because of the expected low grain loading at the sampling location during the blowing mode, the sampling train was operated at the maximum constant flow rate through the impactor consistent with isokinetic sampling. For this reason the 15-μm cyclone precutter did not provide a 15-μm cut point. The aerodynamic size ranges determined for the particle size runs conducted during the blowing mode ranged from a maximum diameter of 10.9 μm to a minimum of 0.4 μm.

The cumulative and fractional particulate concentrations and the emission rates for each particle size run are presented in Tables 38 and 39.

The particulate concentrations and emission rates for the eight size ranges were calculated for each sample run by multiplying the total measured value by the cumulative weight percent less than each cut point, as determined from the individual particle size distribution curves.

The particulate concentrations for the particle size runs are reported in milligrams per dry normal cubic meters (mg/dNm^3) and grains per dry standard cubic feet (gr/dscf). Emission rates are expressed in kilograms per hour and pounds per hour. The product of the concentration measured by the particle size runs and the average volumetric flow rate measured by the preliminary velocity traverses is the mass emission rate.

TABLE 38. SUMMARY OF FILTERABLE PARTICULATE CONCENTRATIONS FOR THE PARTICLE SIZE RUNS

Run No.	Date (1983)	Cumulative less than indicated size																	
		Total		Stage 0		Stage 1		Stage 2		Stage 3		Stage 4		Stage 5		Stage 6		Stage 7	
		mg/dNm³[a]	gr/dscf[b]	mg/dNm³	gr/dscf	mg/dNm³	gr/dscf	mg/dNm³	gr/dscf	mg/dNm³	gr/dscf	mg/dNm³	gr/dscf	mg/dNm³	gr/dscf	mg/dNm³	gr/dscf	mg/dNm³	gr/dscf
Charging mode																			
PSMC-1 cutpoint µm	1/18-1/19	165	0.072	124 8.9	0.054	111 7.8	0.049	102 5.1	0.045	97 3.3	0.042	89 1.8	0.039	70 0.9	0.031	43 0.7	0.019	18 0.4	0.008
PSMC-2 cutpoint µm	1/19	94	0.041	70 8.9	0.031	63 7.8	0.027	59 5.0	0.026	55 3.2	0.024	52 1.7	0.023	46 0.8	0.020	36 0.6	0.016	18 0.3	0.008
PSMC-3 cutpoint µm	1/20	98	0.043	80 9.2	0.035	72 8.2	0.031	67 5.3	0.029	65 3.4	0.028	62 1.9	0.027	48 1.0	0.021	32 0.7	0.014	17 0.4	0.008
PSMC-4 cutpoint µm	1/20	132	0.058	101 9.2	0.044	87 8.1	0.038	59 5.2	0.026	48 3.3	0.021	39 1.8	0.017	32 0.9	0.014	22 0.6	0.009	11 0.3	0.005
PSMC-5 cutpoint µm	1/22	157	0.068	105 9.4	0.046	91 8.3	0.040	80 5.4	0.035	74 3.5	0.032	64 1.9	0.028	42 1.0	0.018	23 0.7	0.010	12 0.4	0.005
Skimming mode																			
PSSS-1 cutpoint µm	1/18-1/19	40	0.018	35 8.3	0.015	31 7.3	0.014	28 4.7	0.012	27 3.0	0.012	25 1.6	0.011	22 0.8	0.010	16 0.5	0.007	10 0.3	0.004
PSSS-2 cutpoint µm	1/20	77	0.033	67 8.7	0.029	61 7.7	0.027	53 4.9	0.023	51 3.2	0.022	44 1.7	0.019	36 0.8	0.016	20 0.6	0.009	7 0.3	0.003
PSSS-3 cutpoint µm	1/22	64	0.028	54 8.7	0.023	50 7.7	0.022	50 5.0	0.022	48 3.2	0.021	45 1.8	0.020	39 0.9	0.017	21 0.7	0.009	8 0.4	0.003
Blowing mode																			
PSB-1 cutpoint µm	1/18-1/19	25	0.011	3 10.9	0.001	3 9.6	0.001	3 6.2	0.001	3 4.0	0.001	3 2.2	0.001	2 1.1	0.001	2 0.7	0.0007	1 0.4	0.0003
PSB-2 cutpoint µm	1/20	107	0.047	46 10.4	0.020	45 9.2	0.020	44 6.0	0.019	42 3.8	0.018	39 2.1	0.017	27 1.0	0.012	14 0.7	0.006	4 0.4	0.002
PSB-3 cutpoint µm	1/20	45	0.020	1 10.4	0.0006	1 9.2	0.0005	1 6.0	C.0005	1 3.8	0.0005	1 2.1	0.0004	1 1.0	0.0003	1 0.7	0.0003	0.0[c] 0.4	0.0002
PSB-4 cutpoint µm	1/22	13	0.006	1 10.4	0.0006	1 9.2	0.0006	1 5.9	C.0005	1 3.8	0.0005	1 2.1	0.0004	1 1.0	0.0001	1 0.7	0.0003	0.0[c] 0.4	0.0001

[a] Milligrams per dry normal cubic meter.

[b] Grains per dry standard cubic foot.

Reproduced from
best available copy.

TABLE 39. SUMMARY OF FILTERABLE PARTICULATE EMISSION RATES FOR THE PARTICLE SIZE RUNS[a]

Run No.	Date (1983)	Cumulative less than indicated size																	
		Total		Stage 0		Stage 1		Stage 2		Stage 3		Stage 4		Stage 5		Stage 6		Stage 7	
		kg/h[b]	lb/h[c]	kg/h	lb/h	kg/h	lb/h	kg/h	lb/h	kg/h	lb/h	kg/h	lb/h	kg/h	lb/h	kg/h	lb/h	kg/h	lb/h
		Charging mode																	
PSMC-1 cutpoint µm	1/18-1/19	35.4	78.3	26.6 8.9	58.7	23.8 7.8	53.3	21.9 5.1	49.0	20.8 3.3	45.7	19.1 1.8	42.4	15.0 0.9	33.7	9.2 0.7	20.7	3.9 0.4	8.7
PSMC-2 cutpoint µm	1/19	20.1	44.6	15.0 8.9	33.7	13.5 7.8	29.4	12.6 5.0	28.3	11.9 3.2	26.1	30.2 1.7	25.0	9.9 0.8	21.8	7.7 0.6	17.4	3.9 0.3	8.7
PSMC-3 cutpoint µm	1/20	21.0	46.8	17.1 9.2	38.1	15.4 8.2	33.7	14.4 5.3	31.5	13.9 3.4	30.5	13.3 1.9	29.4	10.3 1.0	22.8	6.9 0.7	15.2	3.6 0.4	8.7
PSMC-4 cutpoint µm	1/20	28.3	63.1	21.6 9.2	47.9	18.6 8.1	41.3	12.6 5.2	28.3	10.3 3.3	22.8	8.4 1.8	18.5	6.9 0.9	15.2	4.7 0.6	9.8	2.4 0.3	5.4
PSMC-5 cutpoint µm	1/22	33.6	74.0	22.5 9.4	50.0	19.5 8.3	43.5	17.1 5.4	38.1	15.9 3.5	34.8	13.7 1.9	30.5	9.0 1.0	19.6	4.9 0.7	10.9	2.6 0.4	5.4
		Skimming mode																	
PSSS-1 cutpoint µm	1/18-1/19	8.6	19.6	7.5 8.3	16.3	6.6 7.3	15.2	6.0 4.7	13.1	5.8 3.0	13.1	5.4 1.6	12.0	4.7 0.8	10.9	3.4 0.5	7.6	2.1 0.3	4.4
PSSS-2 cutpoint µm	1/20	16.5	35.9	14.4 8.7	31.5	13.1 7.7	29.4	11.4 4.9	25.0	10.9 3.2	23.9	9.4 1.7	20.7	7.7 0.8	17.4	4.3 0.6	9.8	1.5 0.3	3.3
PSSS-3 cutpoint µm	1/22	13.7	30.5	11.6 8.7	25.0	10.7 7.7	23.9	10.7 5.0	23.9	10.3 3.2	22.8	9.6 1.8	21.8	8.4 0.9	18.5	4.5 0.7	9.8	1.7 0.4	3.3
		Blowing mode																	
PSB-1 cutpoint µm	1/18-1/19	3.2	7.2	0.4 10.9	0.7	0.4 9.6	0.7	0.4 6.2	0.7	0.4 4.0	0.7	0.4 2.2	0.7	0.3 1.1	0.7	0.3 0.7	0.5	0.1 0.4	0.2
PSB-2 cutpoint µm	1/20	13.8	30.8	5.9 10.4	13.1	5.8 9.2	13.1	5.7 6.0	12.4	5.4 3.8	11.8	5.0 2.1	11.1	3.5 1.0	7.9	1.8 0.7	3.9	0.5 0.4	1.3
PSB-3 cutpoint µm	1/20	5.8	13.1	0.1 10.4	0.4	0.1 9.2	0.3	0.1 6.0	0.3	0.1 3.8	0.3	0.1 2.1	0.3	0.1 1.0	0.2	0.1 0.7	0.2	0.0[d] 0.4	0.1
PSB-4 cutpoint µm	1/22	1.7	3.9	0.1 10.4	0.4	0.1 9.2	0.4	0.1 5.9	0.3	0.1 3.8	0.3	0.1 2.1	0.3	0.1 1.0	0.3	0.1 0.7	0.2	0.0[d] 0.4	0.07

---

[a] Emission rate based on average volumetric flow rates of 2149 dNm^3/min (76,359 dscfm) during low flow (blow mode) and 3571 dNm^3/min (126,924 dscfm) during high flow (charging and slaging modes)

[b] Kilograms per hour.

[c] Pounds per hour.

The moisture content measured by the corresponding particulate/arsenic test was used to calculate the particle size parameters for each sample run.

During the charging mode, the total particulate concentration measured by the particle size runs ranged between 94 mg/dNm³ (0.041 gr/dscf) and 165 mg/dNm³ (0.072 gr/dscf). One reason the particulate concentration varied during the charging mode is that the different materials charged into the converter during each tested cycle caused significant variations. The visible emissions varied during the charging modes. Another reason is that the converter was not operated consistently throughout the charging mode. During some of the charging segments, the converter was rolled out and the primary hood was raised up and left that way from one charging of a ladle of material to the next. Visual emissions decreased significantly in the periods between each charge. On other occasions the converter was rolled out for the charging mode and the primary hood was raised, but the hood was lowered again over the converter mouth after each ladle of material was charged. Particle size sampling was conducted while the primary hood was left up between ladles of material being charged (high flow mode), as this was considered to be part of the charging mode. The reduced particulate emissions at these times caused the overall sample to show a lower concentration.

The total particulate emission rate as determined from the particle size distribution tests during the charging mode ranged between 20.1 kg/h (44.6 lb/h) and 35.4 kg/h (78.3 lb/h). These values show the same variations as the concentration results because an average flue gas flow rate of 3571 dNm³ (126,924 dscfm) as measured during the specific mode tests was used for all of the emission rate calculations.

During the skimming mode, the particle size runs showed a total particulate concentration ranging between 40 mg/dNm³ (0.018 gr/dscf) and 77 mg/dNm³ (0.033 gr/dscf). The same operating procedures were followed during the charging mode; sometimes the primary hood was left up between pourings of ladles of slag or copper and sometimes it was lowered. This resulted in the same dilution effects in the measured concentrations during the particle size runs. The visible emissions decreased significantly between ladles of slag or copper being poured. During both the charging and skimming modes, the time between ladles of material being charged or skimmed varied throughout the testing period, depending on process operations.

The total particulate emission rate during the skimming mode ranged between 8.6 kg/h (19.6 lb/h) and 16.5 kg/h (35.9 lb/h). The average high-flow-mode exhaust gas flow rate of 3571 dNm^3/m (126,924 dscfm) was also used for all of the skimming emission rate calculations.

During the blowing mode, the total particulate concentrations measured by the particle sizing runs ranged between 13 mg/dNm^3 (0.006 gr/dscf) and 107 mg/dNm^3 (0.047 gr/dscf). This large variation in particulate concentrations resulted from a very high concentration during one run (Run No. PSB-2), during which the primary hood draft malfunctioned and emissions normally captured by the primary hood escaped and were collected by the air curtain exhaust system. Visual observations of the process during the blowing mode indicates that the visible emissions were very low (not visible) while the primary hood was operating correctly. This explains why the particulate concentrations measured by the particle size runs were much lower during the blowing mode than during the charging and skimming modes.

The total particulate emission rate during the blowing mode ranged between 1.7 kg/h (3.9 lb/h) and 13.8 kg/h (30.8 lb/h). The average low-flow-mode flue gas flow rate of 2149 dNm^3/min (76,359 dscfm) was used to calculate all of the particulate emission rates for the blowing mode.

Figures 16 through 18 present particle size distribution curves for each of the three converter modes tested. These graphs show that the size of the particulate generated during each of the three modes differ.

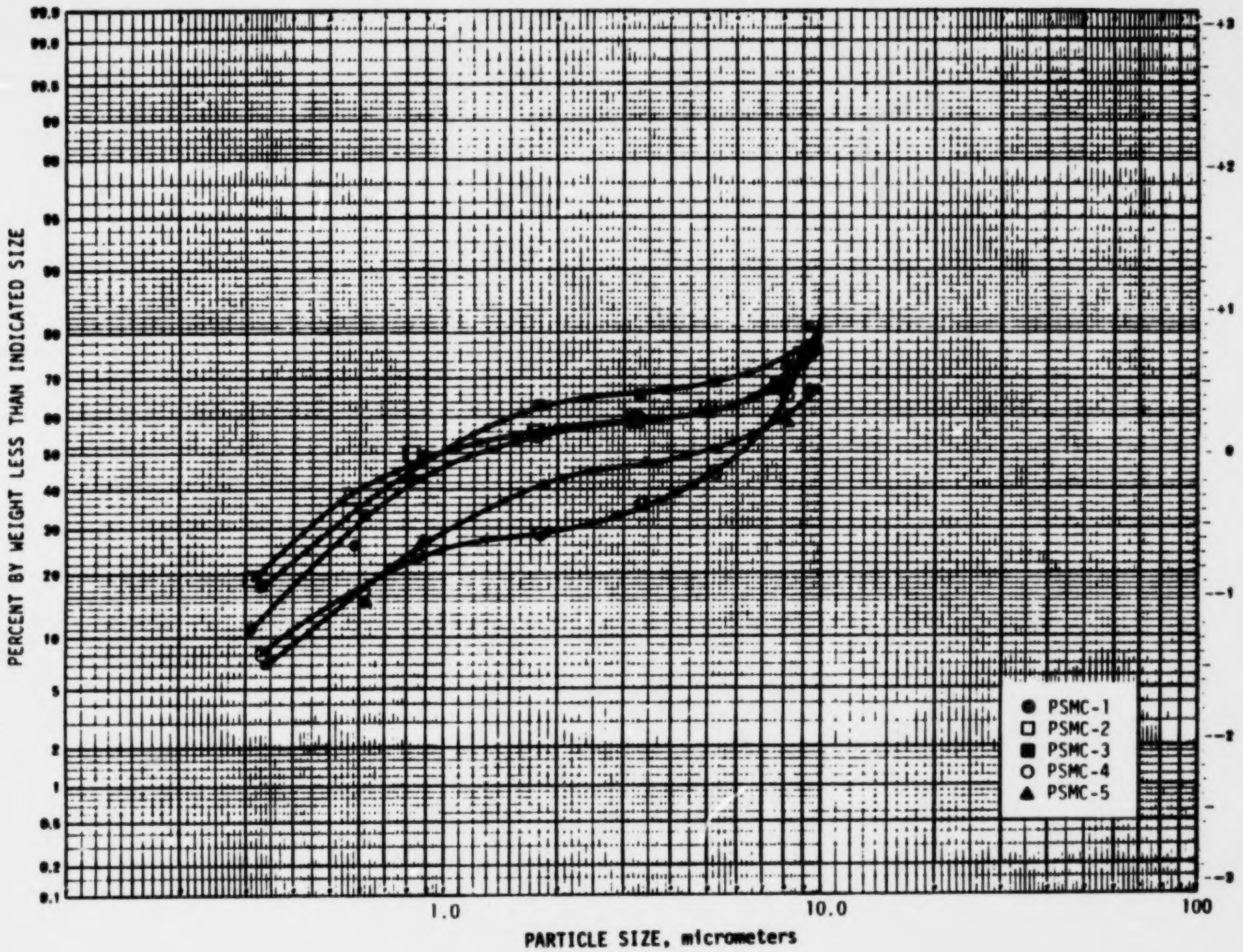

Figure 16. Individual particle size distributions for the charging mode sample runs.

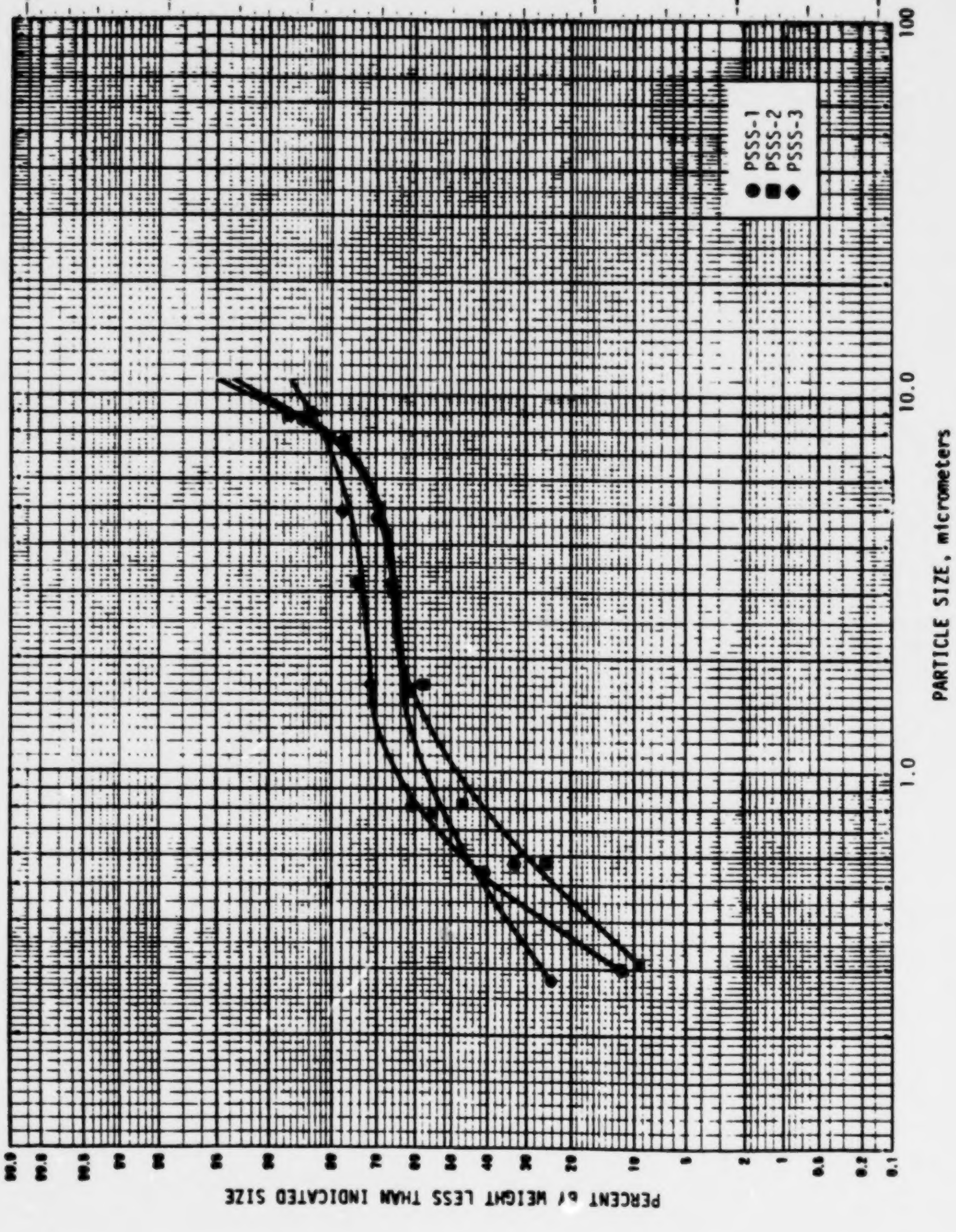

Figure 17. Individual particle size distributions for the skimming mode sample runs.

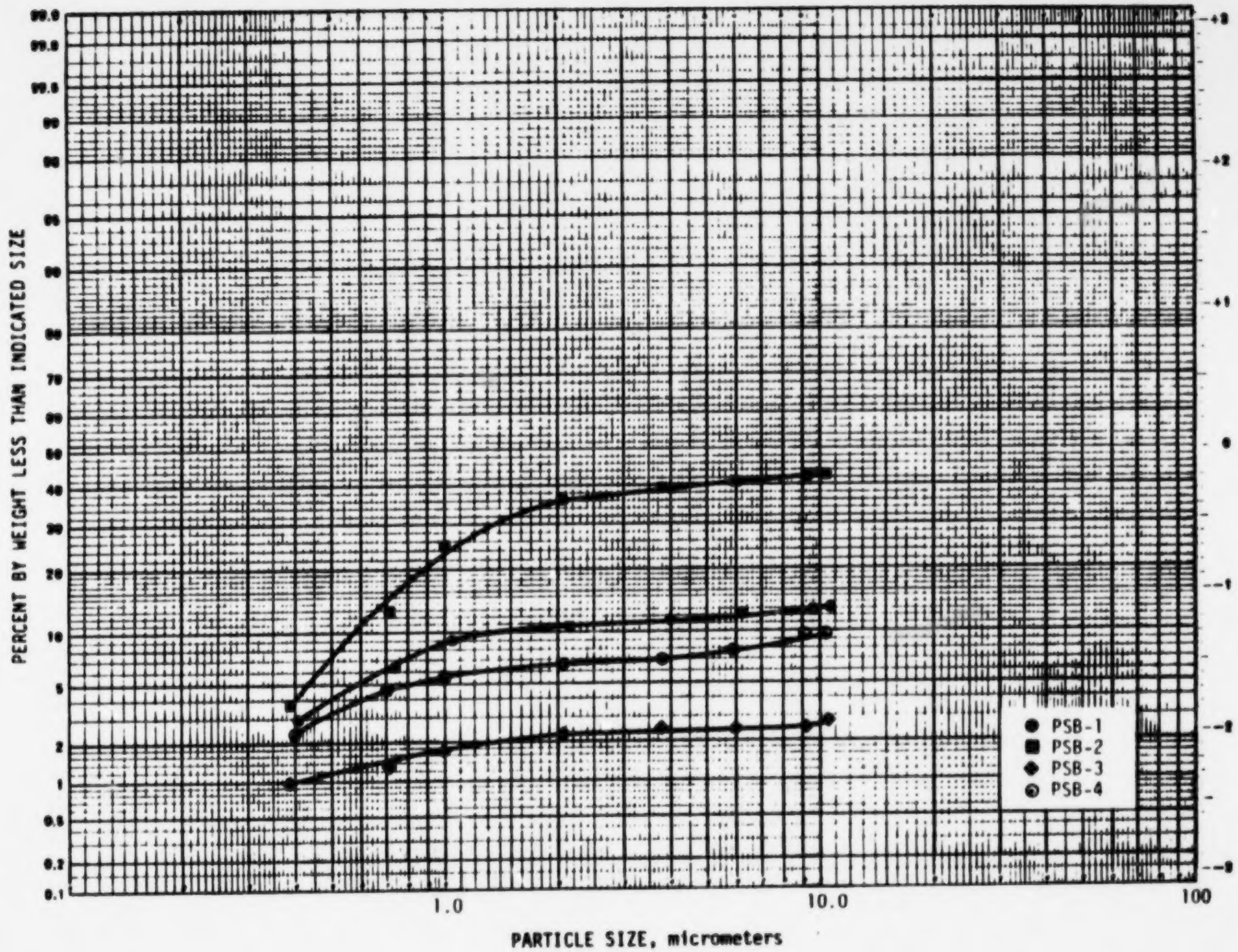

Figure 18. Individual particle size distributions for the blowing mode sample runs.

The particle size distribution curves, however, for each individual sample run conducted during the charging and skimming modes compare closely with each other for each specific mode tested. This indicates that the size of the particulate emitted during the charging and skimming modes was fairly consistent during the testing period. Consequently, the individual particle size distribution curves for the sample runs conducted during the blowing mode do not compare closely with each other. The particle size results for Run PSB-2 show a much larger percentage of particles less than 10 μm in size than the other three sample runs. The large variation in particle sizes during Run PSB-2 resulted from an upset in the primary hood, which caused particulate normally captured by the primary hood to escape and be collected in the air curtain exhaust system.

Figures 19 through 21 present average particle size distribution curves for each of three converter operating modes tested (charging, skimming, and blowing). The highest and lowest measured values are shown for each indicated cut point.

The average particle size curves for the charging and skimming modes show that most of the particulate emissions captured by the air curtain exhaust system are in the inhalable particulate (IP) range (<10 μm), and that a large percentage of the emissions are in the fine particulate (FP) range (<2.5 μm).

The average particle size distribution curves for the blowing mode shows that most of the particulate emissions captured by the secondary exhaust system are greater than 10 μm and not in the inhalable particulate range.

5.4.2 Inhalable Particulate Emission Data

Tables 40 and 41 present the IP and FP concentration and emission rate results for each particle size run conducted. Inhalable particulate (<10 μm) and fine particulate (<2.5 μm) concentrations and emission rates are calculated for each specific operating mode tested by multiplying the total measured value by the cumulative weight percent less than the stated value as

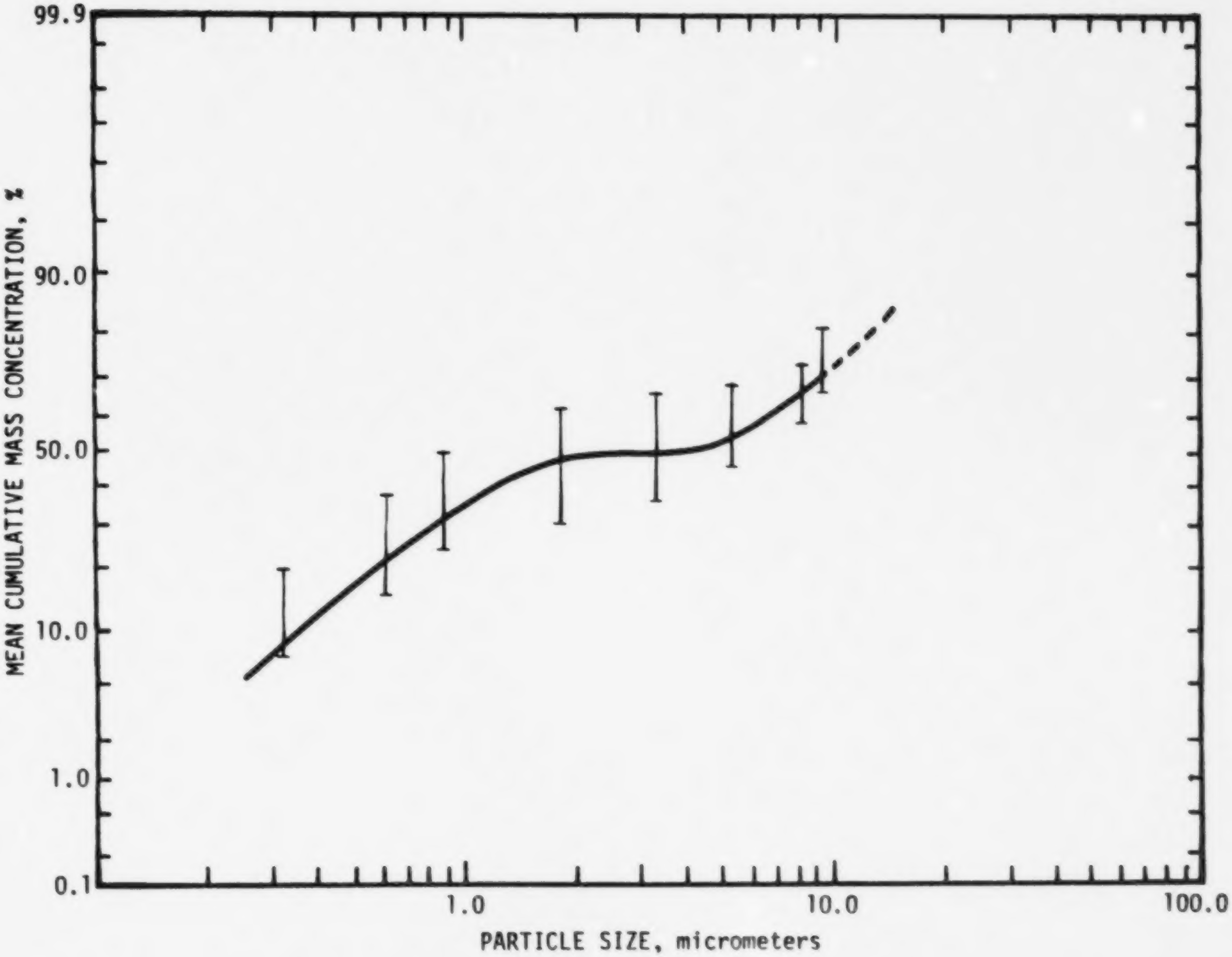

Figure 19. Average particle size distribution for the charging mode.

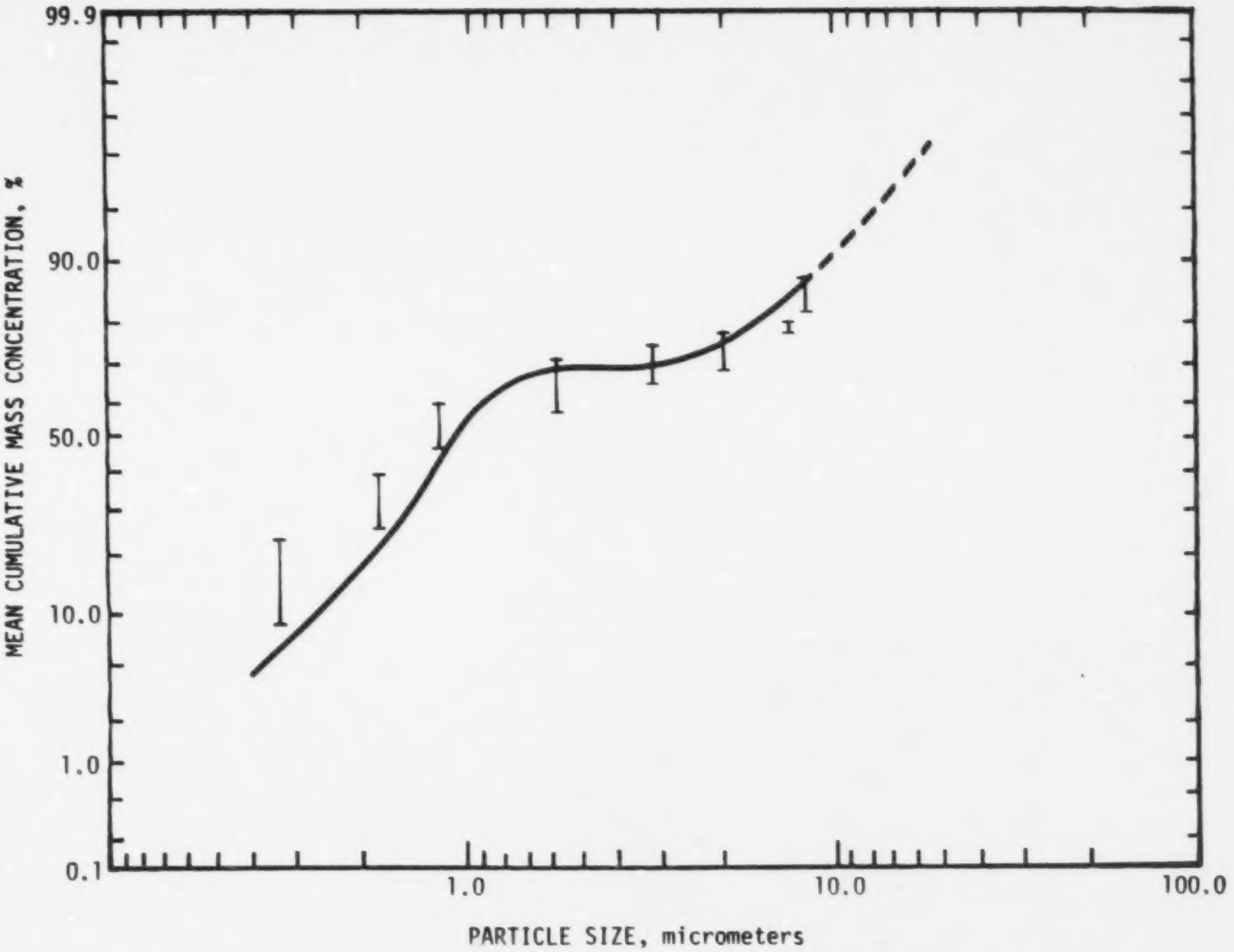

Figure 20. Average particle size distribution for the skimming mode.

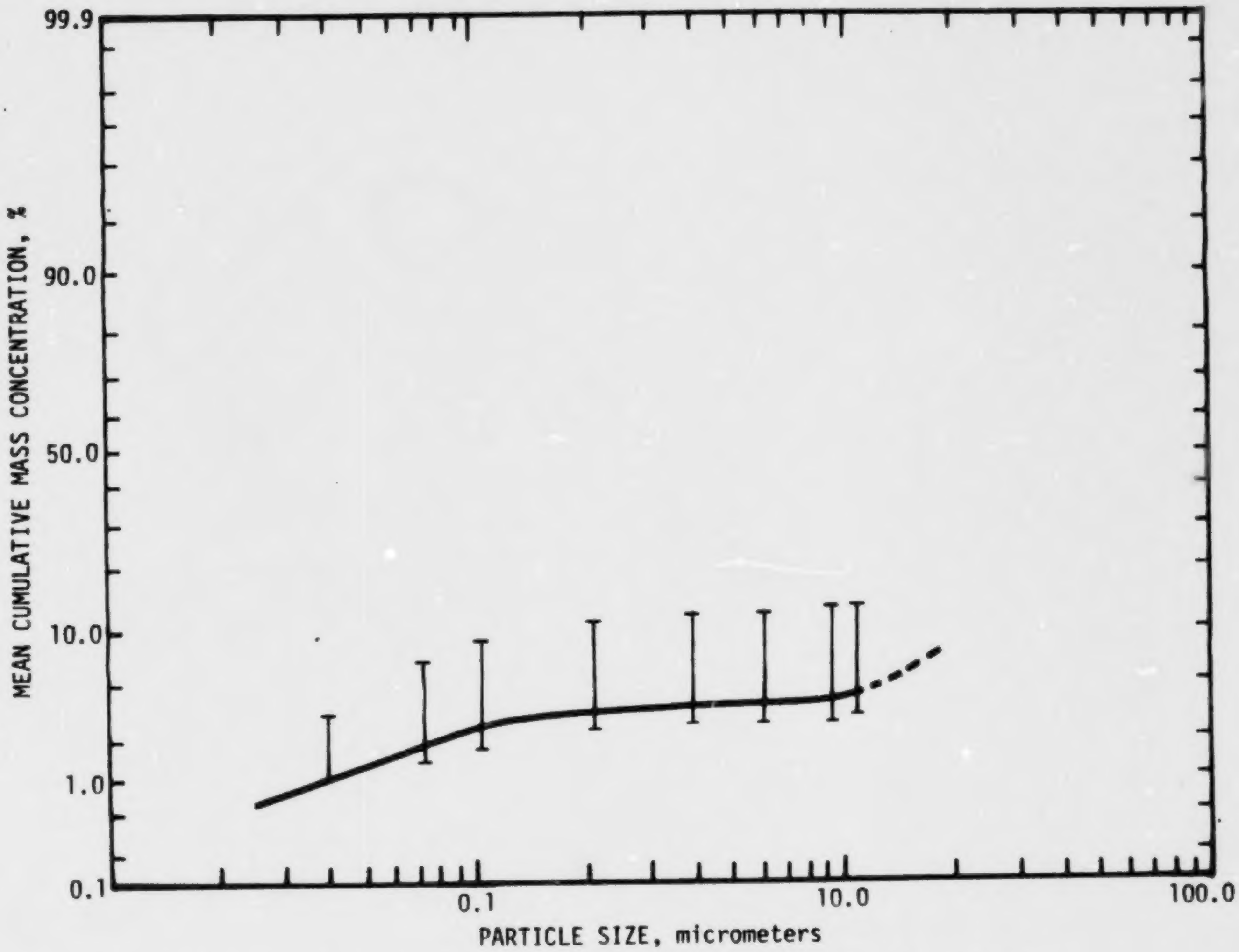

Figure 21. Average particle size distribution for the blowing mode.

TABLE 40. SUMMARY OF INHALABLE PARTICULATE CONCENTRATIONS DURING THE PARTICLE SIZE RUNS

Run No.	Date (1983)	Cumulative less than indicated size							
		Total		10 μm > X		5 μm > X		2.5 μm > X	
		mg/dNm³[a]	gr/dscf[b]	mg/dNm³	gr/dscf	mg/dNm³	gr/dscf	mg/dNm³	gr/dscf
Charging mode[c]									
PSMC-1	1/18-19	165	0.072	129	0.056	102	0.045	94	0.041
PSMC-2	1/19	94	0.041	72	0.032	59	0.026	54	0.023
PSMC-3	1/20	98	0.043	82	0.036	67	0.029	64	0.027
PSMC-4	1/20	132	0.058	110	0.048	57	0.025	42	0.019
PSMC-5	1/22	157	0.068	110	0.048	79	0.034	71	0.031
Skimming mode[c]									
PSSS-1	1/18-19	40	0.018	36	0.016	28	0.013	26	0.012
PSSS-2	1/20	77	0.033	71	0.030	53	0.023	50	0.021
PSSS-3	1/22	64	0.028	55	0.024	50	0.022	47	0.020
Blowing mode									
PSB-1	1/18-19	25	0.011	3	0.001	3	0.001	3	0.001
PSB-2	1/20	107	0.047	45	0.020	43	0.019	40	0.017
PSB-3	1/20	45	0.020	1	0.0005	1	0.0005	1	0.0004
PSB-4	1/22	13	0.006	1	0.0006	1	0.0005	1	0.0004

[a] Milligrams per dry normal cubic meter.

[b] Grains per dry standard cubic foot.

[c] The 10-μm cutpoint is extrapolated from the particle size distribution curves.

TABLE 41. SUMMARY OF INHALABLE PARTICULATE EMISSION RATES DURING THE PARTICLE SIZE RUNS[a]

Run No.	Date (1983)	Cumulative less than indicated size							
		Total		10 µm > X		5 µm > X		2.5 µm > X	
		kg/h[b]	lb/h[c]	kg/h	lb/h	kg/h	lb/h	kg/h	lb/h
Charging mode[d]									
PSMC-1	1/18-1/19	35.4	78.3	27.6	60.9	21.9	49.0	20.1	44.6
PSMC-2	1/19	20.1	44.6	15.4	34.8	12.6	28.3	11.6	25.0
PSMC-3	1/20	21.0	46.8	17.6	39.2	14.4	31.5	13.7	29.4
PSMC-4	1/20	28.3	63.1	23.6	52.2	12.2	27.2	8.6	18.5
PSMC-5	1/22	33.6	74.0	23.6	52.2	16.9	37.0	15.2	33.7
Skimming mode[d]									
PSSS-1	1/18-1/19	8.6	19.6	7.7	17.4	6.0	14.1	5.6	13.1
PSSS-2	1/20	16.5	35.9	15.2	32.6	11.4	25.0	10.7	22.8
PSSS-3	1/22	13.7	30.5	11.8	26.1	10.7	23.9	10.1	21.8
Blowing mode									
PSB-1	1/18-1/19	3.2	7.2	0.4	0.7	0.4	0.7	0.4	0.7
PSB-2	1/20	13.8	30.8	5.8	13.1	5.5	12.4	5.2	11.1
PSB-3	1/20	5.8	13.1	0.1	0.3	0.1	0.3	0.1	0.3
PSB-4	1/22	1.7	3.9	0.1	0.4	0.1	0.3	0.1	0.3

[a] Emission rate based on the average volumetric flow rates of 2149 dNm^3/min (76,359 dscfm) during low flow (blowing mode) and 3571 dNm^3/min (126,924 dscfm) during the high flow (charging and skimming modes).

[b] Kilograms per hour.

[c] Pounds per hour.

[d] The 10-µm cutpoint is extrapolated from the particle size distribution curves.

determined from the individual particle size distribution curves. During the charging and skimming modes, the desired 10 μm diameter was determined from extrapolated portions of the best-fit curves generated for each individual sample run. The results of the particle size distribution tests conducted during the charging and skimming modes indicate that most of the particulate emissions collected by the air curtain exhaust system are in the IP range.

During the charging mode, the amount of particulate in the IP range varied between 70 and 84 percent of the total particulate emissions, whereas the amount of particulate in the FP range varied between 32 and 65 percent. The results of the particle size runs conducted during the charging mode show that the IP concentration varied between 72 mg/dNm³ (0.032 gr/dscf) and 129 mg/dNm³ (0.056 gr/dscf), while the FP concentration varied between 42 mg/dNm³ (0.019 gr/dscf) and 94 mg/dNm³ (0.041 gr/dscf). The IP emission rate during the charging mode ranged between 15.4 kg/h (34.8 lb/h) and 27.6 kg/h (60.9 lb/h), and the FP emission rate averaged between 9.0 kg/h (20.7 lb/h) and 20.1 kg/h (44.6 lb/h).

During the skimming mode, the amount of particulate in the IP range varied between 86 and 92 percent of the total particulate emissions, whereas the amount in the FP range varied between 65 and 73 percent. The results of the particle size runs conducted during the skimming mode show that the IP concentration varied between 36 mg/dNm³ (0.016 gr/dscf) and 71 mg/dNm³ (0.030 gr/dscf), and the FP concentration varied between 26 mg/dNm³ (0.012 gr/dscf) and 50 mg/dNm³ (0.021 gr/dscf). The IP emission rate during the skimming mode ranged between 7.7 kg/h (17.4 lb/h) and 15.2 kg/h (32.6 lb/h), and the FP emission rate ranged between 5.6 kg/h (13.1 lb/h) and 10.7 kg/h (22.8 lb/h).

During the blowing mode, the amount of particulate measured in the IP and FP ranges varied between 2 and 12 percent, excluding the results of Run PSB-2, which was not considered to be representative of normal operating conditions because it was conducted during an upset in the primary hood system.

A reasonable explanation of why particle sizes measured during the blowing mode were larger than those measured during the charging and skimming modes is that the primary hood operates only during the blowing mode and thus captures most of the process emissions generated. The particulate matter collected by the air curtain exhaust system during the blowing mode represents fugitive emissions from inside the converter building. These fugitive emissions, which were visually observed in the converter building during the test series, are attributable to the general operation of the plant (i.e., crane operation, housekeeping practices, etc.). Uncontrolled fugitive emissions also emanated from the operations of the other two converters during the test series.

The results of the particle size runs conducted during the charging mode (excluding Run PSB-2) show that the IP and FP concentrations varied between 1 mg/dNm^3 (0.0004 gr/dscf) and 3 mg/dNm^3 (0.001 gr/dscf). The IP and FP emission rates during the blowing mode varied between 0.1 kg/h (0.7 lb/h) and 0.4 kg/h (0.7 lb/h). Because of the small percentage of particles in the IP range and the low IP emission rate, the particulate matter collected by the air curtain hooding system during the blowing mode should not be considered significant.

5.4.3 Elemental Analysis of the Particle Size Runs

Selected individual particle size runs were analyzed by Atomic Absorption Spectrophotometry for six elements (arsenic, selenium, cadmium, antimony, lead, and bismuth). The runs selected for elemental analysis had measurable particulate concentrations throughout the particle size distribution. Each particle size sample run selected for elemental analysis was subdivided into three size ranges. The criterion for the selection of the three size ranges was to choose the actual cut points closest to the inhalable particulate (IP) cut point of 10 μm and fine particulate (FP) cut point of 2.5 μm. This would ideally yield size ranges of greater than 10 μm, between 10 μm and 2.5 μm, and less than 2.5 μm.

The results of the elemental analysis is presented separately for the three different operating modes tested (charging, blowing, and skimming).

Charging Mode--

Tables 42 through 47 present the concentration and mass emission rates for the elemental analysis performed on the five particle size runs conducted during the charging mode. The data are presented for each element on a total basis for the entire particle size run and individually for each of the three size ranges selected.

The total concentration of arsenic measured from the particle size runs ranged between 4.0 mg/dNm³ (0.002 gr/dscf) and 28.0 mg/dNm³ (0.012 gr/dscf). This corresponds to a mass emission rate ranging between 0.9 kg/h (2.2 lb/h) and 6.0 kg/h (13.1 lb/h).

The total concentration of selenium measured from the particle size runs ranged from less than 0.05 mg/dNm³ (0.00002 gr/dscf) to 0.1 mg/dNm³ (0.00006 gr/dscf). This corresponds to a mass emission rate of less than 0.05 kg/h (0.1 lb/h) for all of the sample runs.

The total concentration of cadmium measured from the particle size runs ranged between 0.05 mg/dNm³ (0.00002 gr/dscf) and 0.9 mg/dNm³ (0.0004 gr/dscf). For one sample run the mass emission rate was 0.2 kg/h (0.4 lb/h); all of the other sample runs had measurement rates of less than 0.05 kg/h (0.1 lb/h).

The total concentration of antimony measured from the particle size runs ranged between 0.2 mg/dNm³ (0.0007 gr/dscf) and 1.8 mg/dNm³ (0.0008 gr/dscf). This corresponds to a mass emission rate ranging than 0.05 kg/h (0.1 lb/h) to 0.4 kg/h (0.9 lb/h).

The total concentration of lead measured from the particle size runs ranged between 6.2 mg/dNm³ (0.003 gr/dscf) and 30.4 mg/dNm³ (0.013 gr/dscf). This corresponds to a mass emission rate ranging between 1.5 kg/h (3.3 lb/h) and 6.4 kg/h (14.1 lb/h).

TABLE 42. SUMMARY OF ARSENIC CONCENTRATION AND MASS EMISSION RATE FOR THE PARTICLE SIZE RUNS FOR THE CHARGING MODE[a]

Run No.	Date (1983)	Concentration							
		Total		$x \geq 9.1$ μm		9.1 μm > x > 3.4 μm		x < 3.4 μm	
		mg/dNm^3[b]	gr/dscf[c]	mg/dNm^3	gr/dscf	mg/dNm^3	gr/dscf	mg/dNm^3	gr/dscf
PSMC-1	1/18-19	20.0	0.009	1.6	0.0007	1.4	0.0006	17.0	0.007
PSMC-2	1/19	4.0	0.002	0.5	0.0002	0.4	0.0001	3.1	0.001
PSMC-3	1/20	28.0	0.012	2.0	0.0009	1.9	0.0008	24.0	0.010
PSMC-4	1/20	10.5	0.005	1.5	0.0006	1.5	0.0007	7.5	0.003
PSMC-5	1/22	9.4	0.004	1.0	0.0005	1.4	0.0006	7.0	0.003

Run No.	Date (1983)	Emission rate							
		Total		$x \geq 9.1$ μm		9.1 μm > x > 3.4 μm		x < 3.4 μm	
		kg/h[d]	lb/h[e]	kg/h	lb/h	kg/h	lb/h	kg/h	lb/h
PSMC-1	1/18-19	4.3	9.8	0.3	0.8	0.3	0.7	3.6	7.6
PSMC-2	1/19	0.9	2.2	0.1	0.2	0.05	0.1	0.5	1.1
PSMC-3	1/20	6.0	13.1	0.4	1.0	0.4	0.9	5.1	10.9
PSMC-4	1/20	2.2	5.4	0.4	0.7	0.3	0.8	1.6	3.3
PSMC-5	1/22	2.0	4.4	2.5	0.5	0.3	0.7	1.5	3.3

[a] Emission rate based on average volumetric flow rates of 2149 dNm^3/min (76,359 dscfm) during low flow blowing mode) and 3571 dNm^3/min (126,924 dscfm) during high flow (charging and skimming modes).

[b] Milligrams per dry normal cubic meter.

[c] Grains per dry standard cubic foot.

[d] Kilograms per hour.

[e] Pounds per hour.

TABLE 43. SUMMARY OF SELENIUM CONCENTRATION AND MASS EMISSION RATE FOR THE PARTICLE SIZE RUNS FOR THE CHARGING MODE[a]

Run No.	Date (1983)	Concentration							
		Total		$x \geq 9.1$ μm		9.1 μm $> x >$ 3.4 μm		$x < 3.4$ μm	
		mg/dNm^3[b]	gr/dscf[c]	mg/dNm^3	gr/dscf	mg/dNm^3	gr/dscf	mg/dNm^3	gr/dscf
PSMC-1	1/18-19	0.1	0.00006	0.02	0.000008	0.01	0.000005	0.2	0.00005
PSMC-2	1/19	0.04	0.00002	0.006	0.000003	0.003	0.000001	0.03	0.00001
PSMC-3	1/20	0.05	0.00002	0.005	0.000002	0.003	0.000001	0.05	0.00002
PSMC-4	1/20	0.03	0.00001	0.008	0.000004	0.008	0.000003	0.02	0.000007
PSMC-5	1/22	0.05	0.00002	0.01	0.000006	0.007	0.000003	0.03	0.00001

Run No.	Date (1983)	Emission rate							
		Total		$x \geq 9.1$ μm		9.1 μm $> x >$ 3.4 μm		$x < 3.4$ μm	
		kg/h[d]	lb/h[e]	kg/h	lb/h	kg/h	lb/h	kg/h	lb/h
PSMC-1	1/18-19	0.03	0.07	0.004	0.009	0.002	0.055	0.02	0.05
PSMC-2	1/19	0.01	0.002	0.001	0.003	0.005	0.001	0.005	0.01
PSMC-3	1/20	0.01	0.002	0.001	0.002	0.001	0.01	0.01	0.02
PSMC-4	1/20	0.005	0.01	0.002	0.004	0.001	0.003	0.003	0.008
PSMC-5	1/22	0.01	0.02	0.003	0.007	0.001	0.003	0.005	0.01

[a] Emission rate based on average volumetric flow rates of 2149 dNm^3/min (76, 359 dscfm) during low flow (blowing mode) and 3571 dNm^3/min (126,924 dscfm) during high flow (charging and skimming modes).

[b] Milligrams per dry normal cubic meter.

[c] Grains per dry standard cubic foot.

[d] Kilograms per hour.

[e] Pounds per hour.

TABLE 44. SUMMARY OF CADMIUM CONCENTRATION AND MASS EMISSION RATE FOR THE PARTICLE SIZE RUNS FOR THE CHARGING MODE[a]

		Concentration							
		Total		$x \geq 9.1$ μm		9.1 μm > x > 3.4 μm		x < 3.4 μm	
Run No.	Date (1983)	mg/dNm^3[b]	gr/dscf[c]	mg/dNm^3	gr/dscf	mg/dNm^3	gr/dscf	mg/dNm^3	gr/dscf
PSMC-1	1/18-19	0.9	0.0004	0.5	0.00002	0.06	0.00002	0.8	0.0004
PSMC-2	1/19	0.2	0.00009	0.01	0.000005	0.01	0.000005	0.2	0.00007
PSMC-3	1/20	0.2	0.00008	0.01	0.000005	0.01	0.000005	0.2	0.00007
PSMC-4	1/20	0.07	0.00003	0.02	0.000007	0.02	0.000007	0.04	0.00002
PSMC-5	1/22	0.05	0.00002	0.02	0.000008	0.01	0.000004	0.02	0.00001

		Emission rate							
		Total		$x \geq 9.1$ μm		9.1 μm > x > 3.4 μm		x < 3.4 μm	
Run No.	Date (1983)	kg/h[d]	lb/h[e]	kg/h	lb/h	kg/h	lb/h	kg/h	lb/h
PSMC-1	1/18-19	0.2	0.4	0.01	0.02	0.01	0.02	0.2	0.4
PSMC-2	1/19	0.04	0.1	0.002	0.005	0.002	0.005	0.03	0.08
PSMC-3	1/20	0.04	0.09	0.002	0.005	0.002	0.005	0.03	0.08
PSMC-4	1/20	0.01	0.03	0.003	0.008	0.003	0.008	0.01	0.02
PSMC-5	1/22	0.01	0.02	0.004	0.009	0.002	0.004	0.005	0.01

[a] Emission rate based on average volumetric flow rates of 2149 dNm^3/min (76,359 dscfm) during low flow (blowing mode) and 3571 dNm^3/min (126,924 dscfm) during high flow (charging and skimming modes).

[b] Milligrams per dry normal cubic meter.

[c] Grains per dry standard cubic foot.

[d] Kilograms per hour.

[e] Pounds per hour.

TABLE 45. SUMMARY OF ANTIMONY CONCENTRATION AND MASS EMISSION RATE FOR THE PARTICLE SIZE RUNS FOR THE CHARGING MODE[a]

Run No.	Date (1983)	Concentration							
		Total		x ≥ 9.1 μm		9.1 μm > x > 3.4 μm		x < 3.4 μm	
		mg/dNm³[b]	gr/dscf[c]	mg/dNm³	gr/dscf	mg/dNm³	gr/dscf	mg/dNm³	gr/dscf
PSMC-1	1/18-19	1.6	0.0007	0.2	0.00009	0.2	0.00008	1.2	0.0005
PSMC-2	1/19	0.2	0.0001	0.06	0.00003	0.03	0.00001	0.1	0.00005
PSMC-3	1/20	1.8	0.0008	0.1	0.00005	0.09	0.00004	1.6	0.0007
PSMC-4	1/20	0.7	0.0003	0.1	0.00006	0.2	0.00009	0.4	0.0002
PSMC-5	1/20	0.6	0.0002	0.1	0.00006	0.1	0.00004	0.3	0.0001

Run No.	Date (1983)	Emission rate							
		Total		x ≥ 9.1 μm		9.1 μm > x > 3.4 μm		x < 3.4 μm	
		kg/h[d]	lb/h[e]	kg/h	lb/h	kg/h	lb/h	kg/h	lb/h
PSMC-1	1/18-19	0.3	0.8	0.4	0.1	0.04	0.09	0.2	0.5
PSMC-2	1/19	0.05	0.1	0.01	0.03	0.005	0.01	0.02	0.05
PSMC-3	1/20	0.4	0.9	0.02	0.05	0.02	0.04	0.3	0.8
PSMC-4	1/20	0.1	0.3	0.03	0.07	0.04	0.1	0.1	0.2
PSMC-5	1/22	0.1	0.2	0.03	0.07	0.02	0.04	0.05	0.1

[a] Emission rate based on average volumetric flow rates of 2149 dNm³/min (76,359 dscfm) during low flow (blowing mode) and 3571 dNm³/min (126,924 dscfm) during high flow (charging and skimming modes).

[b] Milligrams per dry normal cubic meter.

[c] Grains per dry standard cubic foot.

[d] Kilograms per hour.

[e] Pounds per hour.

TABLE 46. SUMMARY OF LEAD CONCENTRATION AND MASS EMISSION RATE FOR THE PARTICLE SIZE RUNS FOR THE CHARGING MODE[a]

Run No.	Date (1983)	Concentration							
		Total		$x \geq 9.1$ µm		9.1 µm > x > 3.4 µm		x < 3.4 µm	
		mg/dNm^3[b]	gr/dscf[c]	mg/dNm^3	gr/dscf	mg/dNm^3	gr/dscf	mg/dNm^3	gr/dscf
PSMC-1	1/18-19	30.4	0.013	2.7	0.001	2.7	0.001	24.9	0.011
PSMC-2	1/19	6.2	0.0026	0.7	0.0003	0.6	0.0003	4.9	0.002
PSMC-3	1/20	8.6	0.0036	0.8	0.0003	0.6	0.0003	7.3	0.003
PSMC-4	1/20	8.0	0.0035	1.6	0.0007	1.8	0.0008	4.6	0.002
PSMC-5	1/22	9.9	0.0043	1.7	0.0007	1.3	0.0006	6.9	0.003

Run No.	Date (1983)	Emission rate							
		Total		$x \geq 9.1$ µm		9.1 µm > x > 3.4 µm		x < 3.4 µm	
		kg/h[d]	lb/h[e]	kg/h	lb/h	kg/h	lb/h	kg/h	lb/h
PSMC-1	1/18-19	6.4	14.1	0.5	1.1	0.5	1.1	5.4	12.0
PSMC-2	1/19	1.5	3.3	0.1	0.3	0.1	0.3	1.0	2.2
PSMC-3	1/20	2.0	4.4	0.1	0.3	0.1	0.3	1.5	3.3
PSMC-4	1/20	1.5	3.3	0.3	0.8	0.4	0.9	1.0	2.2
PSMC-5	1/22	2.0	4.4	0.3	0.8	0.3	0.7	1.5	3.3

[a] Emission rate based on average volumetric flow rates of 2149 dNm^3/min (76,359 dscfm) during low flow (blowing mode) and 3571 dNm^3/min (126,924 dscfm) during high flow (charging and skimming modes).

[b] Milligrams per dry normal cubic meter.

[c] Grains per dry standard cubic foot.

[d] Kilograms per hour.

[e] Pounds per hour.

TABLE 47. SUMMARY OF BISMUTH CONCENTRATION AND MASS EMISSION RATE FOR THE PARTICLE SIZE RUNS FOR THE CHARGING MODE[a]

		Concentration							
		Total		$x \geq 9.1$ µm		9.1 µm > x > 3.4 µm		x < 3.4 µm	
Run No.	Date (1983)	mg/dNm^3[b]	gr/dscf[c]	mg/dNm^3	gr/dscf	mg/dNm^3	gr/dscf	mg/dNm^3	gr/dscf
PSMC-1	1/18-19	0.6	0.0024	0.05	0.00002	0.05	0.00002	0.5	0.002
PSMC-2	1/19	0.3	0.00009	0.02	0.00001	0.02	0.00001	0.1	0.00007
PSMC-3	1/20	0.2	0.0001	0.02	0.00001	0.02	0.000008	0.2	0.00008
PSMC-4	1/20	0.2	0.00008	0.04	0.00002	0.05	0.00002	0.09	0.00004
PSMC-5	1/22	0.1	0.00006	0.04	0.00002	0.03	0.00001	0.07	0.00003

		Emission rate							
		Total		$x \geq 9.1$ µm		9.1 µm > x > 3.4 µm		x < 3.4 µm	
Run No.	Date (1983)	kg/h[d]	lb/h[e]	kg/h	lb/h	kg/h	lb/h	kg/h	lb/h
PSMC-1	1/18-19	0.1	0.3	0.01	0.02	0.01	0.02	0.1	0.2
PSMC-2	1/19	0.04	0.1	0.005	0.01	0.005	0.01	0.03	0.08
PSMC-3	1/20	0.05	0.1	0.005	0.01	0.004	0.009	0.04	0.09
PSMC-4	1/20	0.04	0.09	0.01	0.02	0.01	0.02	0.02	0.04
PSMC-5	1/22	0.03	0.07	0.01	0.02	0.005	0.01	0.01	0.03

[a] Emission rate based on average volumetric flow rates of 2149 dNm^3/min (76,359 dscfm) during low flow (blowing mode) and 3571 dNm^3/min (126,924 dscfm) during high flow (charging and skimming modes).

[b] MIlligrams per dry normal cubic meter.

[c] Grains per dry standard cubic foot.

[d] Kilograms per hour.

[e] Pounds per hour.

The total concentration of bismuth measured from the particle size runs ranged between 0.1 mg/dNm^3 (0.00006 gr/dscf) and 0.6 mg/dNm^3 (0.00024 gr/dscf). For two sample runs the mass emission rates were 0.1 and 0.05 kg/h (0.3 and 0.1 lb/h); all of the other sample runs had mass emission rates of less than 0.05 kg/h (0.1 lb/h).

The data presented in Tables 42 through 47 indicate that arsenic and lead comprised the majority of the measurable elemental concentration for the particle size runs conducted during the charging mode. The concentrations of selenium, cadmium, antimony, and bismuth measured in the particle size runs conducted during the charging mode are also presented in Tables 42 through 47.

The variations in the concentrations of arsenic and lead during the testing period can be attributed to the fact that the material being charged to the converter during the particle size runs was not consistent. A comparison of the material charged to the measured elemental concentration indicates that the greater the number of matte charges sampled by a particle size run, the higher the measured concentrations of arsenic and lead.

Figures 22 and 23 present a breakdown of the elemental concentrations for the three size ranges selected for analysis from the size runs conducted during the charging mode. These figures indicate that for all six elements measured, the majority of elemental concentrations are in the fine particulate range.

Skimming Mode--

Tables 48 through 53 present the concentration and mass emission rates for the elemental analysis performed on the three particle size runs conducted during the skimming mode. The data are presented in the same format as that used for the charging mode results.

The total concentration of arsenic measured from the particle size runs ranged between 2.0 mg/dNm^3 (0.0009 gr/dscf) and 5.6 mg/dNm^3 (0.002 gr/dscf). This corresponds to a mass emission rate ranging between 0.4 kg/h (1.0 lb/h) and 1.0 kg/h (2.2 lb/h).

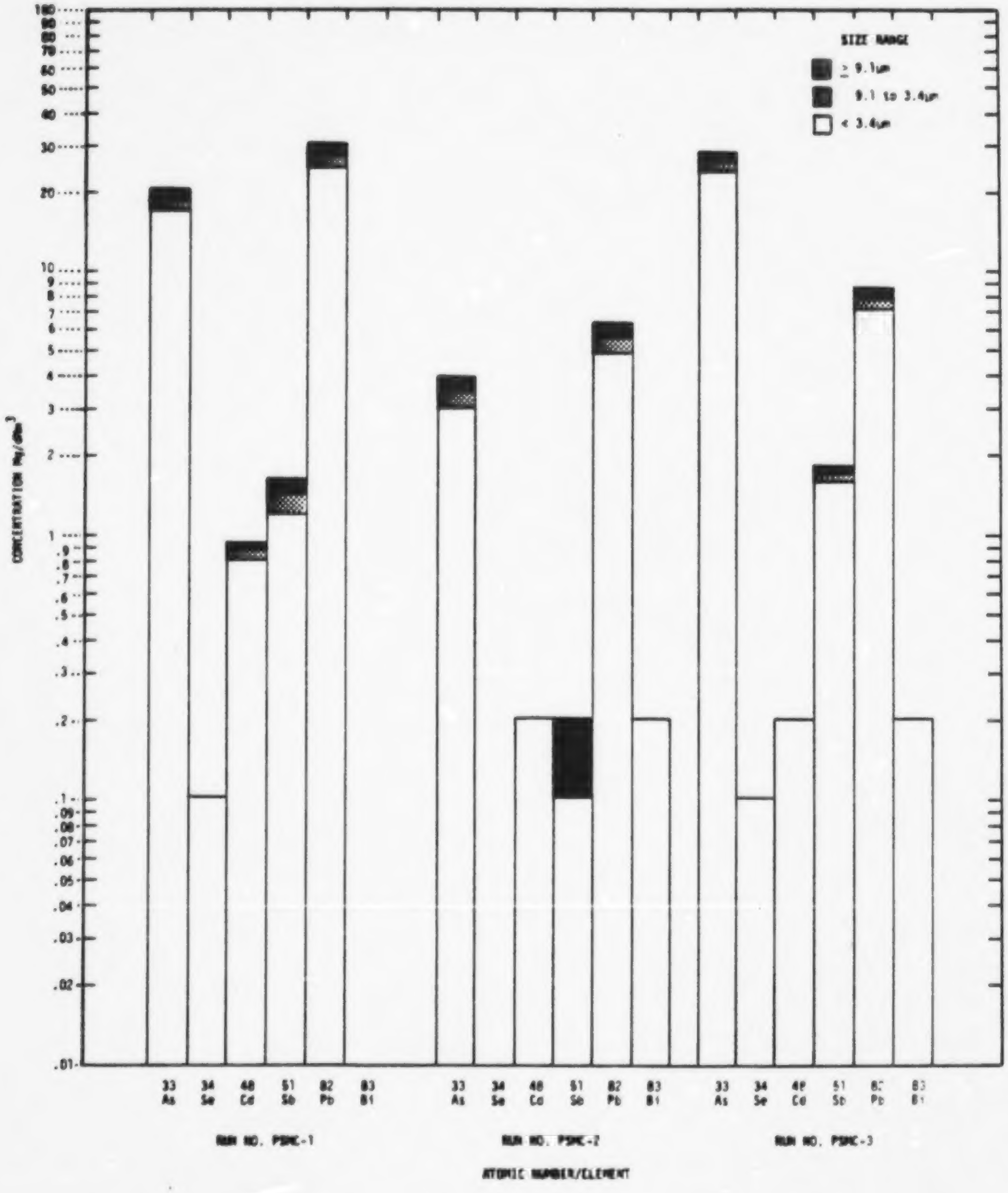

Figure 22. Comparison of elemental concentrations for the charging mode (Run Nos. PSMC-1, -2, -3.)

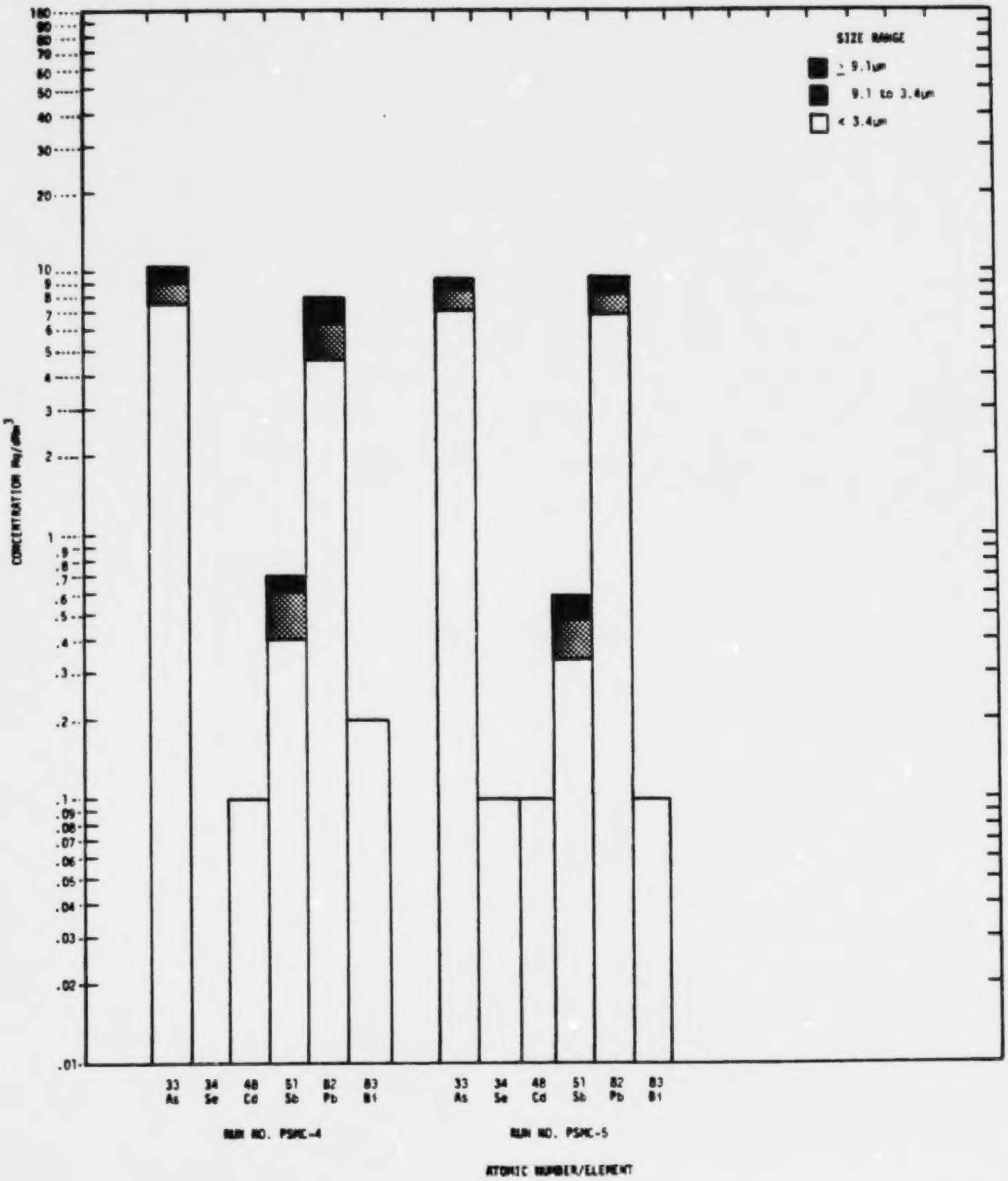

Figure 23. Comparison of elemental concentrations for the charging mode (Run Nos. PSMC-4, -5).

TABLE 48. SUMMARY OF ARSENIC CONCENTRATION AND MASS EMISSION RATE FOR THE PARTICLE SIZE RUNS FOR THE SKIMMING MODE[a]

Run No.	Date (1983)	Concentration							
		Total		$x \geq 8.6$ μm		8.6 μm > x > 3.1 μm		x < 3.1 μm	
		mg/dNm^3[b]	gr/dscf[c]	mg/dNm^3	gr/dscf	mg/dNm^3	gr/dscf	mg/dNm^3	gr/dscf
PSSS-1	1/18-19	2.0	0.0009	0.1	0.00004	0.1	0.00005	1.8	0.0008
PSSS-2	1/20	5.6	0.0024	0.4	0.0002	0.5	0.0002	4.7	0.002
PSSS-3	1/22	4.8	0.0022	0.2	0.0001	0.3	0.0001	4.3	0.002

Run No.	Date (1983)	Emission rate							
		Total		$x \geq 8.6$ μm		8.6 μm > x > 3.1 μm		x < 3.1 μm	
		kg/h[d]	lb/h[e]	kg/h	lb/h	kg/h	lb/h	kg/h	lb/h
PSSS-1	1/18-19	0.4	1.0	0.02	0.04	0.02	0.05	0.4	0.9
PSSS-2	1/20	1.0	2.2	0.1	0.2	0.1	0.2	1.0	2.2
PSSS-3	1/22	1.0	2.2	0.05	0.1	0.05	0.1	1.0	2.2

[a] Emission rate based on average volumetric flow rates of 2149 dNm^3/min (76,359 dscfm) during low flow (blowing mode) and 3571 dNm^3/min (126,924 dscfm) during high flow (charging and skimming modes).

[b] Milligrams per dry normal cubic meter.

[c] Grains per dry standard cubic foot.

[d] Kilograms per hour.

[e] Pounds per hour.

TABLE 49. SUMMARY OF SELENIUM CONCENTRATION AND MASS EMISSION RATE FOR THE PARTICLE SIZE RUNS FOR THE SKIMMING MODE[a]

Run No.	Date (1983)	Concentration							
		Total		$x \geq 8.6$ μm		8.6 μm > x > 3.1 μm		x < 3.1 μm	
		mg/dNm³[b]	gr/dscf[c]	mg/dNm³	gr/dscf	mg/dNm³	gr/dscf	mg/dNm³	gr/dscf
PSSS-1	1/18-19	2.1	0.0009	0.005	0.000002	0.01	0.000006	2.10	0.0009
PSSS-2	1/20	0.04	0.00002	0.005	0.000002	0.006	0.000002	0.03	0.00001
PSSS-3	1/22	0.05	0.00002	0.003	0.000001	0.002	0.0000009	0.05	0.00002

Run No.	Date (1983)	Emission rate							
		Total		$x \geq 8.6$ μm		8.6 μm > x > 3.1 μm		x < 3.1 μm	
		kg/h[d]	lb/h[e]	kg/h	lb/h	kg/h	lb/h	kg/h	lb/h
PSSS-1	1/18-19	0.4	1.0	0.001	0.002	0.003	0.007	0.4	1.0
PSSS-2	1/20	0.01	0.02	0.001	0.002	0.001	0.002	0.005	0.01
PSSS-3	1/22	0.01	0.02	0.0005	0.001	0.0004	0.001	0.01	0.02

[a] Emission rate based on average volumetric flow rates of 2149 dNm³/min (76,359 dscfm) during low flow (blowing mode) and 3571 dNm³/min (126, 924 dscfm) during high flow (charging and skimming modes).

[b] Milligrams per dry normal cubic meter.

[c] Grains per dry standard cubic foot.

[d] Kilograms per hour.

[e] Pounds per hour.

TABLE 50. SUMMARY OF CADMIUM CONCENTRATION AND MASS EMISSION RATE FOR THE PARTICLE SIZE RUNS FOR THE SKIMMING MODE[a]

Run No.	Date (1983)	Concentration							
		Total		$x \geq 8.6$ µm		8.6 µm > x > 3.1 µm		x < 3.1 µm	
		mg/dNm^3[b]	gr/dscf[c]	mg/dNm^3	gr/dscf	mg/dNm^3	gr/dscf	mg/dNm^3	gr/dscf
PSSS-1	1/18-19	0.02	0.000008	0.002	0.0000008	0.002	0.000001	0.01	0.000006
PSSS-2	1/20	0.1	0.000067	0.007	0.000003	0.01	0.000004	0.1	0.00006
PSSS-3	1/22	0.07	0.000033	0.003	0.000001	0.004	0.000002	0.07	0.00003

Run No.	Date (1983)	Emission rate							
		Total		$x \geq 8.6$ µm		8.6 µm > x > 3.1 µm		x < 3.1 µm	
		kg/h[d]	lb/h[e]	kg/h	lb/h	kg/h	lb/h	kg/h	lb/h
PSSS-1	1/18-19	0.004	0.009	0.0004	0.0009	0.0005	0.001	0.003	0.007
PSSS-2	1/20	0.03	0.07	0.001	0.003	0.002	0.004	0.03	0.07
PSSS-3	1/22	0.01	0.03	0.0005	0.001	0.001	0.002	0.01	0.03

[a] Emission rate based on average volumetric flow rates of 2149 dNm^3/min (76,359 dscfm) during low flow (blowing mode) and 3571 dNm^3/min (126,924 dscfm) during high flow (charging and skimming modes).

[b] Milligrams per dry normal cubic meter.

[c] Grains per dry standard cubic foot.

[d] Kilograms per hour.

[e] Pounds per hour.

TABLE 51. SUMMARY OF ANTIMONY CONCENTRATION AND MASS EMISSION RATE FOR THE PARTICLE SIZE RUNS FOR THE SKIMMING MODE[a]

Run No.	Date (1983)	Concentration							
		Total		$x \geq 8.6$ µm		8.6 µm > x > 3.1 µm		x < 3.1 µm	
		mg/dNm^3[b]	gr/dscf[c]	mg/dNm^3	gr/dscf	mg/dNm^3	gr/dscf	mg/dNm^3	gr/dscf
PSSS-1	1/18-19	0.18	0.00008	0.03	0.00001	0.03	0.00001	0.12	0.00005
PSSS-2	1/20	0.80	0.00036	0.05	0.00002	0.08	0.00004	0.67	0.0003
PSSS-3	1/22	0.57	0.00022	0.03	0.00001	0.03	0.00001	0.52	0.0002

Run No.	Date (1983)	Emission rate							
		Total		$x \geq 8.6$ µm		8.6 µm > x > 3.1 µm		x < 3.1 µm	
		kg/h[d]	lb/h[e]	kg/h	lb/h	kg/h	lb/h	kg/h	lb/h
PSSS-1	1/18-19	0.04	0.09	0.005	0.01	0.005	0.01	0.02	0.05
PSSS-2	1/20	0.1	0.3	0.01	0.02	0.02	0.04	0.1	0.03
PSSS-3	1/22	0.1	0.3	0.005	0.01	0.005	0.01	0.1	0.2

[a] Emission rate based on average volumetric flow rates of 2149 dNm^3/min (76,359 dscfm) during low flow (blowing mode) and 3571 dNm^3/min (126,924 dscfm) during high flow (charging and skimming modes).

[b] Milligrams per dry normal cubic meter.

[c] Grains per dry standard cubic foot.

[d] Kilograms per hour.

[e] Pounds per hour.

TABLE 52. SUMMARY OF LEAD CONCENTRATION AND MASS EMISSION RATE FOR THE PARTICLE SIZE RUNS FOR THE SKIMMING MODE[a]

		Concentration							
		Total		$x \geq 8.6$ µm		8.6 µm > x > 3.1 µm		$x < 3.1$ µm	
Run No.	Date (1983)	mg/dNm^3[b]	gr/dscf[c]	mg/dNm^3	gr/dscf	mg/dNm^3	gr/dscf	mg/dNm^3	gr/dscf
PSSS-1	1/18-19	4.9	0.002	0.2	0.0001	0.3	0.0001	4.3	0.002
PSSS-2	1/20	18.4	0.008	0.8	0.0003	1.1	0.0005	16.5	0.007
PSSS-3	1/22	16.6	0.0075	0.4	0.0002	0.6	0.0003	15.6	0.007

		Emission rate							
		Total		$x \geq 8.6$ µm		8.6 µm > x > 3.1 µm		$x < 3.1$ µm	
Run No.	Date (1983)	kg/h[d]	lb/h[e]	kg/h	lb/h	kg/h	lb/h	kg/h	lb/h
PSSS-1	1/18-19	1.0	2.2	0.05	0.1	0.05	0.1	1.0	2.2
PSSS-2	1/20	3.9	8.7	0.1	0.3	0.2	0.5	3.5	7.6
PSSS-3	1.22	3.5	7.6	0.1	0.2	0.1	0.3	3.5	7.6

[a] Emission rate based on average volumetric flow rates of 2149 dNm^3/min (76,359 dscfm) during low flow blowing mode) and 3571 dNm^3/min (126,924 dscfm) during high flow (charging and skimming modes).

[b] Milligrams per dry normal cubic meter.

[c] Grains per dry standard cubic foot.

[d] Kilograms per hour.

[e] Pounds per hour.

TABLE 53. SUMMARY OF BISMUTH CONCENTRATION AND MASS EMISSION RATE FOR THE PARTICLE SIZE RUNS FOR THE SKIMMING MODE[a]

Run No.	Date (1983)	Concentration							
		Total		x ≥ 8.6 µm		8.6 µm > x > 3.1 µm		x < 3.1 µm	
		mg/dNm³[b]	gr/dscf[c]	mg/dNm³	gr/dscf	mg/dNm³	gr/dscf	mg/dNm³	gr/dscf
PSSS-1	1/18-19	0.17	0.00007	0.005	0.000002	0.007	0.000003	0.16	0.00007
PSSS-2	1/20	0.54	0.00022	0.02	0.000009	0.03	0.00001	0.49	0.0002
PSSS-3	1/22	0.42	0.0002	0.01	0.000005	0.01	0.000005	0.40	0.0002

Run No.	Date (1983)	Emission rate							
		Total		x ≥ 8.6 µm		8.6 µm > x > 3.1 µm		x < 3.1 µm	
		kg/h[d]	lb/h[e]	kg/h	lb/h	kg/h	lb/h	kg/h	lb/h
PSSS-1	1/18-19	0.03	0.08	0.001	0.002	0.001	0.003	0.03	0.08
PSSS-2	1/20	0.1	0.2	0.004	0.01	0.005	0.01	0.1	0.2
PSSS-3	1/22	0.1	0.2	0.002	0.005	0.002	0.005	0.1	0.2

[a] Emission rate based on average volumetric flow rates of 2149 dNm³/min (76,359 dscfm) during low flow (blowing mode) and 3571 dNm³/min (126,924 dscfm) during high flow (charging and skimming modes).

[b] Milligrams per dry normal cubic meter.

[c] Grains per dry standard cubic foot.

[d] Kilograms per hour.

[e] Pounds per hour.

The total concentrations of selenium measured from the particle size runs ranged from less than 0.05 mg/dNm³ (0.00002 gr/dscf) to 2.1 mg/dNm³ (0.0009 gr/dscf). This corresponds to a mass emission rate ranging from less than 0.05 kg/h (0.1 lb/h) to 0.4 kg/h (1.0 lb/h). The reason for the large concentration of selenium measured in Run No. PSSS-1 could not be determined from the converter's observation log and is therefore considered suspect.

The total concentration of cadmium measured from the particle size runs ranged from less than 0.05 mg/dNm³ (0.00002 gr/dscf) to 0.15 mg/dNm³ (0.00006 gr/dscf). This corresponds to a mass emission rate of less than 0.05 kg/h (0.1 lb/h).

The total concentration of antimony measured from the particle size runs ranged between 0.18 and 0.57 mg/dNm³ (0.00008 and 0.003 gr/dscf). This corresponds to a mass emission rate ranging from less than 0.05 kg/h to 0.1 kg/h (0.00002 to 0.3 lb/h).

The total concentration of lead measured from the particle size runs ranged between 4.9 mg/dNm³ (0.002 gr/dscf) and 18.4 mg/dNm³ (0.008 gr/dscf). This corresponds to a mass emission rate ranging between 1.0 kg/h (2.2 lb/h) and 3.9 kg/h (8.7 lb/h).

The total concentration of bismuth measured from the particulate size runs ranged between 0.17 and 0.54 mg/dNm³ (0.00007 and 0.0002 gr/dscf). This corresponds to a mass emission rate ranging from less than 0.05 kg/h to 0.1 kg/h (0.1 to 0.2 lb/h).

Figure 24 presents a breakdown of the elemental concentration for the three size ranges selected for analysis from the particle size runs conducted during the skimming mode. This figure indicates that for all six elements measured the majority of the elemental concentrations are in the fine particulate range.

The concentrations for five of the six elements appear to follow a pattern; Run No. PSSS-1 had the lowest concentration, Run No. PSSS-2 the highest concentration, and Run No. PSSS-3 a concentration in between the two previous runs. The total particulate concentrations for the particle size runs also follow this same pattern.

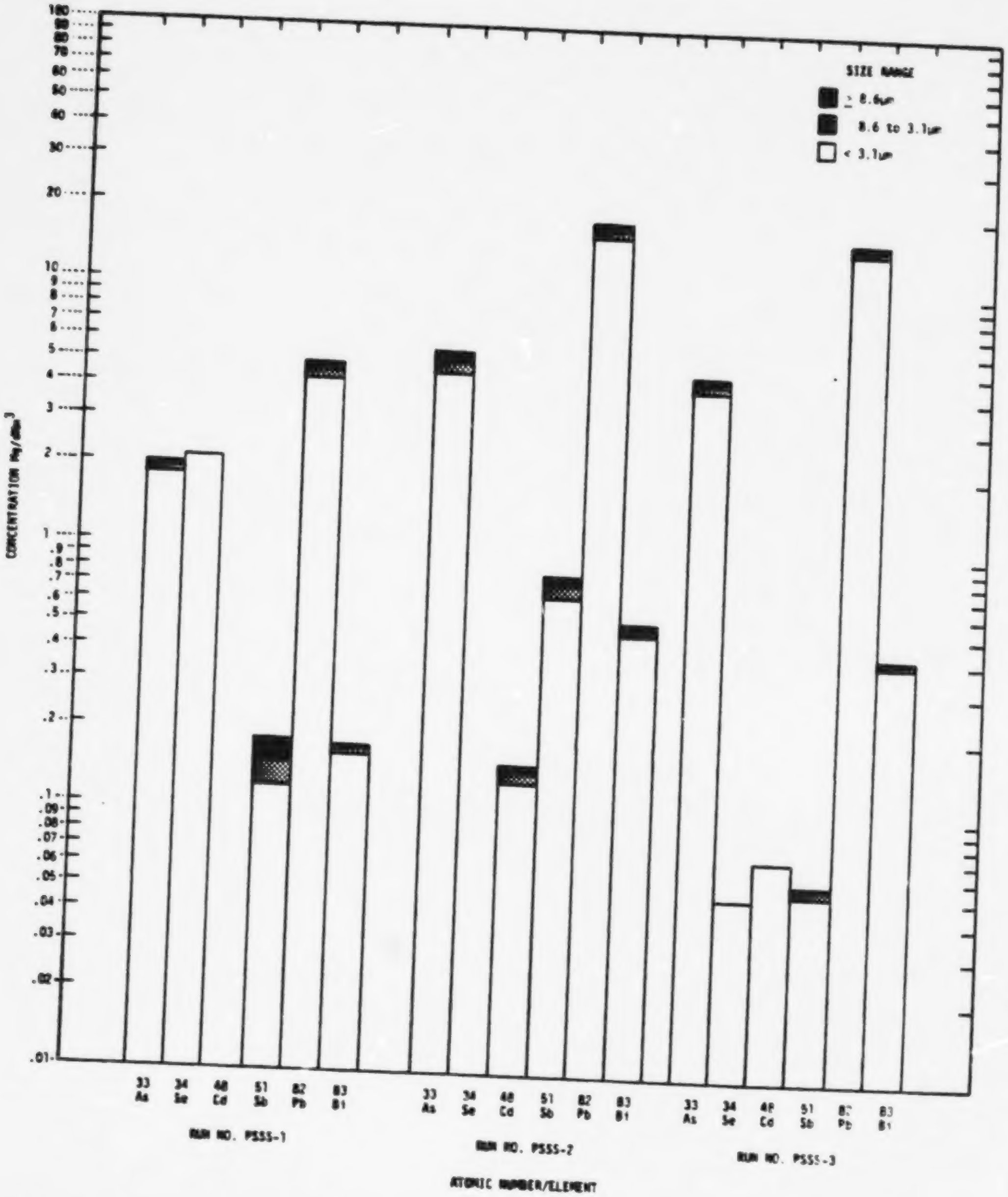

Figure 24. Comparison of elemental concentrations for the skimming mode.

Blowing Mode--

Tables 54 through 59 present the concentration and mass emission rates for the elemental analysis performed on two of the particle size runs conducted during the blowing mode. These data are presented in the same format as that used for the charging mode results.

The total concentrations of arsenic, antimony, lead, and bismuth measured for the two particle size runs varied significantly. The reason for this large variation is that during Run No. PSB-2, the primary hood malfunctioned and emissions normally captured by the primary hood escaped and were collected by the air curtain system. This indicates that the elemental concentration measured by Run No. PSB-2 is biased high.

The elemental analyses for selenium and cadmium for the two particle size runs show that the concentrations of these elements are less than the detectable level.

Figure 25 presents a breakdown of the elemental concentration for the three size ranges selected for analysis from the two chosen particle size runs conducted during the blowing mode. This figure indicates that a higher percentage of the elemental concentration is comprised of larger particulate compared to the charging and skimming modes.

Table 60 presents a comparison of the total particulate concentration with the elemental concentrations measured for the particle size runs.

For the charging mode the particulate concentration determined by adding the individual concentrations from the elemental analysis comprised between 12.2 and 39.5 percent of the total particulate concentration measured by the particle size runs. The concentration of arsenic in these runs ranged between 4.6 and 28.2 percent of the total particle size concentration, while the concentration of lead ranged between 5.6 and 18.2 percent. The concentration of the remaining four elements (selenium, cadmium, antimony, and bismuth) comprised between 0.6 and 2.3 percent of the total particle size concentration.

TABLE 54. SUMMARY OF ARSENIC CONCENTRATION AND MASS EMISSION RATE FOR THE PARTICLE SIZE RUNS FOR THE BLOWING MODE[a]

Run No.	Date (1983)	Concentration							
		Total		$x \geq 9.9$ µm		9.9 µm > x > 2.1 µm		x < 2.1 µm	
		mg/dNm^3[b]	gr/dscf[c]	mg/dNm^3	gr/dscf	mg/dNm^3	gr/dscf	mg/dNm^3	gr/dscf
PSB-1	1/18	0.37	0.0002	0.13	0.00006	0.03	0.00001	0.21	0.00009
PSB-2	1/20	23.7	0.01	1.5	0.0007	2.2	0.0009	20.1	0.009

Run No.	Date (1983)	Emission rate							
		Total		$x \geq 9.9$ µm		9.9 µm > x > 2.1 µm		x < 2.1 µm	
		kg/h[d]	lb/h[e]	kg/h	lb/h	kg/h	lb/h	kg/h	lb/h
PSB-1	1/18	0.01	0.1	0.02	0.04	0.003	0.07	0.03	0.06
PSB-2	1/20	3.0	6.5	0.2	0.5	0.3	0.6	2.7	5.9

[a] Emission rate based on average volumetric flow rates of 2149 dNm^3/min (76,359 dscfm) during low flow (blowing mode) and 3571 dNm^3/min (126,924 dscfm) during high flow (charging and skimming modes).

[b] Milligrams per dry normal cubic meter.

[c] Grains per dry standard cubic foot.

[d] Kilograms per hour.

[e] Pounds per hour.

TABLE 55. SUMMARY OF SELENIUM CONCENTRATION AND MASS EMISSION RATE FOR THE PARTICLE SIZE RUNS FOR THE BLOWING MODE[a]

Run No.	Date (1983)	Concentration							
		Total		x ≥ 9.9 µm		9.9 µm > x > 2.1 µm		x < 2.1 µm	
		mg/dNm³[b]	gr/dscf[c]	mg/dNm³	gr/dscf	mg/dNm³	gr/dscf	mg/dNm³	gr/dscf
PSB-1	1/18	0.007	0.000003	0.005	0.0000002	<0.0004	<0.0000002	0.001	0.0000006
PSB-2	1/20	0.02	0.000008	0.01	0.000006	<0.002	<0.0000007	0.003	0.000001

Run No.	Date (1983)	Emission rate							
		Total		x ≥ 9.9 µm		9.9 µm > x > 2.1 µm		x < 2.1 µm	
		kg/h[d]	lb/h[e]	kg/h	lb/h	kg/h	lb/h	kg/h	lb/h
PSB-1	1/18	0.001	0.002	0.0006	0.001	<0.00006	<0.0001	0.0002	0.0004
PSB-2	1/20	0.002	0.005	0.002	0.004	<0.0002	<0.0005	0.0003	0.0007

[a] Emission rate based on average volumetric flow rates of 2149 dNm³/min (76,359 dscfm) during low flow (blowing mode) and 3571 dNm³/min (126,924 dscfm) during high flow (charging and skimming modes).

[b] Milligrams per dry normal cubic meter.

[c] Grains per dry standard cubic foot.

[d] Kilograms per hour.

[e] Pounds per hour.

TABLE 56. SUMMARY OF CADMIUM CONCENTRATION AND MASS EMISSION RATE FOR THE PARTICLE SIZE RUNS FOR THE BLOWING MODE[a]

Run No.	Date (1983)	Concentration							
		Total		$x \geq 9.9$ µm		9.9 µm $> x >$ 2.1 µm		$x <$ 2.1 µm	
		mg/dNm^3[b]	gr/dscf[c]	mg/dNm^3	gr/dscf	mg/dNm^3	gr/dscf	mg/dNm^3	gr/dscf
PSB-1	1/18	0.006	0.000003	0.002	0.000001	<0.0004	<0.0000002	0.004	0.000002
PSB-2	1/20	0.03	0.00001	0.02	0.000007	0.01	0.000004	0.008	0.000003

Run No.	Date (1983)	Emission rate[e]							
		Total		$x \geq 9.9$ µm		9.9 µm $> x >$ 2.1 µm		$x <$ 2.1 µm	
		kg/h[d]	lb/h[e]	kg/h	lb/h	kg/h	lb/h	kg/h	lb/h
PSB-1	1/18	0.001	0.002	0.0003	0.0007	0.00006	0.0001	0.0006	0.001
PSB-2	1/20	0.003	0.007	0.002	0.005	0.001	0.003	0.0009	0.002

[a] Emission rate based on average volumetric flow rates of 2149 dNm^3/min (76,359 dscfm) during low flow (blowing mode) and 3571 dNm^3/min (126,924 dscfm) during high flow (charging and skimming modes).

[b] Milligrams per dry normal cubic meter.

[c] Grains per dry standard cubic foot.

[d] Kilograms per hour.

[e] Pounds per hour.

TABLE 57. SUMMARY OF ANTIMONY CONCENTRATION AND MASS EMISSION RATE FOR THE PARTICLE SIZE RUNS FOR THE BLOWING MODE[a]

Run No.	Date (1983)	Concentration							
		Total		$x \geq 9.9$ µm		9.9 µm $> x >$ 2.1 µm		$x <$ 2.1 µm	
		mg/dNm^3[b]	gr/dscf[c]	mg/dNm^3	gr/dscf	mg/dNm^3	gr/dscf	mg/dNm^3	gr/dscf
PSB-1	1/18	0.09	0.00004	0.07	0.00003	0.001	0.0000006	0.01	0.000006
PSB-2	1/20	1.75	0.0008	0.27	0.0001	0.10	0.00004	1.38	0.0006

Run No.	Date (1983)	Emission rate[e]							
		Total		$x \geq 9.9$ µm		9.9 µm $> x >$ 2.1 µm		$x <$ 2.1 µm	
		kg/h[d]	lb/h[e]	kg/h	lb/h	kg/h	lb/h	kg/h	lb/h
PSB-1	1/18	0.01	0.03	0.009	0.02	0.0002	0.0004	0.002	0.004
PSB-2	1/20	0.24	0.5	0.03	0.07	0.01	0.03	0.2	0.4

[a] Emission rate based on average volumetric flow rates of 2149 dNm^3/min (76,359 dscfm) during low flow (blowing mode) and 3571 dNm^3/min (126,924 dscfm) during high flow (charging and skimming modes).

[b] Milligrams per dry normal cubic meter.

[c] Grains per dry standard cubic foot.

[d] Kilograms per hour.

[e] Pounds per hour.

TABLE 58. SUMMARY OF LEAD CONCENTRATION AND MASS EMISSION RATE FOR THE PARTICLE SIZE RUNS FOR THE BLOWING MODE[a]

Run No.	Date (1983)	Concentration							
		Total		$x \geq 9.9$ µm		9.9 µm $> x >$ 2.1 µm		$x <$ 2.1 µm	
		mg/dNm^3[b]	gr/dscf[c]	mg/dNm^3	gr/dscf	mg/dNm^3	gr/dscf	mg/dNm^3	gr/dscf
PSB-1	1/18	0.71	0.0003	0.45	0.0002	0.03	0.00001	0.23	0.0001
PSB-2	1/20	8.97	0.004	2.0	0.0009	0.70	0.0003	6.3	0.003

Run No.	Date (1983)	Emission rate[e]							
		Total		$x \geq 9.9$ µm		9.9 µm $> x >$ 2.1 µm		$x <$ 2.1 µm	
		kg/h[d]	lb/h[e]	kg/h	lb/h	kg/h	lb/h	kg/h	lb/h
PSB-1	1/18	0.09	0.2	0.06	0.1	0.003	0.007	0.03	0.07
PSB-2	1/20	1.2	2.6	0.3	0.6	0.09	0.2	0.9	2.0

[a] Emission rate based on average volumetric flow rates of 2149 dNm^3/min (76,359 dscfm) during low flow (blowing mode) and 3571 dNm^3/min (126,924 dscfm) during high flow (charging and skimming modes).

[b] Milligrams per dry normal cubic meter.

[c] Grains per dry standard cubic foot.

[d] Kilograms per hour.

[e] Pounds per hour.

TABLE 59. SUMMARY OF BISMUTH CONCENTRATION AND MASS EMISSION RATE FOR THE PARTICLE SIZE RUNS FOR THE BLOWING MODE[a]

Run No.	Date (1983)	Concentration							
		Total		$x \geq 9.9$ μm		9.9 μm > x > 2.1 μm		x < 2.1 μm	
		mg/dNm^3[b]	gr/dscf[c]	mg/dNm^3	gr/dscf	mg/dNm^3	gr/dscf	mg/dNm^3	gr/dscf
PSB-1	1/18	0.01	0.000005	0.007	0.000003	0.0008	0.0000004	0.005	0.000002
PSB-2	1/20	0.30	0.0001	0.05	0.000002	0.03	0.00001	0.2	0.0001

Run No.	Date (1983)	Emission rate[e]							
		Total		$x \geq 9.9$ μm		9.9 μm > x > 2.1 μm		x < 2.1 μm	
		kg/h[d]	lb/h[e]	kg/h	lb/h	kg/h	lb/h	kg/h	lb/h
PSB-1	1/18	0.001	0.003	0.0009	0.002	0.0001	0.0003	0.0006	0.001
PSB-2	1/20	0.03	0.07	0.006	0.01	0.003	0.007	0.03	0.07

[a] Emission rate based on average volumetric flow rates of 2149 dNm^3/min (76,359 dscfm) during low flow (blowing mode) and 3571 dNm^3/min (126,924 dscfm) during high flow (charging and skimming modes).

[b] Milligrams per dry normal cubic meter.

[c] Grains per dry standard cubic foot.

[d] Kilograms per hour.

[e] Pounds per hour.

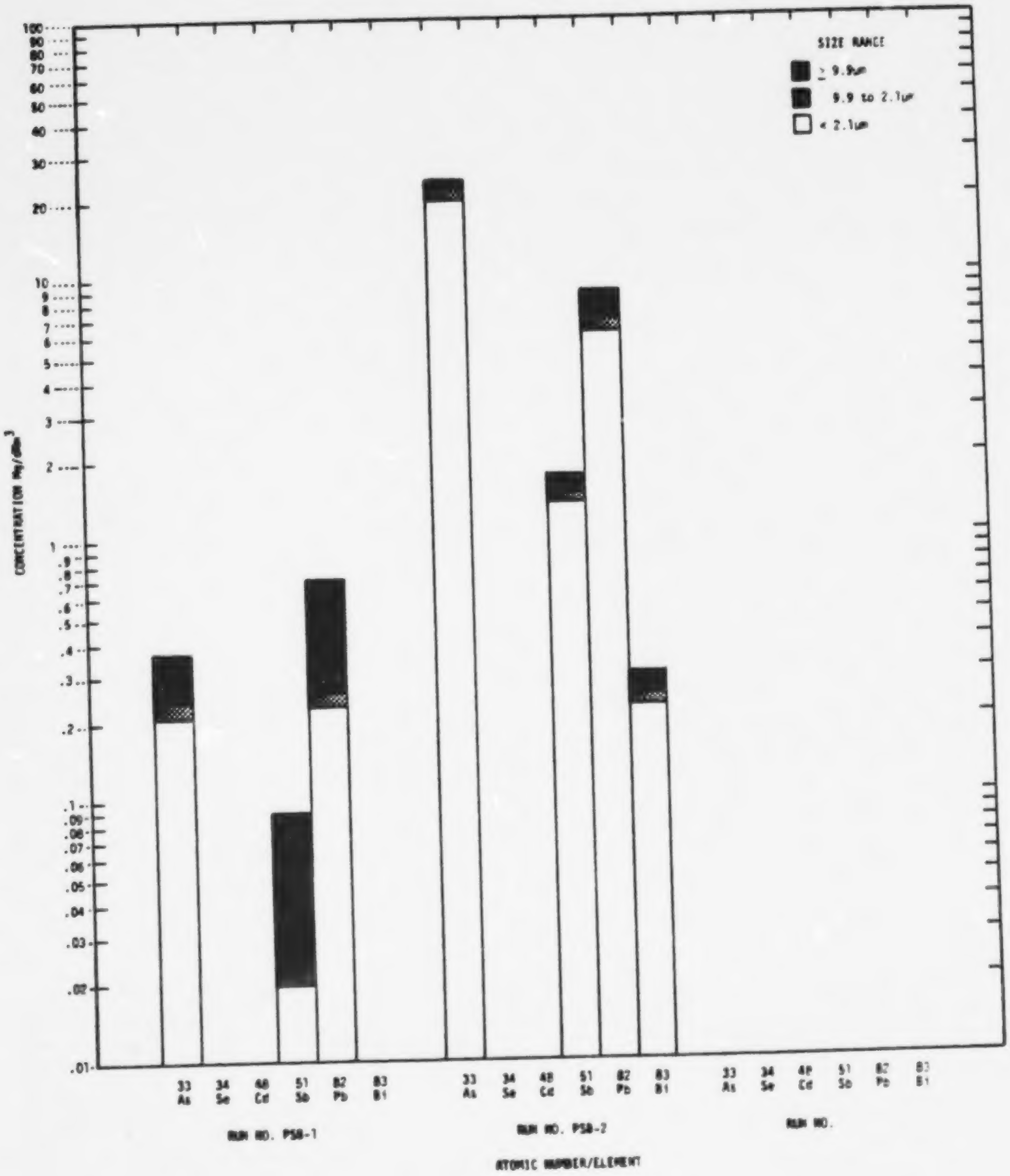

Figure 25. Comparison of elemental concentrations for the blowing mode.

TABLE 60. COMPARISON OF THE TOTAL PARTICULATE CONCENTRATION MEASURED BY THE PARTICLE SIZE RUNS TO THE ELEMENTAL CONCENTRATIONS

Run No.	Total particulate concentration, mg/dNm³ (gr/dscf)	Percent of the total particulate concentration determined from the total elemental concentration	Percent of the total particulate concentration for each element measured					
			As	Se	Cd	Sb	Pb	Bi
Charging mode								
PSMC-1	165 (0.072)	32.5	12.3	0.07	0.5	1.0	18.2	0.4
PSMC-2	94 (0.041)	12.2	4.6	0.04	0.2	0.2	7.0	0.2
PSMC-3	98 (0.043)	39.5	28.2	0.05	0.2	1.8	9.0	0.2
PSMC-4	132 (0.058)	14.7	8.3	0.02	0.05	0.5	5.6	0.2
PSMC-5	157 (0.068)	12.6	6.0	0.03	0.03	0.4	6.1	0.08
Blowing mode								
PSB-1	25 (0.011)	4.8	1.5	0.02	0.02	0.4	2.8	0.04
PSB-2	107 (0.047)	32.7	22.1	0.02	0.02	1.6	8.4	0.3
Skimming mode								
PSSS-1	40 (0.018)	23.2	5.3	5.3	0.04	0.5	11.7	0.4
PSSS-2	77 (0.033)	32.8	6.7	0.06	0.2	1.0	24.1	0.7
PSSS-3	64 (0.028)	26.2	7.3	0.08	0.1	0.9	25.5	0.7

For the blowing mode the particulate concentration determined by adding the individual concentrations from the elemental analysis for the two sample runs comprised 4.7 and 32.4 percent of the total particulate concentration measured by the particle size runs.

The concentrations of arsenic in these two runs were 1.5 and 22.1 percent, while the concentrations of antimony were 0.4 and 1.6 percent and lead 2.8 and 8.4 percent of the total particle size concentration. The remaining three elements (selenium, cadmium, and bismuth) comprised less than 1 percent of the total particle size concentration.

For the skimming mode the particulate concentration determined by adding the individual concentrations from the elemental analysis comprised between 23.2 and 32.7 percent of the total particulate concentration measured by the particle size runs. The concentration of arsenic in these runs ranged between 5.3 and 7.3 percent of the total particle size concentration. The concentration of selenium was between 0.0 and 5.3 percent and lead between 11.7 and 25.5 percent of the total particle size concentration. The remaining three elements (cadmium, antimony, and bismuth) comprised between 0.9 and 1.9 percent of the total particle size concentration.

5.5 TRACE METALS--ANTIMONY, BISMUTH, CADMIUM, LEAD, AND SELENIUM

Table 61 summarizes the concentrations of antimony (Sb), bismuth (Bi), cadmium (Cd), lead (Pb), and selenium (Se). Aliquots of samples from tests PATC and PASM were analyzed by atomic absorption techniques at the completion of the particulate and arsenic analysis. The reported concentrations represent the combined filterable and gaseous fractions of each metal. Mass emission rates were calculated by use of the volumetric flows presented in Sections 5.2, Table 33. In the total cycle tests, the concentrations of antimony, bismuth, cadmium, and selenium were less than 1.0 mg/dNm^3 (0.0004 gr/dscf), and the lead concentrations ranged from 3.44 mg/dNm^3 (0.0015 gr/dscf) to 8.79 mg/dNm^3 (0.004 gr/dscf).

TABLE 61. SUMMARY OF TRACE METAL EMISSION RESULTS

Cycle Test No.	Run No.	Date (1983)	Total concentration[a], mg/dNm³ (gr/dscf)					Mass emission rate[b], kg/h (lb/h)				
			Sb	Bi	Cd	Pb	Se	Sb	Bi	Cd	Pb	Se
1	PATC-1	1/18-19	0.23 (0.0001)	0.12 (0.00005)	0.08 (0.00004)	4.79 (0.002)	0.38 (0.0002)	0.04 (0.08)	0.02 (0.04)	0.01 (0.03)	0.73 (1.6)	0.07 (0.16)
1	PASM-1	1/18-19	0.51 (0.0002)	0.17 (0.00007)	0.19 (0.00008)	9.49 (0.004)	1.0 (0.0004)	0.10 (0.22)	0.04 (0.08)	0.04 (0.09)	2.0 (4.4)	0.20 (0.44)
2	PATC-2	1/20	0.81 (0.0004)	0.29 (0.0001)	0.09 (0.00004)	8.79 (0.004)	0.05 (0.00002)	0.15 (0.32)	0.04 (0.08)	0.01 (0.03)	1.45 (3.2)	0.01 (0.02)
2	PASM-2	1/20	1.44 (0.0006)	0.38 (0.0002)	0.18 (0.00008)	18.9 (0.008)	0.07 (0.00003)	0.29 (0.65)	0.10 (0.22)	0.04 (0.09)	3.95 (8.7)	0.01 (0.03)
3	PATC-3	1/22	0.15 (0.00007)	0.10 (0.00004)	0.02 (0.00001)	3.44 (0.0015)	0.23 (0.0001)	0.03 (0.06)	0.01 (0.03)	0.004 (0.008)	0.54 (1.2)	0.04 (0.08)
3	PASM-3[c]	1/22	0.75 (0.0003)	1.09 (0.0005)	0.15 (0.0004)	21.7 (0.009)	0.10 (0.00004)	0.15 (0.33)	0.24 (0.54)	0.02 (0.04)	4.4 (9.8)	0.02 (0.04)

[a] Total concentration (filterable and gaseous fractions) of antimony (Sb), bismuth (Bi), cadmium (Cd), lead (Pb), and selenium (Se).

[b] Calculations of mass emission rate were based on measured concentration and volumetric flows reported in Table 5-9.

[c] Slag skimming only.

During specific mode Tests PASM-1 and 2, antimony concentrations ranged from 0.51 mg/dNm³ (0.0002 gr/dscf) to 1.44 mg/dNm³ (0.0006 gr/dscf). Bismuth and cadmium concentrations were less than 0.5 mg/dNm³ (0.0002 gr/dscf) and selenium concentrations ranged from 0.07 mg/dNm³ (0.00003 gr/dscf) during Test PASM-2 to 1.0 mg/dNM³ (0.004 gr/dscf) during Test PASM-1. Lead concentrations during these tests were 9.49 mg/dNm³ (0.004 gr/dscf) and 18.9 mg/dNm³ (0.008 gr/dscf), respectively.

Test Run PASM-3, which was conducted only during slag skimming operations, showed a lead concentration of 21.7 mg/dNm³ (0.009 gr/dscf).

The trace metal emission data support conclusions drawn in Subsections 5.1 through 5.3 that the majority of fugitive emissions from the No. 4 converter are generated during converter roll-out modes. Data from Test PASM-3, conducted only during slag skim operations, indicate that lead and bismuth emissions are generated primarily during the converter skimming mode. Emission data from Test PATC-2, during which the malfunction in the primary hood system occurred, show higher levels of antimony and bismuth than the other PATC test runs.

5.6 PROCESS SAMPLES

Table 62 summarizes analytical results for arsenic and lead in the process samples collected by ASARCO personnel during the test program. Results for each element are expressed as percent by weight. Samples were digested according to procedures described in draft EPA Method 108 and analyzed by atomic absorption. Although lead analysis was not required for these samples, the results are reported to validate the lead results obtained during the particulate and particle size distribution tests.

The El Indio and Le Panto concentrates are high in arsenic (~11%). All the other charge materials are comparatively low in arsenic (generally less than 0.2%). Also presented in Table 62 are the percentages of concentrate ore (by weight) charged during the January test period. As shown, the concentrate charge accounted for 79.74 percent of the total charge (the remainder of 20.26 percent represents other inert materials) and of this total, 19.88 percent or approximately one fourth of the total ore charge was high arsenic Le Panto concentrate.

TABLE 62. ARSENIC AND LEAD IN PROCESS SAMPLES

Sample description	Arsenic (As), %	Lead (Pb), %	Concentrate charge - 1/83 % by weight
Test No. 1 (1/19) - Charge 79 - cleanup blow	0.09	4.8	
Test No. 1 (1/19) - Charge 79 - 2nd blow	0.15	3.5	
Test No. 1 (1/19) - Charge 79 - 3rd blow	0.13	4.5	
Test No. 1 (1/19) - Charge 79 - 4th blow	0.18	2.9	
Test No. 2 (1/20) - Charge 80 - cleanup	0.07	2.9	
Test No. 2 (1/20) - Charge 80 - 1st blow	0.17	1.1	
Test No. 2 (1/20) - Charge 80 - 2nd blow	0.22	1.6	
Test No. 2 (1/20) - Charge 80 - 3rd blow	0.15	2.8	
Test No. 2 (1/20) - Charge 80 - 4th blow	0.13	2.3	
Test No. 3 (1/22) - Charge 81 - cleanup	0.19	0.7	
Test No. 3 (1/22) - Charge 81 - 3rd skim	0.12	3.6	
Test No. 3 (1/22) - Charge 81 - 4th skim	0.14	2.2	
Test No. 3 (1/22) - Charge 81 - 5th skim	0.24	1.9	
Reverberatory matte - composite as received from ASARCO	0.70	3.0	
Gibraltor concentrates	0.008	0.05	9.99
Lornex concentrates	0.08	0.03	39.01
El Indio concentrates	10.8	0.09	-
Le Panto concentrates	11.1	0.13	19.88
St. Joe	NSR	-	7.74
Troy	NSR	-	3.12
		Total	79.74

NSR = No sample received.

SECTION 6

QUALITY ASSURANCE

Because the end product of testing is to produce representative emission results, quality assurance is one of the main facets of stack sampling. Quality assurance guidelines provide the detailed procedures and actions necessary for defining and producing acceptable data. Five such documents were used in this test program to ensure the collection of acceptable data and to provide a definition of unacceptable data. The following documents comprise the source-specific test plan prepared by PEDCo and reviewed by EPA-IERL: the source-specific Quality Assurance plan prepared by PEDCo and reviewed by EPA-IERL; the EPA Quality Assurance Handbook Volume III, EPA-600/4-77-027; the PEDCo Environmental Emission Test Quality Assurance Plan; and the PEDCo Environmental Laboratory Quality Assurance Plan. The last two, which are PEDCo's general guideline manuals, define the company's standard operating procedures and are followed by the emission testing groups and the laboratory groups.

For this test program, the following steps were taken to ensure that the testing and analytical procedures produced quality data.

- Calibration of all field sampling equipment. (Appendix E describes calibration guidelines in more detail.)
- Checks on train configuration and calculations.
- Onsite quality assurance checks (i.e., sampling train, pitot tube, and Orsat line leak checks) and quality assurance checks of all test equipment prior to use.
- Use of designated analytical equipment and sampling reagents.

- Internal and external audits to ensure accuracy in sampling and analysis.

Table 63 lists the sampling equipment used to perform the particulate/arsenic, particle size, and SO_2 tests as well as the calibration guidelines and limits. In addition to the pre-test and post-test calibrations, a field audit was performed on the metering system used for the particulate/arsenic, particle size, and SO_2 sample runs. Figures 26 through 29 show an example audit run for each dry gas meter used for particulate/arsenic, particle size, and SO_2 tests.

As a check on the reliability of the method used to analyze the filters for the particulate tests, sets of filters that had been preweighed in the lab were resubmitted for replicate analysis. Table 64 summarizes the results of a blank filter and reagent analysis.

An impactor run was made to determine if the gaseous emissions generated by the process biased the particle size results. Two absolute filters were placed prior to the impactor to remove filterable particulate emissions. The impactor's filter stages were recovered and analyzed in the same manner as during the test runs. As the data in Table 64 show, the filtered stack gas did not react with the filter media.

The atomic absorption (AA) spectrophotometer used for the trace metal analysis was calibrated for the specific analysis each time a batch of samples was analyzed by use of NBS traceable 1000-ppm solutions of the individual metals. Table 65 presents results of the QA audit performed on samples supplied by EMSL/QAD.

Audit solutions prepared by the EPA were used to check the analytical procedures and reagent used for the manual SO_2 sampling and onsite analysis. Figure 30 presents the results of these analytical audits. The audit results show that the analytical techniques were good.

The simultaneously performed manual SO_2 test results were compared with the monitor data to assure proper CEM operations.

TABLE 63. FIELD EQUIPMENT CALIBRATION

Equipment	Test No.	Calibrated against	Allowable deviation	Actual deviation	Within allowable limits	Comments
Meter box	FB-4	Wet test meter	(Y ±0.05 Y pre-test) ΔH @ ±0.15 (Y ±0.05 Y post-test)	-0.003 -0.06 -0.006	X X X	Used for particulate/arsenic tests
	FB-5			-0.008 -0.11 -0.001	X X X	Used for particulate/arsenic and SO_2 tests
	FB-7			-0.019 -0.03 +0.008	X X X	Used for particle size tests
	FB-9			-0.022 -0.03 -0.004	X X X	Used for particle size tests
Pitot tube	015 032 278 284	Geometric specifications	See Appendix E	0.046 0.075 0.017	X X X	Cp = 0.84
Thermocouple	133 147 202 203	ASTM-3F	1.5%	-0.50% 0.19% -1.07% -0.61%	X X X X	
Digital indicator	124 221	Millivolt signals	0.5%	-0.41% -0.06%	X X	
Impinger thermometer		ASTM-3F	±2°F			
Dry gas meter thermometer	FB-4 Inlet FB-4 Outlet	ASTM-2 or 3F	±5°F	3.0°F 1.3°F	X X	
	FB-5 Inlet FB-5 Outlet			4.0°F 2.5°F	X X	
	FB-7 Inlet FB-7 Outlet			3.0°F 2.5°F	X X	
	FB-9 Inlet FB-9 Outlet			1.0°F 1.0°F	X X	
Trip balance	270	Type S weights	±0.5 g	0.0 g	X	
Barometer	229	NBS traceable barometer	+0.10 in.Hg (0.20 post-test)	0.01 in.	X	
Probe nozzle	PATC 2-111 PATC 3-116 PASM 2-221 PSMCP PSSSP PSBP PS Blank	Caliper	Dn ±0.004 in.	0.00 in. 0.00 in. 0.00 in. 0.002 in. 0.003 in. 0.001 in. 0.002 in.	X X X X X X X	

AUDIT REPORT DRY GAS METER

DATE: 8/12/83

CLIENT: USEPA

BAROMETRIC PRESSURE (P_{bar}): 30.04 in. Hg

METER BOX NO. FB-4

ORIFICE NO. 73

PRETEST γ: 1.037

ORIFICE K FACTOR: 4.591×10^{-4}

AUDITOR: DRO

Orifice manometer reading ΔH in H_2O	Dry gas meter reading V_i/V_f ft^3	Temperatures: Ambient T_{ai}/T_{af} °F	Temperatures: Dry gas meter: Inlet T_{ii}/T_{if} °F	Temperatures: Dry gas meter: Outlet T_{oi}/T_{of} °F	Duration of run Ø min	
1.79	451.000	58	63	57	15:06.8	Vac
	461.400	60	64	58	15.113	14.5

Dry gas meter volume V_m ft^3	Average temperatures: Ambient T_a °F	Average temperatures: Dry gas meter T_m °F	$V_{m_{std}}$ ft^3	$V_{m_{act}}$ ft^3	Audit γ	γ deviation %
10.400	59	60.5	10.639	11.006	1.034	−0.3

$V_{m_{std}}$	$V_{m_{act}}$
$\frac{(17.647)(V_m)(P_{bar} + \Delta H/13.6)}{(T_m + 460)}$	$\frac{(1203)(\emptyset)(K)(P_{bar})}{(T_a + 460)^{1/2}}$

Audit γ	γ deviation, %
$\frac{V_{m_{act}}}{V_{m_{std}}}$	$\frac{(\gamma \text{ audit} - \gamma \text{ pre-test})(100\%)}{(\gamma \text{ audit})}$

Audit γ must be in the range, pre-test γ ±0.05

Figure 26. Audit report dry gas meter (Meter Box No. FB-4).

AUDIT REPORT DRY GAS METER

DATE: 1/12/83
CLIENT: USEPA
BAROMETRIC PRESSURE (P_{bar}): 29.98 in. Hg
METER BOX NO. FB-5
ORIFICE NO. 10
PRETEST γ: .988
ORIFICE K FACTOR: 4.798×10^{-4}
AUDITOR: DRO

Orifice manometer reading ΔH in H_2O	Dry gas meter reading V_i/V_f ft^3	Temperatures			Duration of run $\emptyset$ min
		Ambient T_{ai}/T_{af} °F	Dry gas meter Inlet T_{ii}/T_{if} °F	Dry gas meter Outlet T_{oi}/T_{of} °F	
1.98	517.000	67	77	70	15.08.8
	528.700	65	77	70	15.147

Vac
19.8

Dry gas meter volume V_m ft^3	Average temperatures Ambient T_a °F	Average temperatures Dry gas meter T_m °F	$V_{m_{std}}$ ft^3	$V_{m_{act}}$ ft^3	Audit γ	γ deviation %
11.700	66	73.5	11.640	11.409	.980	-0.8

$V_{m_{std}}$	$V_{m_{act}}$
$\frac{(17.647)(V_m)(P_{bar} + \Delta H/13.6)}{(T_m + 460)}$	$\frac{(1203)(\emptyset)(K)(P_{bar})}{(T_a + 460)^{1/2}}$

Audit γ	γ deviation, %
$\frac{V_{m_{act}}}{V_{m_{std}}}$	$\frac{(\gamma \text{ audit} - \gamma \text{ pre-test})(100\%)}{(\gamma \text{ audit})}$

Audit γ must be in the range, pre-test γ ±0.05

Figure 27. Audit report dry gas meter (Meter Box No. FB-5).

AUDIT REPORT DRY GAS METER

DATE: 1/12/87 CLIENT: USEPA
BAROMETRIC PRESSURE (P_{bar}): 29.93 in. Hg METER BOX NO. FB-7
ORIFICE NO. 5 PRETEST γ: 1.001
ORIFICE K FACTOR: 5.412×10^{-4} AUDITOR: DRG

Orifice manometer reading ΔH in H_2O	Dry gas meter reading V_i/V_f ft^3	Temperatures			Duration of run Ø min	
		Ambient T_{ai}/T_{af} °F	Dry gas meter			
			Inlet T_{ii}/T_{if} °F	Outlet T_{oi}/T_{of} °F		Vac
2.31	93.000	67	79	69	15:10.5	
	106.200	65	77	70	15.175	19.1

Dry gas meter volume V_m ft^3	Average temperatures		$V_{m_{std}}$ ft^3	$V_{m_{act}}$ ft^3	Audit γ	γ deviation %
	Ambient T_a °F	Dry gas meter T_m °F				
13.200	66	73.75	13.136	12.893	.982	-1.9

$V_{m_{std}}$	$V_{m_{act}}$
$\frac{(17.647)(V_m)(P_{bar} + \Delta H/13.6)}{(T_m + 460)}$	$\frac{(1203)(Ø)(K)(P_{bar})}{(T_a + 460)^{1/2}}$

Audit γ	γ deviation, %
$\frac{V_{m_{act}}}{V_{m_{std}}}$	$\frac{(\gamma \text{ audit} - \gamma \text{ pre-test})(100\%)}{(\gamma \text{ audit})}$

Audit γ must be in the range, pre-test γ ±0.05

Figure 28. Audit report dry gas meter (Meter Box No. FB-7).

AUDIT REPORT DRY GAS METER

DATE: 1/12/83
CLIENT: USEPA
BAROMETRIC PRESSURE (P_{bar}): 30.04 in. Hg
METER BOX NO. FB-9
ORIFICE NO. 5
PRETEST γ: .910
ORIFICE K FACTOR: 5.412 x10^-4
AUDITOR: DRO

Orifice manometer reading ΔH in H_2O	Dry gas meter reading V_i/V_f ft³	Temperatures Ambient T_{ai}/T_{af} °F	 Dry gas meter Inlet T_{ii}/T_{if} °F	 Outlet T_{oi}/T_{of} °F	Duration of run Ø min
2.72	143.000	56	52	53	15:10.3 15.172
	156.100	57	53	54	

Vac
20.3

Dry gas meter volume V_m ft³	Average temperatures Ambient T_a °F	 Dry gas meter T_m °F	$V_{m_{std}}$ ft³	$V_{m_{act}}$ ft³	Audit γ	γ deviation %
13.100	56.5	53	13.627	13.057	.958	-2.3

$V_{m_{std}}$	$V_{m_{act}}$
$\frac{(17.647)(V_m)(P_{bar} + \Delta H/13.6)}{(T_m + 460)}$	$\frac{(1203)(\text{Ø})(K)(P_{bar})}{(T_a + 460)^{1/2}}$

Audit γ	γ deviation, %
$\frac{V_{m\,act}}{V_{m\,std}}$	$\frac{(\gamma \text{ audit} - \gamma \text{ pre-test})(100\%)}{(\gamma \text{ audit})}$

Audit γ must be in the range, pre-test γ ±0.05

Figure 29. Audit report dry gas meter (Meter Box No. FB-9).

TABLE 64. EXAMPLE BLANK FILTER AND REAGENT ANALYSIS

Sample type	Original tare weight, mg	Blank weight, mg	Net weight, mg
Particulate			
87-mm Reeve Angel 934 AH No. 0002439	370.4	370.9	+0.5
Particle size			
64-mm Reeve Angel 934 AH			
BG-05	160.0	160.3	+0.3
BG-14	142.7	142.7	0.0
BG-91	161.0	161.0	0.0
BG-36	143.9	143.8	-0.1
BG-01	161.4	161.9	+0.5
BF-52	148.4	148.2	-0.2
BG-27	168.6	168.6	0.0
BF-82	143.0	143.0	0.0
Backup 0000005	217.8	219.0	+1.2
Acetone blank (780 ml volume)	103,264.7	103,272.9	+8.9 = 0.028 mg/g[a]

[a] 0.01 mg/g used in calculations.

TABLE 65. ARSENIC AND SELENIUM QA AUDIT

	Arsenic			Selenium		
Audit[a] Sample No.	Measured value, mg/liter	True value, mg/liter	95% confidence interval, mg/liter	Measured value, mg/liter	True value, mg/liter	95% confidence interval, mg/liter
1	0.027	0.024	0.017-0.032	<0.012	0.0087	none listed
2	0.194	0.182	0.129-0.230	0.046	0.048	
3	0.072	0.061	0.043-0.078	0.014	0.016	

[a] Received from Mr. Guy Simes, EMSL/QAD Cincinnati.

PLANT Asarco PN NUMBER 3490-9

DATE SAMPLES RECEIVED 1/20/83 DATE ANALYZED 1/20/83

SAMPLES ANALYZED BY Paul Clarke

REVIEWED BY 2-15-83 DATE OF REVIEW T. Wagner

Sample No.	mg SO_2/dscm determined	Source of sample	Accepted value	Percent difference
8423 0282	2321	USEPA Per T. Wagner	2325.9	-0.2

Figure 30. Audit report SO_2 analysis.

As shown in Table 66, the manual SO_2 and CEM SO_2 emission data compare closely over the segments tested.

TABLE 66. COMPARISON OF MANUAL AND CEM SO_2 RESULTS

Date (1983)	Run No.	Manual M-6 SO_2 concentration, ppm	Average CEM SO_2 concentration, ppm
1/14	PS02-1	10.6	7.2
1/14	PS02-2	35.5	54.2
1/14	PS02-3	39.9	40.8
1/14	PS02-4	16.0	15.5
1/14	PS02-5	67.0	61.6
1/14	PS02-6	69.0	60.2
1/14	PS02-7	1.7	1.0

Standard quality assurance guidelines were followed throughout the tracer study. All sample equipment was calibrated according to applied EPA criteria prior to its use. The Perkin-Elmer Model 3920 gas chromatograph was calibrated and checked daily prior to sample analysis (as described in Appendix D). Also, the limiting orifice associated with the SF_6 injection system was calibrated prior to and after each sustained injection by use of a 0-10 cc scale bubble meter and stop watch.

Background tests to determine the presence of SF_6 were performed daily prior to the hood capture efficiency tests. Background samples were obtained by collecting flue gas samples from the exhaust duct and from the air curtain control area and analyzed for SF_6. Table 67 summarizes the background analytical results.

Reported SF_6 concentrations were less than 5×10^{-12}, which was below the working range of the GC calibration curves. Samples BR-A and B were designed to preclude the possibility of SF_6 recirculating within the air curtain control area. The SF_6 was

TABLE 67. SUMMARY OF SF_6 BACKGROUND ANALYSIS

Sample No.	Sample location	Date (1983)	SF_6 concentration - v/v[a] ($\leq$ indicated values)
BRA	Air curtain control area	1/13	5×10^{-12}
BRB	Air curtain control area	1/13	5×10^{-12}
B-1	Exhaust duct	1/13	5×10^{-12}
B-2	Air curtain control area	1/13	5×10^{-12}
B-3	Exhaust duct	1/14	5×10^{-12}
B-4	Ambient	1/14	5×10^{-12}
B-5	Exhaust duct	1/17	5×10^{-12}
B-6	Air curtain control area	1/17	5×10^{-12}
B-7	Ambient	1/17	5×10^{-12}
B-8	Ambient	1/18	5×10^{-12}
B-9	Air curtain control area	1/18	5×10^{-12}
B-10	Exhaust duct	1/19	5×10^{-12}
B-11	Air curtain control area	1/19	5×10^{-12}
B-12	Air curtain control area	1/20	5×10^{-12}
B-13	Air curtain control area	1/20	5×10^{-12}

[a] Reported concentrations are out of the working range of the ECD calibration.

injected in the control area for a sustained period of time. After the SF_6 probe was removed, approximately 3 minutes were allowed to elapse before samples were collected at the secondary exhaust sample location and analyzed for SF_6. As shown, the values obtained were comparable to standard background data.

Before the transmissometer was shipped to ASARCO, the instrument was inspected and serviced by a Lear Siegler field service engineer. The instrument was assembled in the laboratory during this service inspection, and PEDCo personnel were instructed in the proper optical and electronic alignment procedures. After the transmissometer arrived on site and before its installation on the air curtain system, it was set up in a smoke-free environment at a distance equal to the measurement distance, and the optical and electronic alignment was checked. A general operational check was also conducted. The instrument was then installed on the air curtain system while the No. 4 converter was down. After the installation and while the No. 4 converter was still down, alignment and calibration checks were conducted and necessary adjustments were made.

Before their use, the strip chart recorders used to record transmissometer output were calibrated with a multimeter calibrator. Each day before the start of testing, the optical alignment of the transmissometer was checked and zero and span calibration checks were conducted.

SECTION 7

SAMPLING AND ANALYTICAL PLAN

This section describes the sampling sites and the test methods used to characterize the emissions captured by the air curtain system on ASARCO's No. 4 Copper Converter.

Table 68 presents a sample matrix outlining the number of segments tested during the particulate/arsenic and particle size sample runs.

A PEDCo representative stationed in the converter building coordinated all tests with a plant representative and with the personnel operating the sampling trains to assure that sampling was conducted during the proper segments of the converter cycle.

7.1 SAMPLE LOCATION

The manual testing, continuous monitoring, and tracer study tests were conducted in the air curtain exhaust duct, as shown in Figure 31.

Four 15-2-cm (6-in.) inside diameter (I.D.) sample ports, located 8 stack diameters downstream and 2 diameters upstream from the nearest flow disturbance, were used to collect the particulate/arsenic, SO_2, particle size, and tracer gas samples in the 1.5-m (5 ft) I.D. round duct.

The SO_2 CEM samples were obtained in a 6.4-cm (2½-in.) port located ~112-cm (~44 in.) below the four sampling ports. These sampling sites met all criteria specified in EPA Method 1.*

7.2 VELOCITY AND GAS TEMPERATURE

A Type S pitot tube and an inclined draft gauge manometer were used to measure the gas velocity pressures at the manual

TABLE 68. SAMPLE MATRIX

Sample train type	Run No.	Date (1983)	Segments sampled during the converter cycle							
			Matte charge, No. of ladles tested	Cold additions, No. of ladles tested	Slag addition, No. of ladles tested	Slag skim, No. of ladles tested	No. of blows tested	Cleanup blows tested	Finish blows tested	Copper pour, No. of ladles tested
Particulate/arsenic continuous sampling train	PATC-1	1/18 1/19	14	8	4.50	10.75	4	1	1	10
	PATC-2	1/20	14	10[a]		9.75	4	1	1	
	PATC-3	1/22	4	14[b]		7.25	3	1	1	9
Particulate/arsenic specific segment sampling train	PASM-1	1/18 1/19	14	7	4.50	10.75				10
	PASM-2	1/20	14	10[a]		9.75				
	PASM-3	1/22				7.25				
Andersen Mark III impactor (charging mode)	PSMCP-1	1/14	9	4						
	PSMC-1	1/18 1/19	14	1	4.50					
	PSMC-2	1/19	2	7						
	PSMC-3	1/20	10	4						
	PSMC-4	1/20	4	6[a]						
	PSMC-5	1/22	4	12[b]						
Andersen Mark III impactor (skimming mode)	PSSSP-1	1/14				10.75				
	PSSS-1	1/18 1/19				10.75				10
	PSSS-2	1/20				9.25				
	PSSS-3	1/22				7.25				
Andersen Mark III impactor with 15-μm precutter (blowing mode)	PSBP-1	1/14					4			
	PSB-1	1/18 1/19					4	1	1	
	PSB-2	1/20					2			
	PSB-3	1/20					1	1	1	
	PSB-4	1/22					1	1	1	

[a] Four of the cold additions were blocks of blister.

[b] Seven of the cold additions were blocks of blister.

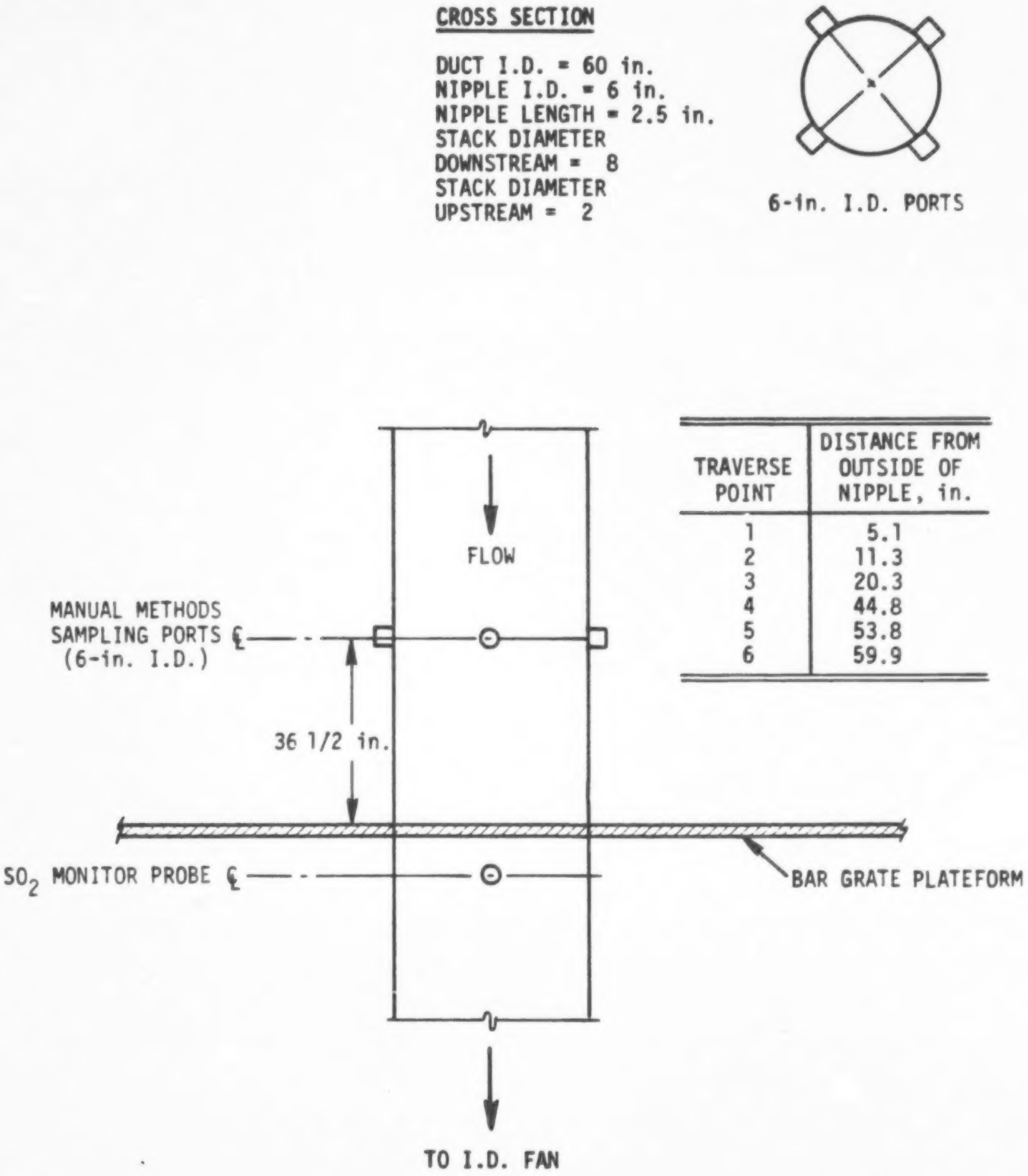

CROSS SECTION

DUCT I.D. = 60 in.
NIPPLE I.D. = 6 in.
NIPPLE LENGTH = 2.5 in.
STACK DIAMETER
DOWNSTREAM = 8
STACK DIAMETER
UPSTREAM = 2

TRAVERSE POINT	DISTANCE FROM OUTSIDE OF NIPPLE, in.
1	5.1
2	11.3
3	20.3
4	44.8
5	53.8
6	59.9

Figure 31. No. 4 converter air curtain exhaust duct sample site.

methods test site. Velocity pressures were measured at each sampling point across the duct to determine an average value. Measurements were taken in accordance with procedures outlined in Method 2 of the Federal Register.* The temperature at each sampling point was measured with a thermocouple and digital readout.

7.3 MOLECULAR WEIGHT

Flue gas composition was determined in accordance with procedures described in Method 3.* Grab samples were collected at the manual test site during the preliminary impactor runs, and an Orsat Gas Analyzer was used to analyze the bag contents for oxygen and carbon dioxide. Because these results verified that the gas streams were essentially air, additional samples were not collected.

7.4 PARTICULATE/ARSENIC

Methods 5* and 108** (as described in the Federal Register*) were used to measure particulate and arsenic concentrations. All tests were conducted isokinetically by regulating the sample flow rate relative to the gas velocity in the duct (as measured by the pitot tube and thermocouple attached to the sampling probe). The continuous sampling train traversed the cross-sectional area of the duct, whereas the specific mode train was run at a single point of average velocity. The sampling train consisted of a heated glass-lined probe, a heated 7.6-cm (3-in.) diameter glass fiber (Whatman Reeve Angel 934AH) filter, and a series of six Greenburg-Smith impingers followed by a vacuum line, vacuum gauge, leak-free vacuum pump, dry gas meter, thermometers, and a calibrated orifice.

---

[*] 40 CFR 60, Appendix A, Reference Methods 1, 2, 3 and 5, July 1, 1981.

[**] Method 108 is a proposed method.

An acetone rinse of the nozzle, probe, and filter holder portions of the sampling train was made at the end of each test. Upon completion of the acetone rinse, an additional rinse with 0.1 N NaOH was performed. The acetone rinse and particulate caught on the filter media were dried at room temperature, desiccated to a constant weight, and weighed on an analytical balance. Total filterable particulate matter was determined by adding these two values. The volume of water collected in the impinger section of the sampling train was measured at the end of each sample run to determine the moisture content of the flue gas. The contents of the first two impingers were transferred to a polyethylene container. The impingers and all connecting glassware, including the back half of the filter holder, were rinsed with 0.1 N NaOH and the rinse was added to the container. The contents of the third, fourth, and fifth impingers were transferred to a polyethylene container. The impingers and all connecting glassware were rinsed with distilled water and added to the container. Upon completion of the gravimetric analysis, the filter acetone rinse and solids contained in the 0.1 N NaOH rinse of the front half of the sampling train were prepped, combined, and analyzed for arsenic (by atomic absorption). The contents of the first two impingers and 0.1 N NaOH rinse also were analyzed for arsenic by atomic absorption. The contents of the third, fourth, and fifth impingers and distilled water rinse were titrated with NaOH to determine SO_2 concentrations.

7.5 PARTICLE SIZE DISTRIBUTION

Particle size samples at the manual methods test site were collected with an Andersen Mark III cascade impactor. The Mark III is an in-stack, multistage cascade impactor that yields a total of eight particle cut sizes normally ranging from 0.5 to 15 μm. Substrates for this impactor were 64-mm-diameter glass fiber filters.

A cyclone precutter was attached to the front of the impactor used to sample during the blowing portions of the converter cycle. This removed the larger particles and avoided the need to use buttonhook nozzles. Because the sampling rate could not be adjusted to obtain the 15-μm cut point of the cyclone precutter, the weight of particulate collected by the cyclone was added to the weight in the first stage of the respective impactor.

All particle size samples were collected at a point of average velocity near the centroid of the duct. The isokinetic sampling rate was based on initial measurements of velocity, pressure, and temperature. Constant cut-point characteristics were maintained during sampling, but velocity pressures and temperatures were measured periodically at the sampling point to evaluate the actual variation in isokinetic rate. Nozzles were selected to keep sampling rates in the recommended range of 0.3 to 0.75 acfm. Each filter was recovered, desiccated, and weighed on an analytical balance. The inlet chamber and nozzle were brushed and rinsed with acetone, and the rinse was evaporated, desiccated, and weighed. This weight was added to the first stage of the impactor.

Upon completion of the gravimetric analysis, the samples were analyzed by atomic absorption spectrometry to determine the concentrations of selected trace metals (arsenic, cadmium, lead, antimony, selenium, and bismuth).

7.6 SULFUR DIOXIDE MANUAL METHOD

The EPA Method 6 sampling procedure described in the Federal Register* was used to measure the sulfur dioxide concentration for comparison with the CEM measurements. A single sampling point located approximately in the center of the duct was sampled at a constant rate for 20 minutes.

The EPA Method 6 sampling train consisted of a heated glass-lined probe (containing a plug of glass wool at the probe tip), a series of Greenburg-Smith impingers, a vacuum line, a dry gas meter, and a leak-free diaphragm vacuum pump.

---

*40 CFR 60, Appendix A, Reference Method 6, July 1, 1981.

Upon completion of each sample run, the sampling train was leak-checked and then purged with ambient air for 15 minutes. The samples were recovered and analyzed for sulfur dioxide on site by the barium-thorin titration method.

7.7 CONTINUOUS MONITORING FOR SULFUR DIOXIDE

A Thermo-Electron Model 40 SO_2 analyzer operating on the principle of pulsed fluorescence was used for continual measuring of the SO_2 concentration in the gas stream. During the testing period, a continuous sample was extracted from the duct at a representative sampling point by use of an unheated stainless steel probe. This gas then passed through an unheated coalescing filter to remove particulate matter and moisture droplets, and then into the Teflon sample line, which transported it to the analyzer. The sample line pressure was indicated on a manometer placed just prior to the analyzer.

Triplicate injections of each standard gas were made into the analyzer during the initial startup period. The analyzer was also calibrated daily by use of appropriate mid-range or span calibration gases. A sample line integrity check also was conducted daily during the testing period.

The CEM data collected during the test series were manually reduced to a maximum SO_2 concentration and average SO_2 concentration in units of parts per million for each discernible event (i.e., one SO_2 peak resulting from one ladle of matte charged was counted as one event, but two emission peaks that merged as a result of two ladles of copper blister poured in rapid succession also were treated as one event). The average SO_2 concentration, the duration of the event, and the average stack velocity were used to calculate the pounds of SO_2 captured per event. The manual SO_2 results were compared with the corresponding CEM data to verify the CEM results.

7.8 SULFUR HEXAFLUORIDE TRACER AS AN INDICATOR OF HOOD CAPTURE EFFICIENCY

7.8.1 Tracer Gas

Measured quantities of SF_6 tracer gas were injected into the air curtain control area. Measurements of the tracer concentration at the sampling point, combined with flow rate measurements, permitted the calculation of the amount passing the sampling point (i.e., the amount collected by the air curtain and suction plenum). The collection efficiency was then calculated from the amount injected and the amount captured on a mass flow basis.

Sulfur hexafluoride (SF_6), which was used as the tracer, is a colorless, odorless, tasteless gas that is nonflammable and completely nontoxic. It is also stable up to a temperature of 500°C (923°F), and the minimum detection limit by the GC electron capture analytical technique is 5 parts per trillion.

The SF_6 was injected into the controlled area of the air curtain at a constant rate. A constant pressure was maintained on a limiting orifice to ensure a constant injection flow rate. The injection system was calibrated by a bubble meter before and after each sustained injection. The temperature at each injection point was monitored during the injection of the SF_6 to avoid decomposition. The tracer was injected over a selected time period or operation mode, as required.

Single point samples of the secondary hood flue gas were collected at the downstream sampling location by pulling them at a constant rate into a leak-free Tedlar 15-liter bag. Samples were collected over a selected time period or operational mode, as required.

SF_6 analysis was performed by using a Perkin-Elmer Model 3920 gas chromatograph equipped with a Ni-63 electron capture detector and a Valco gas sampling valve with a 1-ml sampling loop. An exponential dilution system was used to construct calibration curves and the electron capture detector's response to SF_6 was determined with a conventional strip chart recorder.

Peak heights were measured to determine response and were compared with calibration curves prepared by use of the exponential dilution system just before analysis to determine the actual concentrations of SF_6.

7.9 OPACITY

The opacity of emissions escaping capture by the air curtain and passing through the slot was monitored by use of a Lear Siegler Model RM4 double-pass transmissometer. The RM4 was chosen for this task because it has a design feature that makes it insensitive to ambient light.

The instrument was installed at the top of the secondary hood below the crane vail. Figure 32 presents a diagram of the secondary hood and transmissometer installation. Visual observation from a position at the top of the secondary hood revealed that emissions escaping the air curtain and exiting through the slot were fairly uniform along the length of the slot. As a result of this observation, the instrument was located near the center of the slot in a position that appeared to allow minimum interference to the measurement beam from the crane cables. In this location the optical path length for the instrument was 5.89 m (19.33 feet) (flange to flange). A Leeds Northrup Speedomax strip chart recorder with a 0 to 20 mA input was coupled to the transmissometer output to record opacity data.

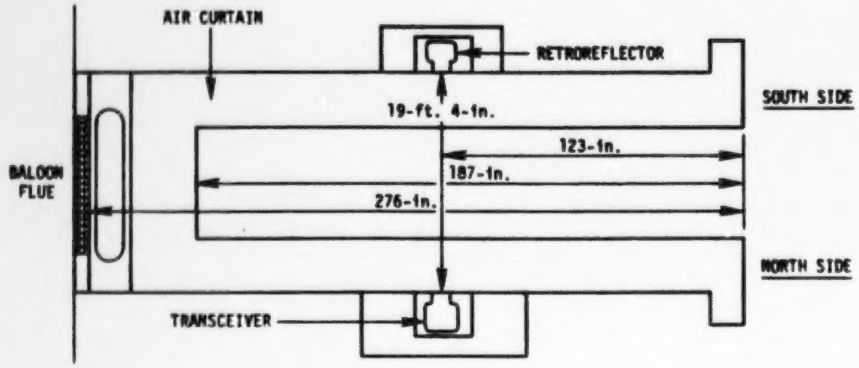

TOP VIEW

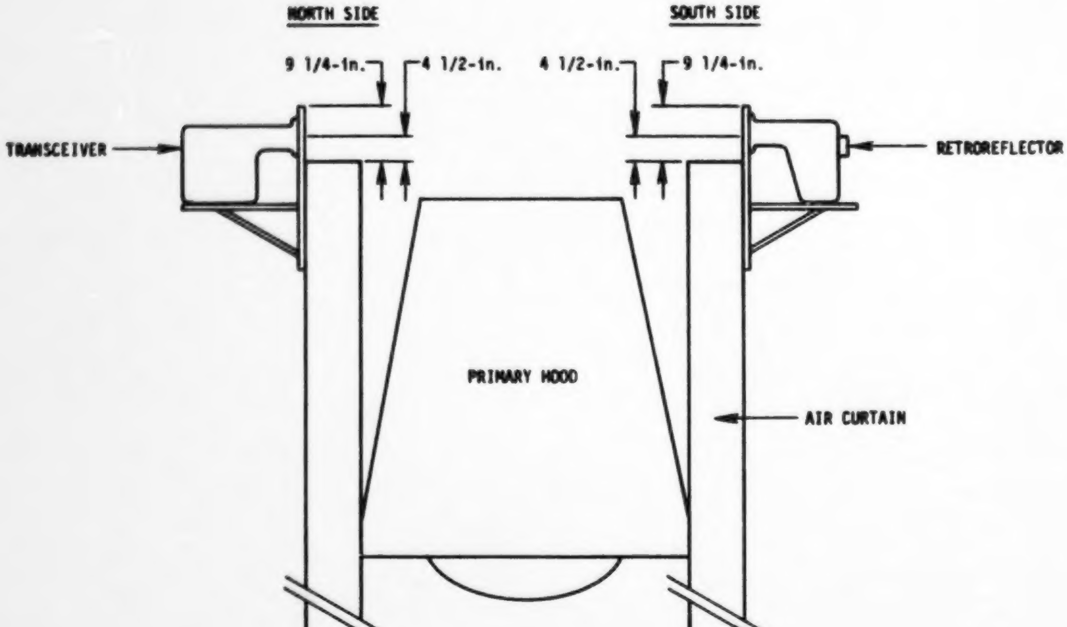

PLAN VIEW

Figure 32. Transmissometer installation on secondary hood.